REMOVAL OF BISPHENOL A APPLYING SONOPHOTOCATALYSIS

SHARMINI A/P SUNASEE

DEPARTMENT OF CIVIL ENGINEERING
FACULTY OF ENGINEERING
UNIVERSITY OF MALAYA
KUALA LUMPUR

2018

REMOVAL OF BISPHENOL A APPLYING SONOPHOTOCATALYSIS

SHARMINI A/P SUNASEE

DISSERTATION SUBMITTED IN FULFILMENT OF THE REQUIREMENTS FOR THE DEGREE OF MASTER OF ENGINEERING SCIENCE

DEPARTMENT OF CIVIL ENGINEERING
FACULTY OF ENGINEERING
UNIVERSITY OF MALAYA
KUALA LUMPUR

2018

UNIVERSITY OF MALAYA
ORIGINAL LITERARY WORK DECLARATION

Name of Candidate: Sharmini D/O Sunasee

Matric No: KGA140016

Name of Degree: Master of Engineering Science

Title of Project Paper/Research Report/Dissertation/Thesis ("this Work"):

Removal Of Bisphenol A Applying Sonophotocatalysis

Field of Study: Environmental Engineering

I do solemnly and sincerely declare that:

(1) I am the sole author/writer of this Work;
(2) This Work is original;
(3) Any use of any work in which copyright exists was done by way of fair dealing and for permitted purposes and any excerpt or extract from, or reference to or reproduction of any copyright work has been disclosed expressly and sufficiently and the title of the Work and its authorship have been acknowledged in this Work;
(4) I do not have any actual knowledge nor do I ought reasonably to know that the making of this work constitutes an infringement of any copyright work;
(5) I hereby assign all and every rights in the copyright to this Work to the University ofMalaya ("UM"), who henceforth shall be owner of the copyright in this Work and that any reproduction or use in any form or by any means whatsoever is prohibited without the written consent of UM having been first had and obtained;
(6) I am fully aware that if in the course of making this Work I have infringed any copyright whether intentionally or otherwise, I may be subject to legal action or any other action as may be determined by UM.

Candidate's Signature Date:

Subscribed and solemnly declared before,

Witness's Signature Date:

Name:

Designation:

REMOVAL OF BISPHENOL A APPLYING SONOPHOTOCATALYSIS

ABSTRACT

Bisphenol A (BPA), a chemical compound that exhibits endocrine disrupting action can be found in aquatic systems. Its complete elimination has been demanded due to its high toxic effects. Initially, the BPA removal by sonophotocatalysis coupled with titanium dioxide (TiO_2, P25) was conducted with various batch tests using energy-based advanced oxidation combining ultrasound (US) and ultraviolet (UV). The kinetics of BPA removal were systematically evaluated with not only various operational parameters such as US frequency and power, mechanical stirring speed, and temperature, but also comparison between sole and coupled system under the optimum condition of US (35 kHz, 50W, 300 rpm stirring speed and 20^oC). The combination of US/UV/P25 was the highest BPA removal rate. The removal of BPA was investigated to identify BPA by-products and intermediates by use of a high-performance liquid chromatography - mass spectrometry (HPLC-MS) and five main intermediates were formed during the sonophotocatalytic degradation. They were monohydroxylated bisphenol A, 4-isopropenylphenol, monohydroxylated 4-isopropenylphenol, dihydroxylated bisphenol A, and 4-hydroxyacetophenone. This study was further investigated to operate energy-saving sonophotocatalysis process and find out the effectiveness of sonophotocatalytic with the presence of nano-structured graphitic carbon nitride (GCN) as environment-friendly sonophotocatalyst. The material was prepared through a facile pyrolysis by using urea as a precursor and it displayed good visible-light-driven photocatalytic performance. There is no any significant effect on pH 4-8 of BPA solution. Therefore, the entire test was carried out at pH 7. The sonophotocatalytic performance was the highest BPA removal rate compared to other Advance Oxidation Process (AOP) application. There were five intermediates, monohydroxylated BPA, dihydroxylated BPA, 4-hydroxyacetophenone, 4-

isopropenylphenol and 4-hydroxybenzaldehyde identified in the presence of GCN under sonophotocatalysis process. Reusability test of GCN was carried out for five times and resulting a good capability of reuse up to third cycle. The advantages of using GCN as sonophotoctalyst were energy save and environment-friendly material because a very good visible light driven and synthesised by non-toxic starting material and the capability of reuse.

Keywords: Sonophotocatalysis. Bisphenol A. Ultrasound. TiO_2. Graphitic carbon nitride.

PENYINGKIRAN BISPHENOL A MENGAPPLIKASIKAN SONO FOTO DAN PEMANGKIN

ABSTRAK

Bisphenol A (BPA) ialah sebatian kimia yang menggangu tindakan endokrin yang boleh didapati di dalam sistem akuatik. Penghapusan BPA yang lengkap telah dituntut kerana kesan toksiknya yang tinggi. Pada mulanya, pelbagai ujian kelompok untuk penyingkiran BPA ditambah dengan pemangkin titanium dioksida (TiO_2, P25) telah dijalankan dengan proses yang berasaskan pengoksidaan yang menggabungkan Ultra bunyi (US) dan Ultra ungu (UV). Kinetik penyingkiran BPA secara sistematik dinilai dengan pelbagai parameter operasi seperti frekuensi dan kuasa US, kelajuan kacau secara mekanikal, dan suhu. Tambahan pula, ujian perbandingan antara sistem pengoksidaan tunggal serta bergabung di bawah keadaan yang optimum (35 kHz , 50W , 300 rpm dan 20°C) telah dijalankan. Proses gabungan antara sono foto dan pemangkin, US/UV/P25 (sonophotocatalysis) telah mencapai kadar penyingkiran BPA yang tertinggi. Penyingkiran BPA telah dikaji untuk mengenal pasti produk atau hasil perantaraan BPA dengan menggunakan kromatografi cecair berprestasi tinggi-spektrometri jisim (HPLC -MS) dan lima produk atau hasil perantaraan BPA yang utama dibentuk semasa degradasi melalui proses gabungan. Monohydroxylated bisphenol A, 4-isopropenylphenol, monohydroxylated 4-isopropenylphenol, dihydroxylated bisphenol A, dan 4-hydroxyacetophenone adalah lima produk atau hasil perantaraan BPA yang telah dikenalpasti. Kajian ini dilanjutkan lagi untuk mengendalikan proses gabungan sono foto dan pemangkin yang berasaskan penjimatan tenaga dan mengenalpasti keberkesanannya dengan kehadiran nano Graphitic carbon nitride (GCN) sebagai pemangkin yang mesra alam. Bahan ini telah disediakan melalui pirolisis mudah dengan menggunakan urea sebagai bahan utama dan ia menunjukkan prestasi yang baik terhadap cahaya kelihatan semasa proses gabungan sono foto dan pemangkin. Cahaya yang digunakan dalam kajian ini merupakan cahaya kelihatan kerana motif untuk menjimatkan tenaga serta mesra alam. . Kajian ke atas pH dalam larutan BPA tidak menunjukan kesan yang besar pada pH 4-8. Oleh itu, larutan BPA dikekalkan dalam keadan neutral iaitu pada pH 7. Kadar penyingkiran BPA dalam proses gabungan sono foto dan pemangkin adalah kadar yang tertinggi berbanding dengan aplikasi proses pengoksidaan yang lain. Terdapat lima hasil produk perantaraan iaitu monohydroxylated BPA, dihydroxylated BPA, 4 - hydroxyacetophenone , 4-isopropenylphenol dan 4- hydroxybenzaldehyde dikenal pasti dalam proses gabungan pengoksidaan. Kajian kebolehgunaan GCN telah dijalankan selama lima kali dan menunjukkan keupayaan penggunaan semula yang baik sehingga kitaran ketiga. Kelebihan menggunakan GCN sebagai pemangkin bagi sono dan fotolisis adalah kerana bahan jimat tenaga dan bahan mesra alam serta disintesis dengan bahan permulaan bukan toksik dan boleh diguna semula.

Keywords: Sonophotocatalysis. Bisphenol A. Ultrasound. TiO_2. Graphitic carbon nitride.

ACKNOWLEDGEMENTS

The first person I would like to express my deepest gratitude is my supervisor, Prof. Dr. Min Jang. He is a great mentor who gave me lots of freedom to work on the study in my way and fully committed whenever I need his guidance and supports on paper writing and experimental works. I appreciate your positive problem solving skills, clear minded and open minded for giving me many chances to attend international conference. I wish him all the best and may him blossom in where he is planted. Next, I would like to thank my co-supervisor, Prof. Shaliza for her continuous support and encouragements on administration and technical work to complete my master degree. I am thankful to Dr. Saravanan Pichiah for supporting me and willing to share his knowledge throughout my study.

I also thank my friend Ranjini for introducing me to my supervisor and willing to assist me during my initial stage of study; Sim Lan Ching for sharing her knowledge; Leong Kah Hon for teaching me UPLC and valuable discussion on our research works and paper writing. Special thanks are given to all of my labmates and friends: Shanmuga, Wong Kien Tek, Mossen, Kang Yee Li, Atiqah, Ilya, Haslina, Anis and Azie who make my life enjoyable in laboratory. Special acknowledgements go to Madam Kalai, Madam Rozita and Alya Shaffiee for their kind technical and administrative supports; Zuliana from INFRA Analytical Laboratory for her excellent contribution in LC/MS analysis.

Lastly, I would like to convey the most important gratitude to my family. Mom and dad, you are the strongest supports to me. Your unconditional love and cares gave me strength to continue this journey. Sincerest thanks to my siblings and beloved husband for providing me transportation and countless support throughout my study.

TABLE OF CONTENTS

CHAPTER 1: INTRODUCTION

CHAPTER 2: LITERATURE REVIEW

CHAPTER 3: MATERIALS AND METHOD

CHAPTER 4: RESULTS AND DISCUSSION

CHAPTER 5: CONCLUSIONS AND RECOMMENDATIONS

LIST OF FIGURES

LIST OF TABLES

LIST OF SYMBOLS AND ABBREVIATIONS

Symbols/Abbreviations	**Meaning**
AOP	advanced oxidation process
ACN	acetonitrile
BPA	bisphenol A
$BaSO_4$	barium sulphate
CB	conduction band
CdS	cadmium sulfide
CH_4N_2O	urea
CO_2	carbon dioxide
EDC	endocrine disrupting compound
EIC	extracted ion chromatography
E_g	band gap energy
e^-	electrons
GCN	graphitic carbon nitride
H_2O	water
H_2O_2	hydrogen peroxide
$H_8MoN_2O_4$	ammonium molybdate
HCl	hydrochloric acid
HNO_3	nitric acid
HPLC/MS	high performance liquid chromatography/ mass spectrometry
$^{\bullet}H$	hydrogen radical
hv	photon energy
h^+	positive holes
IBP	ibuprofen
KI	potassium iodide
MB	methylene blue
MST	magnetically separable titanium dioxide
MWCN	multi-walled carbon nanotubes
NaOH	sodium hydroxide
nm	wavelength

O_2	oxygen
$^{\bullet}OH$	hydroxyl radical
$^{\bullet}O_2^-$	superoxide anion radical
PPCP	pharmaceuticals and personal care products
RhB	rhodamine
RR	reactive red dye
ROS	reactive oxygen species
TiO_2	titanium dioxide
UPLC	ultra performance liquid chromatography
US	ultrasound
UV	ultraviolet
Vis-L	visible light
VB	valence band

CHAPTER 1

INTRODUCTION

1.1 Water and environment

Since the beginning of time, water has been shaping the face of the earth, not only as a geologic agent, cutting valleys and canyons and sculpting rock formations, but also as a major factor in the rise and fall of great civilizations and as a source of conflict and tension between nations. Today, the way we think about water goes to the very heart of the increasing worldwide concern about human health, the environment, and the path towards sustainable development.

The rapid growth of industry has created a series of problems related to energy and environment. Especially, water pollution has become the global risk and continued to threaten the entire ecosystem irrespective of developed and developing nations. This is due to the complexity and variety of new pollutants discharged into the aquatic system by numerous industries. Besides, wastewater reuse has provided a valuable opportunity for protecting the environment by extending the lifetime of available water resources. A considerable diversification of water reuse practices has occurred in the last few years, in areas such as green space and crop irrigation, recreational and various urban uses, and industrial applications (Meneses, Pasqualino, & Castells, 2010; P. Xu, Janex, Savoye, Cockx, & Lazarova, 2002). Thus, it becomes a challenge to identify an ideal treatment process that can meet stringent environmental regulations. The formal treatment methods such as flocculation, adsorption, reverse osmosis, etc. tend to generate secondary pollutants which will inevitably create additional costs for secondary treatment.

1.2 Water pollution

Water industry is faced with the challenge of ensuring a sustained and safe supply of drinking water from sources of varying quality, including the reuse of wastewater. During the last few decades, the focus on chemical pollution has been largely directed toward the well-known ‘‘priority’’ pollutants, especially those displaying persistence in the environment (Daughton & Ternes, 1999).

Natural water environments today are threatened by a variety of hazardous chemical substances derived from man-made products. Other surface water contaminants include a variety of metals, carcinogenic organic compounds, synthetic chemicals, pharmaceutical, veterinary, and illicit drugs, ingredients in cosmetics and other personal care products, and food supplements, together with their respective metabolites and transformation products (Falconer, Chapman, Moore, & Ranmuthugala, 2006; Kolpin et al., 2002).

It is now well established that pharmaceuticals and human hormones are ubiquitous contaminants of wastewater effluents. Most often, these compounds occur at sub-mg/L concentrations. While pharmaceuticals and personal care products (PPCPs) are a mostly well-defined group of compounds, endocrine disrupting chemicals (EDCs) are an extremely diverse group of compounds that interfere with the functioning of natural hormones in animals. It is difficult to determine which chemicals should or should not be classified as endocrine disruptors. The US Environmental Protection

Agency (USEPA) established the Endocrine Disruptor Screening Program (EDSP) to identify screening methods and toxicity testing strategies that can be used to determine whether chemicals are endocrine disruptors, but this process is incomplete (Kim, Cho, Kim, Vanderford, & Snyder, 2007; Snyder, Westerhoff, Yoon, & Sedlak, 2003). Various contaminants such as organochlorine and aromatic hydrocarbons have been detected in drinking water and a number of these chemical components are suspected as endocrine disrupting chemicals (EDCs) (Hong, Wang, & Bush, 1998; Ohko et al., 2001).

1.3 Problem statements

Regardless the nanostructure of TiO_2 in particle form, their photocatalytic efficiency highly depends on its band gap energy (*Eg*). The band gap energy of TiO_2 varies with respect to their crystallographic phase i.e., 3.2 eV for anatase and 3.0 eV for rutile. This wider band gap restricts its excitation to ultraviolet (UV) spectrum only ($\lambda \leq$ 390 nm) that slumps to ~5% by the ozone layer while the visible light contributes as a majority (~43%). Therefore, the sonophocatalyst, graphitic carbon nitride (GCN) which the photoresponse are at visible light spectrum was synthesized for the purpose of sustainable and renewable energy harvesting.

Despite of few researches have been carried out, majority of them utilized UV light in water treatment that is harmful and not readily available (Kočí et al., 2010; Krejčíková et al., 2012). Photocatalysis process with commercial TiO_2 is the common AOP application used in water treatment. A disadvantage of this process is that it cannot utilize solar light as the source of UV light due to the fact that the required UV energy for the photolysis of the oxidizer is not available in the solar spectrum. Thus necessitates the development of photocatalysts that utilize harmless light source sustainably. Collectively all the aforementioned problems provoke the utilization of solar or artificial visible light for both environmental remediation and energy conversion, thereby urging the researchers for their extensive contribution in this specific discipline.

This study focused more on the combination of sonophotocatalysis process in BPA removal. The advantages of using ultrasound are environmentally friendly technology using only electricity as a reactant; energy consumption is reduced; cost effective and safe; and able to treat very toxic wastes at mild conditions. The beneficial effect of coupling photocatalysis with sonolysis can be attributed to the increased production of hydroxyl radicals in the reaction which enhance the reaction rate of BPA degradation. Thus, sonophotocatalysis process with GCN which visible light response was selected in this study.

As the major limitation of this study, the polluted wastewater tried in this study was synthetically prepared in the laboratory. Hence, this solution might be different with the real wastewater because the real wastewater consists of mixture of few types of pollutants such as organic pollutants, inorganic pollutants and dyes. Furthermore, the concentrations of pollutants used might be relatively higher than their detected concentrations in the real water. This limitation may give differences in the real application of developed technology.

1.4 Objective of this Research

In this work, a reactor combined with ultrasound (US) and UV generators was constructed and operated to investigate the BPA removal. The operational parameters such as US frequency, US power, temperature and stirring speed have been optimized through conducting a series of batch tests. In the first phase, the sonophotocatalytic process based on UV light irradiation with the presence of world-widely known commercial TiO_2 (P25) was applied for BPA degradation. Then, as the second phase, the BPA degradation by sonophotocatalytic process based on visible light irradiation with the presence of GCN was investigated to find out the optimum pH and catalyst loading, as well as removal pathway for sonophotocatalysis.

The key scope of the present study is to investigate the BPA degradation by energy based AOPs which includes sonolysis, photolysis, sonocatalysis, photocatalysis and sonophotocatalysis. The studies on BPA degradation conducted by sonophotocatalysis based on UV and visible light irradiations were described as below:

- To find out the effectiveness of energy based Advance Oxidation Processes (AOPs) on the BPA degradation
- To optimize the effects of key operational parameters such as US frequency, US power, temperature and mechanical stirring intensity.
- To elucidate the mineralization mechanism of BPA by conducting kinetic test and LC/MS ananysis and operate energy-saving sonophotocatalysis process.

1.5 Thesis overview

Chapter 1 starts with the introduction on water and environment which is the major subject of discussion of present thesis. This is followed by introductory note water pollution. Then, the major limitations of these specific studies were signified and this was succeeded through precise objectives.

Chapter 2 furnishes the literature survey relevant to the thesis. This chapter elaborated the background of semiconductor photocatalyst, endocrine disrupting compounds, current water treatment and visible light sonophotocatalyst. Finally, the various reports on advance oxidation processes and the application of advance oxidation processes on BPA were presented.

Chapter 3 outlines the detailed synthesis route for GCN, followed by characterization techniques that were involved in understanding the physicochemical nature of the prepared samples. The last section of this chapter elaborates the experimental setup and condition adopted for the degradation of BPA pollutants and the analyses.

Chapter 4 presents the outcome of the thesis findings with comprehensive discussions. This chapter necessitates the insight, importance and influence of the chosen composite. The effect of parameters for the optimized condition, the sonophotocatalystic performance of organic pollutant degradation and its mechanism were presented.

Chapter 5 includes the conclusions and recommendations.

CHAPTER 2

LITERATURE REVIEW

2.1 Titania (TiO_2) Photocatalyst

Semiconductor materials are particularly useful for photocatalytic process because of a favorable combination of electronic structure, light adsorption properties, charge transport characteristics and lift time of excited state. The primary criteria for good semiconductor photocatalysts for organic compound degradation are that the redox potential of the H_2O/•OH (OH- = •OH + e-; *E* 0= -2.8 V) couple lies within the bandgap domain of the material and that they are stable over prolonged periods of time. To be a good photocatalyst, some basic requirements must be met: 1) photoactive; 2) able to utilize visible and/or near UV light; 3) biologically and chemically inert; 4) photostable; 5) inexpensive.

Among the semiconductors, such as ZnO, ZnS, WO_3, CdS, and TiO_2, etc., which have been investigated and reported so far, few of them are appropriate for efficient photocatalytic reaction of a wide range of organic contaminants (Herrmann, Mozzanega, & Pichat, 1983; Keller, Bernhardt, & Garin, 2003). Table 2.1 indicates a wide range of potential semiconductors (TiO_2, ZnO, ZnS, WO_3 and CdS,) for the use of heterogeneous photocatalysis. Titania (TiO_2) is one of the most common types of semiconductor photocatalyst used in heterogeneous photocatalysis to mediate the photoreaction between the adsorbed species and charge transfer (X. Chen & Mao, 2007; Seger & Kamat, 2009).

Table 2.1: Semiconductors used in photocatalysis process (Daghrir, Drogui, & Robert, 2013)

Semiconductors	Band gap energy (ev)	Wavelength (nm)	Light absorption
TiO_2	3.2	387	UV
ZnO	3.2	387	UV
ZnS	3.7	335	UV
WO_3	2.8	443	Visible
CdS	2.5	496	Visible

The renowned TiO_2 photocatalyst P25 produced by Degussa (Germany) is used by several groups studying photocatalysis, because of its high catalytic activity. P25 is manufactured by the Aerosil process in which $TiCl_4$ vapour is hydrolyzed in presence of hydrogen and oxygen in a high temperature flame (> 1200 °C) (Bickley, Gonzalez-Carreno, Lees, Palmisano, & Tilley, 1991; Mills & Le Hunte, 1997). Bickley et al. proposed that this production route gives particles to retain water strongly bound as hydroxyl groups and easily can readsorb water (Bickley et al., 1991). The Aerosil process yields 99.5 % pure TiO_2 as cubic particles with rounded edges consisting of 70% anatase and 30% rutile (Mills & Le Hunte, 1997).

Ohno et al. found by TEM-investigations of P25 approximately 1 % amorphous TiO_2 and that anatase and rutile formed in separete aggregates. The average sizes of anatase and rutile elementary particles were found to be 85 and 25 nm for anatase and rutile, respectively (Ohno, Sarukawa, Tokieda, & Matsumura, 2001). This contradicts previous findings by Bickley et al. who found anatase and rutile in close proximity and related that to the high photoactivity of P25 (Bickley et al., 1991).

2.2 Endocrine disrupting compounds (EDCs)

Endocrine disrupting compounds (EDCs) can be defined as exogenous substances or mixtures that alter the function(s) of the endocrine system and causes adverse health effects on an intact organism or population. Research shows that pharmaceutical residues in water known as EDCs could bioaccumulate in human population. Research conducted in Europe and US have revealed that EDCs are the most common micropollutants found in many water sources and wastewaters. Several papers have reported the presence of PPCPs and EDCs in water sources particularly for drinking purpose (Cleuvers, 2004; Ternes et al., 2002).

The widespread occurrence of organic micropollutants such as pesticides, pharmaceuticals and personal care products, flame retardants, and EDCs in receiving bodies and drinking water influents has been a global issue of concern for academia and environmental agencies for over two decades, and more recently in the general public. In many cases, these pollutants can be traced back to their incomplete removal and discharge from wastewater treatment facilities. Although the direct effect of these compounds on human health is not yet fully understood, the detrimental effect on organisms in these receiving bodies from EDCs has already been demonstrated such as the feminization of male fish due to the release of natural hormones (Rodgers-Gray et al., 2000; Sumpter, 2005). Research on organic micropollutants can be divided into two major areas: upstream treatment and downstream monitoring.

Fent et. al has confirmed that EDCs can cause serious health risks to living organism even at very low concentration (ppb levels) (Fent, Weston, & Caminada, 2006). Also, other studies have reported that EDCs cause health effects such as early puberty and menopause, early breast growth and lactation; and uterine related diseases such as fibroids and endometriosis (Jones, Green, Voulvoulis, & Lester, 2007). These EDCs were found to affect not only the human endocrine system, but also the aquatic wild life, causing ecotoxicological effects (Jermann, Pronk, Boller, & Schäfer, 2009).

Rivers in Malaysia receive treated effluents, municipal and industrial wastewater. However, they supply 98% of water sources which are treated using water treatment processes. There are reports show that endocrine disrupting chemical (EDCs) such as pharmaceuticals and organic wastewater contaminants including BPA do not eliminate completely from the wastewater during the water treatment processes and therefore they can be found in the streams and river (Fulazzaky, Seong, & Masirin, 2010; J.-H. Kang, Kondo, & Katayama, 2006; Santhi, Sakai, Ahmad, & Mustafa, 2012).

2.2.1 Bisphenol A (BPA)

As a representative of EDCs, bisphenol A [BPA, 2,2-bis(4-hydroxyphenyl) propane] is an important industrial chemical which has been used for the production of epoxy resins and polycarbonate in the plastics industry (R. A. Torres, Pétrier, Combet, Moulet, & Pulgarin, 2007). BPA was first synthesized in 1905. It is obtained by the reaction of phenol with acetone in the presence of a catalyst. BPA is a fairly water-soluble compound (300 mg L^{-1} at room temperature) and dissociates in an alkaline environment (pK_a of BPA, 9.9-11.3) (Rykowska & Wasiak, 2006). The chemical structure of BPA is shown in Figure 2.1.

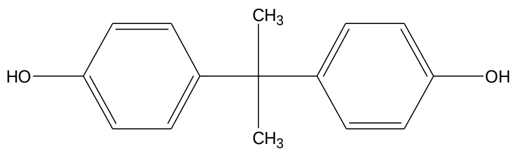

Figure 2.1: Molecular structure of bisphenol A

BPA is mainly used in plastic materials industry, e.g. poly (vinyl chloride), and as an antioxidant in glues, plastics, and ink. In 2001 global production of BPA (started in 1957 in the USA) was estimated to be approximately 2.5 million tons (Rykowska & Wasiak, 2006), and in 2003 it had over 2 million metric tons global production. From 2003 to 2006, the global BPA consumption increased at an average annual rate of about 10% and the demand for BPA was expected to rise at annual rate of 7–8% during 2006–2011 (Garoma & Matsumoto, 2009). It is frequently detected in wastewater discharged from municipal and industrial sources at levels ranging from 0.23 to 149 µg/L (Fuerhacker, 2003; Höhne & Püttmann, 2008; Lee, Peart, Gris, & Chan, 2002; Sánchez-Avila, Bonet, Velasco, & Lacorte, 2009; T. Suzuki, Nakagawa, Takano, Yaguchi, & Yasuda, 2004).

Materials containing BPA have been used in many applications, for example as a varnish on the inside of cans and as other packaging materials used for the storage of food products, beverages, and pharmaceuticals. Polycarbonates have been commonly used for production of components of medical equipment (for dialysis and blood oxygenation), bottles for feeding infants, and kitchen dishes. The wide use of BPA containing polycarbonate polymers follows mainly from their particular properties, light weight, durability, high tensile strength, high modulus of elasticity, high melting point, and high vitrification temperature (Rykowska & Wasiak, 2006).

This compound, found in industrial wastewaters, can be encountered in surface water. With the presentation even at low concentration in water, BPA disturbs the behaviour of aquatic life through its endocrine disrupting effects. BPA can be released into the environment through different sources, such as discharge of wastewater and wash water generated from BPA production facilities or consumer product manufacturing facilities that utilize BPA, discharge of effluent from wastewater treatment plant, leaching from consumer products containing BPA at hazardous waste landfill sites, deposition of particulates or dust from BPA production, processing, or storage facilities, and accidental discharge. According to the toxic release inventory database, the total environmental release of BPA in the U.S. was about 770 tons from 2000 to 2006, with average annual release of 110 tons. In 2006, the total environmental release of BPA was 98 tons, with the breakdown in air release of 54 tons, water release of 1.7 tons, and soil releases of 42 tons (Garoma & Matsumoto, 2009).

According to Shanti's findings, BPA was present in 93% of the surface water samples at level s ranging from below limit of quantification (LOQ: 1.3 ng/L) to 215 ng/L in Langat River basin, Malaysia and low levels of BPA were detected in drinking water. BPA in tap water ranged from 3.5 to 59.8 ng/L with the highest levels detected from the PVC pipes and water filter devices (Santhi et al., 2012).

To some extents, BPA can be eliminated through classical physical, chemical, or biological treatments. However, it is quite difficult to remove completely by biological process. Accordingly, it is necessary to demineralise BPA or transform into environmentally safe by-products that do not have any estrogenic actions (R. A. Torres, Pétrier, Combet, Carrier, & Pulgarin, 2008). Accordingly, environmental scientists have developed best available technologies to render complete removal or considerable destruction of the compound (Gültekin & Ince, 2008; Kaneco, Rahman, Suzuki, Katsumata, & Ohta, 2004; Katsumata, Kawabe, Kaneco, Suzuki, & Ohta, 2004).

2.3 Water treatment

An ideal water treatment process should have the capability to mineralize all the toxic organic components completely without leaving behind any harmful by-products. In broader classification, biological, mechanical, thermal, chemical, or physical treatments, or their combinations may be applied to purify contaminated water. The choice of proper water treatment process depends on the nature of the pollutants present in water, and the allowable contamination level in the treated water. There are many limitations with conventional water treatment system which have a propensity to use more chemical such as coagulant, polymer and chlorine during the extreme weather, which is actually not good for the consumer.

On the other hand, another drawback is its non ability to treat or degrade toxic and non biodegradable pollutants. There are two main purposes of water treatment study – the reduction of contaminant level in the discharge stream to meet environmental regulation, the purification of water to ultrapure water in order to be able to use in semiconductor, microelectronic and pharmaceutical industries (Andreozzi, Caprio, Insola, & Marotta, 1999). Moreover, the cost effectiveness of the water treatment process also plays an important role in choosing the particular process. So new technologies have made growing numbers of water treatment alternatives available and one of them is advance treatment method which assists to reduce our dependent on chemical for treatment process and also helps us to treat various toxics present in wastewater. This can be defined as aqueous phase oxidation methods based on the intermediacy of highly reactive species such as hydroxyl radicals in the mechanisms leading to the destruction of the target pollutant (Comninellis et al., 2008).

2.4 Advance oxidation processes (AOPs)

Although advanced oxidation processes (AOPs) such as ozonation, Fenton, and photo-Fenton, have been developed in the last decades (Jyothi, Yesodharan, & Yesodharan, 2014), energy-based AOPs such as ultrasound (US), ultraviolet (UV) sole or combined with catalysts also get more attentions because of no chemical consumption, its particular efficacy towards volatile and/or hydrophobic compounds, no sludge production and rapid oxidation effect (R. A. Torres, Nieto, Combet, Pétrier, & Pulgarin, 2008).

For the treatment of drinking water and tertiary wastewater, a group of chemical oxidative technologies classified as advanced oxidation processes (AOPs) has garnered a significant level of interest academically and industrially over the last three decades. All AOPs are characterized by the production of highly reactive and non-selective hydroxyl radicals in an aqueous medium (Staehelin & Hoigne, 1985). Hydroxyl radicals are capable of oxidizing nearly all organic compounds to water, carbon dioxide, and mineral salts through a process termed mineralization (Y. Chen & Dionysiou, 2006).

Traditional water disinfection treatment processes such as ozonation and UV disinfection can easily be retrofitted to accomplish advanced oxidation in both water and wastewater treatment plants. There has been over three decades of intense research into many different types of AOPs as well as wide adoption of some of these processes. Of the many AOPs tested, ozonation, UV/ozone, UV/hydrogen peroxide, and

UV/photocatalysis are most commonly studied and used for many applications. The AOP applications are very powerful technology, but the uses are limited in large scale application due to the high operating cost. However, Chongs, et al., have done his research by using the advent of higher efficiency UV lamps, visible light catalysts, and improved reactor design, with the help of computational fluid dynamics and energy modelling. Both UV and solar-based photocatalysis have great potential for large-scale application (Chong, Jin, Chow, & Saint, 2010). However, further research is still needed in developing new immobilised photocatalysis reactors and to improve the performance, the immobilisation, and illumination in the reactor of the photocatalyst.

Complete mineralizations of the organic compound by AOPs are perceived to be expensive but partial oxidation of the initial compounds to less stable intermediates is a viable option. At the same time, the intermediates should degrade itself in the environment and are harmless to the aquatic environment and human health. However, partial oxidation of organic contaminants can in some cases result in the formation of intermediates more toxic than the parent compound (Rizzo, 2011), and the nature and number of the degradation products will depend on the employed oxidation process, reaction time, and water quality metrics.

2.4.1 Photocatalysis (UV/TiO_2)

Titanium dioxide (TiO_2) based photocatalysis is another AOP that has gained considerable attention as a means for water remediation (Bahnemann, 2004). This photocatalysis is categorized as homogeneous and heterogeneous photocatalysis according to the different phases of reactants and photocatalysts employed. Heterogeneous photocatalysis mainly involves the participation of semiconductor photocatalyst to generate active radicals such as superoxide radical anions ($^{\cdot}O_2^{-}$) and hydroxyl radicals ($^{\cdot}OH$) with the presence of sufficient photon energy from different light source (UV, visible light and solar energy).

The mechanism of the photocatalysis process is illustrated in Figure 2.2. First, while the photon energy (hv) is absorbed by the semiconductor photocatalyst, electrons from the valence band (VB) are promoted to conduction band (CB) leaving behind an equal number of positive holes at the VB. Thus the photogenerated electrons (e^{-}) and positive holes (h^{+}) will then migrate to the surface of the semiconductor photocatalyst and react with the strong oxidation and reduction species forming active radicals for oxidation. In the midst most of the electrons and holes tend to recombine and dissipate the energy in the form of heat and light. The organic pollutants are oxidized by $^{\cdot}OH$ and $^{\cdot}O_2^{-}$ to form CO_2, water and non hazardous substances in the complete photocatalytic reaction (R. A. Torres, Nieto, et al., 2008).

The basis of photocatalysis is the photo-excitation of a semiconductor that is solid as a result of the absorption of electromagnetic radiation, often, but not exclusively, in the near UV spectrum. Under near UV irradiation a suitable semiconductor material may be excited by photons possessing energies of sufficient magnitude to produce conduction band electrons and valence band holes. These charge carriers are able to induce reduction or oxidation respectively.

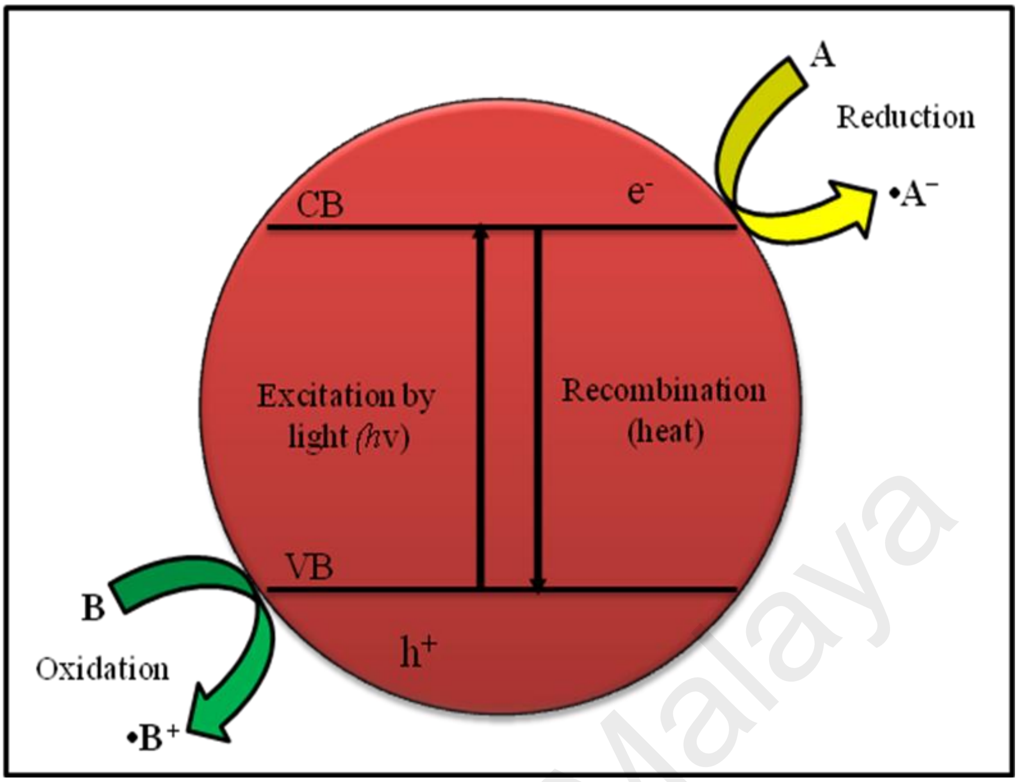

Figure 2.2: Illustration of photocatalysis mechanism

The photocatalytic activity of TiO_2 was discovered by Fujishima in 1967 as a result of research on photoelectrochemical solar cells. TiO_2 is a semiconductor with a wide band gap of ca. 3.0 eV; by irradiation of UV-light (wavelengths in the range 400 to 100 nm). In water, the excited electrons can react with molecular oxygen to form superoxide radical anions ($\cdot O_2^-$) and the holes can react with water to produce hydroxyl radicals ($\cdot OH$). Both the radicals generated by electrons and holes can decompose organic molecules into CO_2 and H_2O, while the oxidative power of the holes is especially important (Fujishima, Rao, & Tryk, 2000). The role of oxygen and all the possible species ($HO^{\cdot}_2$, HO^-_2, H_2O_2 and $\cdot OH$) can be generated from the radical anions which the mechanism is in the following reactions.

$$O_2 + H^+ \rightarrow HO_2^{\cdot} \qquad (2.1)$$

$$H^+ + O_2^- + HO_2^{\cdot} \rightarrow H_2O_2 + O_2 \qquad (2.2)$$

Hydroxide groups on the surface with trapped holes, $Ti(IV)OH^{\cdot +}$, are on the other hand generally accepted to be important for oxidation of organic species, and most photooxidation is found to occur through these groups rather than directly by hole transfer (Mills & Le Hunte, 1997).

After Fujishima's discovery, titanium dioxide has found in many applications as a photocatalyst. For photoelectrochemical purposes, such as light induced electrolysis of water, titanium dioxide was found to have a too low efficiency for practical purposes. Researchers then began to consider other applications for photocatalysis, building upon the knowledge from the photoelectrochemistry research. Now, commercial products which employ the photocatalytic effect of TiO_2 are widely available. Examples are self-cleaning products (windows, tiles, traffic signs), air and water purification systems and self-sterilizating medical equipment (Fujishima et al., 2000).

2.4.2 Sonocatalysis (Ultrasonic/TiO_2)

Application of this technology leads to the decomposition of many complex organic compounds to much simpler compounds during cavitation process. It is one such recent technique which has been found to be substantially beneficial in wastewater treatment. Ultrasound is the term used to describe sound energy at frequencies above the range that is normally audible to human beings (i.e.>16 kHz). At its upper limit ultrasound is not well defined but is generally considered as 5MHz in gases and 500MHz in liquids and solids which are subdivided to reflect applications. The range 20 to 100 kHz (though in certain cases up to 1 MHz) is designates as the power ultrasound reason, while the frequencies up to 1 MHz are known as high frequencies or diagnostics frequencies (Lifka, Ondruschka, & Hofmann, 2003; Petrier, Jeunet, Luche, & Reverdy, 1992)

Sound is composed from longitudinal waves comprising rarefactions (negative pressures) and Compressions (positive pressures). It is these alternating cycles of compression and rarefaction that, in high power ultrasonic applications, can produce a phenomenon known as “cavitation”. Cavitation is described as the formation of microbubbles in solution that implode violently after reaching a critical resonance size. These microbubbles can be produced by a number of mechanisms: 1) Local increase in water velocity as in eddies or vortices, or over boundary contours; 2) Rapid vibration of the boundary through sonication; 3) Separation or parting of a liquid column owing to water hammer; or 4) An overall reduction in static pressure. (R. Torres, Abdelmalek, Combet, Pétrier, & Pulgarin, 2007).

The rapid implosion of cavitation microbubbles results in high temperatures at the bubble/water interface, which can trigger Thermal dissociation of water molecules to form extremely reactive radicals. The extreme conditions generated during cavitation decomposes water to create both oxidizing (•OH) and reducing (•H) radical species. More specifically, ·OH can be produced by the dissociation of water and oxygen (O_2), as well as association reactions occurred inside the collapsing cavitation under extremely high temperature and pressure (Gonze, Fourel, Gonthier, Boldo, & Bernis, 1999; Petrier & Casadonte, 2001).

Sonochemical activity for the degradation of pollutants may take place mainly due to free ·OH that escapes from the interface of bubble-liquid and migrates to the liquid bulk. However, ·OH could recombine to produce H_2O_2 (equation 2.3) which may in turn react with hydrogen radicals (·H) to regenerate ·OH (equation 2.4) (Taghizadeh & Abdollahi, 2011). For the sonolysis, the US frequency/power and temperature have important effects on reaction product distribution and reaction rate (Goel, Hongqiang, Mujumdar, & Ray, 2004; Petrier et al., 1994).

$$\cdot OH + \cdot OH \rightarrow H_2O_2 \tag{2.3}$$

$$H_2O_2 + \cdot H \rightarrow H_2O + \cdot OH \tag{2.4}$$

As a sonocatalyst, Wang, et al. applied nano-sized TiO_2 in the degradation of organic dyes in the system of ultrasound (J. Wang et al., 2011). They found that the production of reactive oxygen species (ROS) such as $\cdot O_2^-$, ·OH, H_2O_2, O_2, etc. is related to amount of nano-TiO_2 and irradiation time. Tang, et al., tried to apply TiO_2 coated activated carbon to degrade a type of dye, Rhodamine B (RhB) (Tang, Teng, Alkarkhi, & Li, 2012). Through sonocatalytic reaction of TiO_2-carbon, the highest removal rate of RhB was achieved with the best operational condition (pH 6, 50 ºC, 60 min irradiation time and 30 kHz US frequency). Song et al., studied on the sono-catalytic effect of graphitic carbon nitride (GCN) to remove methylene blue (MB) in aqueous phase. They found the GCN had a higher activity of sonocatalysis in the degradation of MB compared to the commercial catalyst TiO_2 (P25) (Song, Zhang, Wu, & Wei, 2012). Zhu et al., conducted tests to find out the sonocatalytic activity of multi-walled carbon nanotubes (MWCN) and CdS modified TiO_2 in the degradation of RhB. The composite material MWCN/CdS/TiO_2 had a synergetic effect to remove RhB by sonocatalytic reaction (Zhu, Meng, Park, Ghosh, & Oh, 2013).

The sonolytic degradation of endocrine disrupting compound 4-cumylphenol (4-CyP) in aqueous solution was investigated by Chiha, Hamdaoui, Baup, & Gondrexon, it involved the influence of operating parameters such as initial concentration, frequency, power, pH, temperature and saturating gas. The degradation rate of 4-CyP increased proportionally with increasing ultrasound power from 20 to 100 W and temperature in the range of 20-50 °C. The dependence of the 4-CyP degradation rate in the presence of various saturating gas shows the following order: argon > air> nitrogen and the optimum condition was observed in acidic media. The degradation was inhibited in the presence of nitrogen gas owing to the free radical scavenging effect in vapor phase within the cavitation bubbles. The ultrasonic degradation of 4-CyP was clearly promoted in the presence of bromide ion and the promoting effect on degradation increased with increasing bromide concentration. The improvement of the degradation rate should involve the presence of the dibromine radical anion ($Br_2\cdot^{-}$) coming from the reaction of bromide ion with ·OH radical. This research demonstrated that the sonolytic treatment was more efficient in the natural water compared to pure water (Chiha, Hamdaoui, Baup, & Gondrexon, 2011).

The study of degradation of ibuprofen (IBP) in water using reusable sonocatalyst, magnetically separable titanium dioxide (MST) was done by K. Kang et al. The kinetics of IBP removal by sonolysis or sonocatalysis was evaluated with various operational parameters such as pH, temperature, ultrasound (US) frequency and mechanical mixing intensity. For the first time, authors found that mechanical mixing had an opposite effect on the oxidation rate constants of IBP removal by sonolysis or sonocatalysis according to US frequency (35 > 1000 > 300 > 500 > 700 kHz). Compared to commercial TiO_2 (P25), MST had almost same effective removal rate as (P25) and showed a high reusability because there was no loss in the removal efficiency of IBP by sonocatalysis in five repetitive experiments (K. Kang et al., 2015).

2.4.3 Sonophotocatalysis

Sonophotocatalysis is the combination of two advanced oxidation processes i.e. sonication and photocatalysis. The basic reaction mechanism for both ultrasound initiated degradation and photocatalytic oxidation (either using UV light or solar energy) is the generation of free radicals and subsequent attack by these radicals on the organic pollutant species. If the two modes of irradiations (UV and ultrasound) are operated in combination, more numbers of free radicals are available for the reaction, thereby increasing the rates of reaction.

There have been several studies to depict the synergism and the enhanced rates of degradation. As compared with the sum of the individual processes, the combinatorial operation of sonochemical reactors and photocatalytic oxidation had higher rate constant of degradation process. Madhavan et al. have given an extensive overview of various studies describing the use of sonophotocatalytic oxidation for treatment of ibuprofen (IBP) (Madhavan, Grieser, & Ashokkumar, 2010). The sonolytic, photocatalytic and sonophotocatalytic degradations of IBP in the presence of homogeneous Fe^{3+} and heterogeneous TiO_2 were studied. When compared with sonolysis and photocatalysis, a higher degradation rate was observed for sonophotocatalysis in the presence of TiO_2 or Fe^{3+} and also a slight synergistic enhancement was found with a synergy index of 1.3 and 1.6, respectively.

Work on Sonophotocatalytic destruction of organic contaminants in aqueous systems on TiO_2 powders was done by Davydov et al. They studied the effect of ultrasound on the photodegradation of salicylic acid on four commercial titania powders. The system exhibiting the highest enhancement was isolated. The use of ultrasound during photocatalysis had a pronounced effect on the rate and efficiency of salicylic acid destruction as compared with UV-light photocatalysis alone. The possible reasons of the increased activity under ultrasonication were proposed: aggregate breakage and photocatalytic utilization of species produced by the ultrasound. The combination of the action of ultrasonic waves and UV-assisted photocatalysis yielded synergistic effects for the catalyst with smaller particle size (such as Hombikat), while no enhancement was observed for the largest particle size photocatalyst (Aldrich anatase). Degussa P25 exhibited the highest overall activity for the degradation of salicylic acid and moderate enhancement of activity by ultrasound. The presence of intermediates in the bulk solution was observed during the purely photocatalytic degradation of phenol. The presence of ultrasound, however, allows eliminating the toxic intermediates by the sonolysis in the bulk solution (Davydov, Reddy, France, & Smirniotis, 2001).

The accelerated sonophotocatalytic degradation of Reactive Red (RR) 120 dye under visible light using dye sensitized TiO_2 activated by ultrasound has been carried out by S.K.Kavitha, and P.N.Palanisamy. The effect of sonolysis, photocatalysis and sonophotocatalysis under visible light has been examined to study the influence on the degradation rates by varying the initial substrate concentration, pH and catalyst loading to ascertain the synergistic effect on the degradation techniques. Ultrasonic activation contributes degradation through cavitation leading to the splitting of H_2O_2 produced by both photocatalysis and sonolysis. This increases the amount of reactive radical species including oxidation of the substrate and degradation of intermediates and is mainly responsible for the observed synergy (Kavitha & Palanisamy, 2011).

A lot of work has been done on it in recent years and many papers published for the degradation of dyes, phenolic compounds, herbicides and surfactants. (Bahena, Martínez, Guzmán, & Hernández, 2008; Selli, 2002; Silva, Nouli, Carmo-Apolinário, Xekoukoulotakis, & Mantzavinos, 2007; Y. Suzuki, Arakawa, Maezawa, & Uchida, 1999). But as comparative to these, less work has been done on wastewater treatment. Thus, serious attention should be paid on this issue since a variety of organic pollutant can be detected in surface, ground, and drinking water. The risk is directly proportional to the concentration of the chemical substances in various environmental compartments, and organic pollutants add to that risk if it is not managed properly. In this study, we attempt to study based on advanced treatment options such as combined system of ultrasound and photocatalytic processes for degradation of compounds present in organic pollutant wastewater.

2.5 Graphitic Carbon Nitride

Graphitic carbon nitride (GCN) had very recently attracted tremendous attention of researchers for a robust and stable visible light driven photocatalyst. As compared to other inorganic semiconductor, GCN consists mainly of carbon and nitrogen which are among the most abundant elements in our planet, making it a suitable and environmentally organic semiconductor. The heptazine ring structure and the high condensation degree enable this metal free semiconductor to have various notable advantages such as good physicochemical stability, harvesting visible light with a band gap of 2.7 eV, suitable redox potential to efficiently catalyze reactions, abundant, and inexpensive. These unique properties make GCN to be a promising candidate for visible light enhancement. Nevertheless, pure GCN could be suffered from shortcomings such as rapid recombination rate of photo-generated electron-hole pairs and a small specific surface area. However, its 2-dimensional layered structure could be a good feature for hybridizing with other components to overcome its shortcomings.

In most cases, gcn is prepared by a simple route using nitrogen rich organic molecules as single source precursor under thermal treatment. Yan et al., reported a direct heating of melamine to gcn in a semi-closed system (Yan, Li, & Zou, 2009). Zhang et al., used the thermal polycondensation of cyanamide or dicyadiamide into gcn with a continuous flow of n_2 gas (J. Zhang et al., 2010). Meanwhile, lotsch and schnick employed the thermal transformation of guanylurea dicyanamide to gcn that enable it to render more oxygen containing organic compound (Lotsch & Schnick, 2005). However, some of these precursors are toxic and harmful to human and environment, and some are unstable and difficult to synthesize on a large scale basis. Therefore, by choosing urea as an alternative starting material, drawbacks aforementioned could be overcome (Liu, Zhang, Wang, Dawson, & Chen, 2011). As a common chemical, urea is considered as economic and non-toxic in chemical industry so that it turns out to be the promising precursor for synthesizing gcn (Liu et al., 2011; J. Xu, Li, Peng, Lu, & Li, 2013). Furthermore, it is an active molecular precursor for thermal treatment. First, when the urea is heated under a closed air atmosphere, it decomposes into ammonia and isocyanic acid. Then, it is converted into other intermediates like cyanuric acid, ammalide and ammeline. The formed cyanuric acid further turns into melamine which then condenses to form melem. The gcn will be formed after the polymerization of melam into melon. Liu et al. Had proven mechanism in their studies where they employed a simple pyrolysis of urea under ambient pressure and atmosphere (Liu et al., 2011).

2.6 Application of AOP for BPA

Bisphenol A (BPA) removal process was investigated by many researchers by applying different type of advance oxidation process (AOP). The application and comparison between solo AOP and combination of AOPs was applied such as UV, US, Fenton, Ozone, H_2O_2, Sunlight, photofenton, ptotocatalyst sonocatalyst and more which were organized as in table below.

Table 2.2: Compilation of selected literature reports on application of different type of AOP on BPA removal

Type of AOP	Research Highlights & Findings	Reference
Ozonation	The reaction between BPA and ozone with presence of t-BuOH increased with increase in pH between pH 2-10. The presence of common inorganic anions (chloride, sulphate, nitrate and phosphate ions) at environmental levels did not significantly affect the rate of degradation of BPA by ozone. The degradation products of BPA during ozonation were identified to be 4-(prop 1-en-2-yl)phenol, hydroquinone, 4-hydroxyacetophenone, 2-(2-(4 hydroxy phenyl) propan-2-yl) succinaldehyde, 2-(1-(4 hydroxyphenyl)vinyl) pent-2-enal, 3 formyl-4-(4-hydroxyphenyl)-4 methylpent-2-enoic acid, monohydroxy-BPA and dihydroxy-BPA.	**(Tay, Rahman, & Abas, 2012)**
	An efficient removal of BPA by ozonation can be expected under water treatment conditions. Five major transformation products were evidenced (catechol, orthoquinone, muconic acid derivatives of BPA, benzoquinone and 2-4-hydroxyphenyl-propan-2-ol).	**(Deborde, Rabouan, Mazellier, Duguet, & Legube, 2008)**

Table 2.2, continued

Type of AOP	Research Highlights & Findings	Reference
UV/H_2O_2 & ozonation/H_2O_2	The reaction time and initial H_2O_2 concentration for the more than 85% removal of BPA proved to be 2.0 min and 150 mg/L, respectively in the presence or absence of nitrate. In O_3/H_2O_2 process with nitrate addition, more than 75% of the BPA was removed with initial O_3 concentration of 7.5 mg/L and H_2O_2 concentration of more than 150 mg/L	**(Park et al., 2014)**
Photocatalysis/ TiO_2	The photocatalytic degradation of BPA with initial BPA concentration 175µM in water was totally degraded to carbon dioxide by TiO_2 under UV irradiation for 20 h. TiO_2 photocatalysis could be a useful technology for the purification of water containing BPA without generating ant serious secondary pollution.	**(Ohko et al., 2001)**
	BPA was successfully degraded by different TiO_2 photocatalyst pH 3 and 10. Platinization of TiO_2 photocatalyst (optimum loading between 0.2 and 1.0 wt%) was degraded 3-6 times faster than the bare TiO_2 photocatalyst. 20 ppm of BPA at pH 3 was completely mineralized into CO_2 after 120 min of UV illumination. However, only 20-30 % of the carbon from the BPA was found to be converted into CO_2 for the same illumination time at pH 10.	**(Chiang, Lim, Tsen, & Lee, 2004)**
	The optimization of solar photocatalytic degradation condition (catalyst dosage =500mg; initial subtract concentration =100 µg/ml; temperature = 30°C; pH = 6 & light intensity = 1.3 mW/cm^2) of BPA in water using TiO_2 were identified. All the carbon atoms of BPA were transformed to CO_2.	**(Kaneco et al., 2004)**

Table 2.2, continued

Type of AOP	Research Highlights & Findings	Reference
Fenton & Ultrasound (US)	The BPA sonochemical degradation, ultrasound action was compared to Fenton's reaction in the cases of deionised acidic water (pH 3) and natural water (pH 7.6, main ions concentration: Ca^{2+} = 486 mgL^{-1}, Na^{+} = 9.1 mgL^{-1}, Cl^{-} =10 mgL^{-1}, SO_4^{2-} =1187 mgL^{-1}, $HCO_3{}^{-}$ = 402 mgL^{-1}). Ultrasound was performed at 300 kHz and 80W. Fenton's process was operated using ferrous sulphate (100µmol L^{-1}) and continuous H_2O_2 addition at the rate as it is produced when sonication is applied in water in absence of substrate. This work evidences the efficiency of the Fenton process is totally inhibited, whereas ultrasonic process transforms BPA in biodegradable aliphatic acids that could be eliminated in a subsequent biological treatment.	**(R. Torres et al., 2007)**
US/UV/Iron	BPA degradation (118 µmol L^{-1}) using 300 kHz frequency, with a 80 W electrical power was eliminated by the ultrasound process (90 min). The difficulties in obtaining mineralization of micropollutants like BPA through ultrasonic action alone can be overcome by the Ultrasound/UV/Fe2+ combination and found to be most cost-effective one.	**(R. A. Torres et al., 2007)**
Ultrasonic	118 µmol L^{-1} of BPA solution with the best performance obtained at 300 kHz, 80 W, with oxygen as saturating gas. In these conditions, BPA can be readily eliminated by the ultrasound process (90 min).This study shows that BPA ultrasonic degradation in water occurs mainly through reactions with hydroxyl radicals. Reaction rates are strongly affected by ultrasonic frequency, gas saturation and applied ultrasonic power. The process transforms BPA into biodegradable aliphatic acids that could be treated in a subsequent biological treatment.	**(R. A. Torres, Pétrier, et al., 2008)**

Table 2.2, continued

Type of AOP	Research Highlights & Findings	Reference
	Degradation of bisphenol-A (BPA) by ultrasonic irradiation at 300 kHz was investigated at varying substrate concentrations, pH, hydroxyl radical scavengers and sparge gases. The sonochemical product yield for the decomposition of BPA was found to increase linearly with the input BPA concentration, as a consequence of the possibility of reaction sites other than the bulk liquid at more concentrated solutions. degree of rate inhibition was much larger in the presence of large concentrations of t-butanol than carbonate, showing the significance of interfacial reactions in the destruction pathway of BPA.	**(Gültekin & Ince, 2008)**

CHAPTER 3

MATERIALS AND METHOD

3.1 Materials

Bisphenol A (purity>99%), used as a target compound, was purchased from Sigma Aldrich Co. TiO_2 (P25) was obtained from Degussa Co. Reagent grade potassium biphthalate was purchased from BDH chemicals while potassium iodide (KI), ammonium molybdate ($H_8MoN_2O_4$), sodium hydroxide (NaOH), urea (CH_4N_2O), nitric acid (HNO_3) and hydrochloric acid (HCl) were purchased from R&M Chemicals. The chemicals used for the mobile phase of UPLC detection included HPLC-grade methanol and acetonitrile from Merck Group, as well as Mili-Q ultrapure water (18.2 MΩcm). All chemicals were analytical grade and used as received without any further purification.

3.2 Synthesis of graphitic carbon nitride (GCN)

A facile thermal heating method as reported by Liu et al. was adopted for synthesizing graphitic carbon nitride (Liu et al., 2011). 10 g of urea was dried in a covered crucible at 80 °C. After the overnight drying, the urea calcined at 550 °C for 3 h to complete the reaction. The yellow-coloured product was washed with nitric acid (0.1 M) and distilled water to remove any residual alkaline species such as ammonia adsorbed on the sample surface. Finally, the product was dried at 80 °C for 24 h to form GCN.

3.3 Characterization of GCN

The phase composition of the synthesized sonophotocatalytsts was characterized using X-ray powder diffractometer (XRD, D8 advance, Bruker) operated in the reflection mode with Cu Kα radiation (λ=0.154nm). A Fourier transform infrared (FTIR) spectrum was obtained on a Perkin Elmer Spectrum 400 IR spectrophotometer with scan range of 4000-450 cm^{-1}. Shimadzu UV-2600 spectrophotometer equipped with an integrating sphere attachment and barium sulphate ($BaSO_4$) as a reference was utilised for obtaining diffuse reflectance spectra of prepared samples.

3.4 BPA oxidation by commercial TiO_2 (P25)

This study focused on the degradation of BPA by sonocatalysis, photocatalysis and combined sonophotocatalysis process with the presence of commercial TiO_2 (P25) as a catalyst. In addition, sonolysis, photolysis, and sonophotolysis process were also carried out to compare the AOP applications on the degradation of BPA. The entire tests were run in a reactor which was set accordingly to identify the operational parameters. In this part, the UV light was used as the light source (photo process) which has been discussed as below.

3.4.1 Reactor set up

The schematic diagram of the sonophotocatalytic reactor is shown in Figure 3.1. The temperature in the solution was maintained using a temperature controller, water circulation chiller (HS-28A, 22-240V, 50Hz, HAILEA) and circulation pump (HX 6530, 50W, 200~240V, HAILEA). An over-head stirrer (RZR- 2102 control, Heidolph

Instrument) was used to control the mechanical stirring speed. Four ultraviolet (UV-C) lights (4 W each, Philips) were used as the UV light source which can place into the reactor. Customized double wall stainless steel tank (Φ 11 cm x 170 mm, total volume 1.5 L, effective volume 1 L) with mounting plates and circulation in/out fittings were used for the kinetic evaluation of the sonocatalytic or sonophotocatalytic removal of BPA. The designed stainless steel transducer module (Fulltech, Taiwan) was also coupled with an ultrasonic generator (Flexonic Mirae Ultrasonic Tech., model FX-4FREQ, Korea), of which the US power and US frequency can be adjustable.

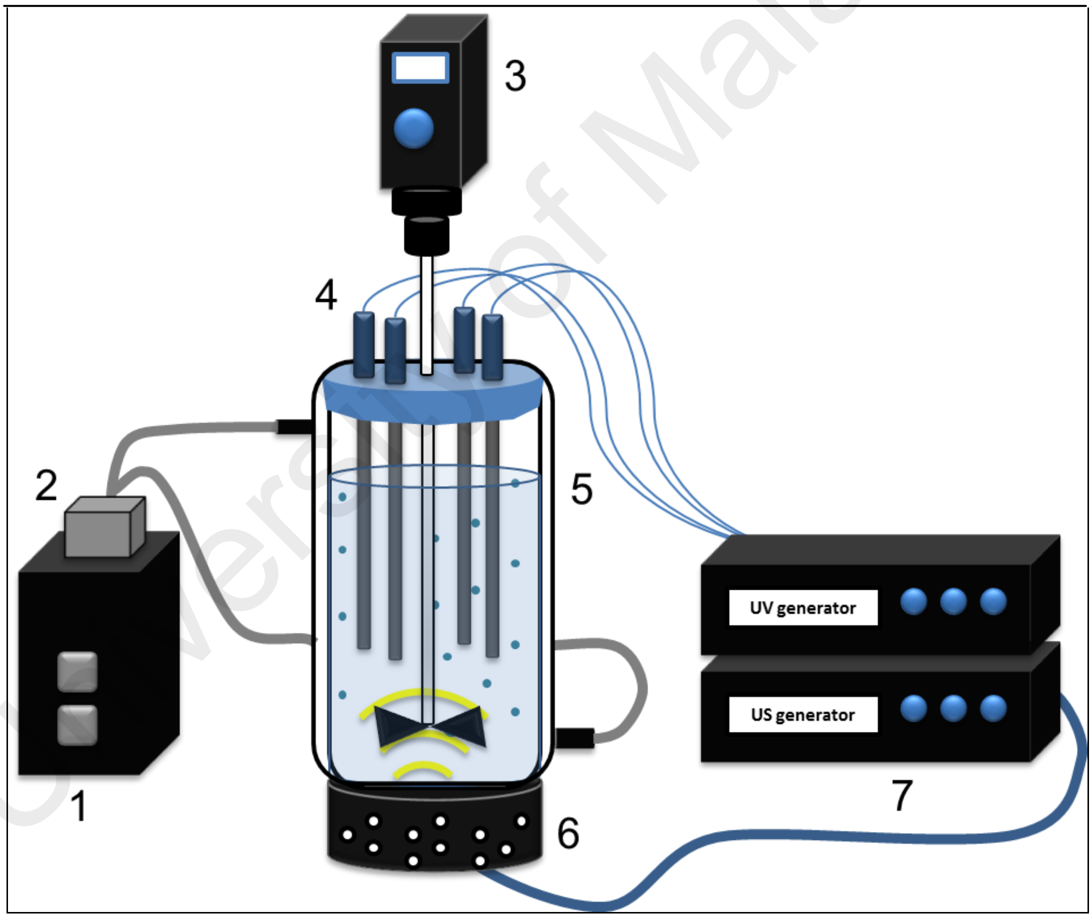

Figure 3.1: Schematic diagram of the sonophotocatalytic reactor: chiller/temperature control (*1*), pump (*2*), mechanical stirring (*3*), UV light (*4*), sonophoto reactor tank (*5*), ultrasound transducer (*6*), ultrasound generator (*7*)

3.4.2 Sonophotocatalysis by P25 (UV light)

The BPA stock solution (100 mg L^{-1}) was prepared by dissolving BPA in methanol followed by distilled water, in which the methanol concentration was 0.10 % (v/v). The solubility of BPA is higher than 30 mg/L and experienced slow dissolution. The addition of 0.10 % of methanol help, especially when added to a suspension of 100-200 ppm of BPA in water. Dissolving BPA in distilled water were not recommended because the tiny particles (non visible through eyes) are dispersed in aqueous medium and this will lead a problem for UPLC analysis. Then, BPA containing water (10 mg L^{-1}) was prepared by adding 100 mL of BPA stock solution into 1000 mL of deionized water. After adding 0.05 g of TiO_2 powder (P25) into 1000 mL BPA solution, the suspension was homogenously mixed using a stirrer at a constant speed in the dark for 1 h to establish an adsorption-desorption equilibrium. Except a series of batch tests conducted for finding out the effect of temperature and stirring speed, the temperature of the solution was set at 20 ± 1 ^{o}C by the temperature controller and stirring speed was fixed at 300 rpm. Table 3.1 shows the operational information of a series of batch tests, in which US frequency and power, temperature and mechanical stirring speed were parameters for sonocatalytic degradation of BPA.

The effect of the US frequency was investigated at 35, 100 and 170 kHz where 35 kHz was the minimum frequency and 170 kHz was the maximum frequency available on the sonication generator. . For these tests, the US power, temperature and mechanical mixing speeds were fixed at 50 W, 20 ^{o}C and 300 rpm, respectively. The effect of US power (20, 50 and 100 W) was also determined at fixed 35 kHz, 20 ^{o}C and 300 rpm. The effect of temperature on the BPA removal was also investigated at 10, 20 and 30 ± 1 ^{o}C. For these tests, the US frequency, US power and mechanical stirring speed were fixed at 35 kHz, 50W and 300 rpm, respectively. The effect of mechanical stirring (0, 100, 200, 300 rpm) on the BPA removal was determined at 35 kHz, 50W and 20 ± 1°C. All the values (US power, temperature and stirring speed) were selected within the range of other studies and references in order to compare with recent study. The maximum measurement of US power and temperature available in the reactor was 100 W and 30 °C respectively. At irradiation time intervals of every 0.5 h, the samples were collected from the mixture and filtered through a 0.22 μm nylon filter before UPLC analysis. Under the optimized condition, comparisons with other oxidation processes (US, UV, US/UV) were also conducted. This process involved without catalyst (TiO_2) to investigate the role of AOP application. After the entire batch test carried out, the LC/MS test was conducted for sonophotocatalysis process to identify intermediate formation.

Table 3.1: Operational Condition for a Series of Batch Tests of BPA oxidation by P25

Series no.	**Catalytic process**	**US frequency (kHz)**	**US power (W)**	**Temperature (°C)**	**Mixing speed (rpm)**	**UV light (W)**	**TiO_2 (g)**
1	Sonocatalysis	35, 100 and 170	50	20 ± 1	300	-	0.05
2	Sonocatalysis	35	20, 50 and 100	20 ± 1	300	-	0.05
3	Sonocatalysis	35	50	10, 20 and 30± 1	300	-	0.05
4	Sonocatalysis	35	50	20 ± 1	0, 100, 200 and 300	-	0.05
5	Photocatalysis	-	-	20 ± 1	300	16	0.05
6	Sonolysis	35	50	20 ± 1	300	-	-
7	Photolysis	-	-	20 ± 1	300	16	-
8	Sono-photocatalysis	35	50	20 ± 1	300	16	0.05

3.5 BPA oxidation by Graphitic Carbon Nitride (GCN)

The research was extended to the study of the degradation of BPA using synthesized reusable sonophotocatalyst, Graphiric Carbon Nitride (GCN) by sonocatalysis, photocatalysis and combined sonophotocatalysis process after the optimum parameters were identified. Comparisons with different type of AOP (sonolysis, photolysis and sonophotolysis) were applied using a reactor which was set accordingly to investigate the BPA oxidation process. This study was focused on the visible light as the light source for the photo process which has been discussed as below.

3.5.1 Reactor set up

The schematic diagram of the sonophotocatalytic reactor is shown in Figure 3.2. The temperature in the solution was maintained with a temperature controller, water circulation chiller (HS-28A, 22-240V, 50Hz, HAILEA) and circulation pump (HX 6530, 50W, 200~240V, HAILEA). An over-head stirrer (RZR- 2102 control, Heidolph Instrument) was used to control the mechanical stirring speed. A tungsten-halogen lamps (500 W) was used as the visible light source which place on the top of the reactor. Customized double wall stainless steel tank (Φ 11 cm x 170 mm, total volume 1.5 L, effective volume 1 L) with mounting plates and circulation in/out fittings were used for the kinetic evaluation of the sonocatalytic or sonophotocatalytic removal of BPA. The designed stainless steel transducer module (Fulltech, Taiwan) was also coupled with an ultrasonic generator (Flexonic Mirae Ultrasonic Tech., model FX- 4FREQ, Korea), of which the US power and US frequency can be adjustable.

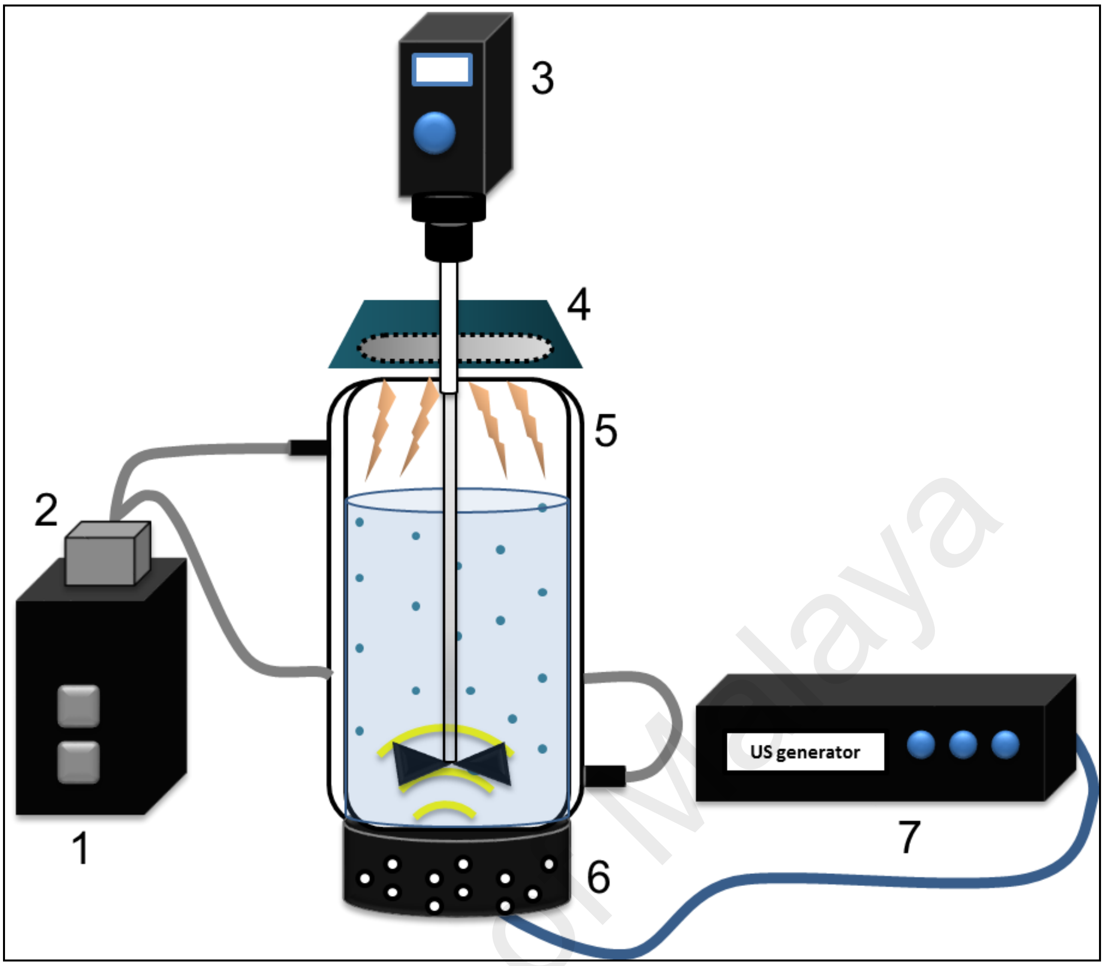

Figure 3.2: Schematic diagram of the sonophotocatalytic reactor: chiller/temperature control (*1*), pump (*2*), mechanical stirring (*3*), visible light (*4*), sonophoto reactor tank (*5*), ultrasound transducer (*6*), ultrasound generator (*7*)

3.5.2 Sonophotocatalysis by GCN (visible light)

1000 mL of BPA solution (10 mg L^{-1}) was employed for the experiment in the reactor containing sono/photo catalyst (dosage, 0.05 g L^{-1}) under the optimum conditions (US frequency - 35 kHz; US power - 50 W; stirring speed - 300 rpm and temperature - 20 °C). Prior to sonophotodegradation, the BPA solution was stirred in the dark for 1 h to establish an adsorption-desorption equilibrium. A 500 W tungsten-halogen lamps was used as a visible light source, any UV light below 400 nm was removed with a high-pass filter (FSQ-GC400, Newport Corp.). Different amounts of catalyst (0.01, 0.05. 0.1, 0.2 and 0.3 g L^{-1}) were tested to identify the optimum dosage of

GCN on BPA removal. Experiments under different pH (2, 4, 6, 7, 8 and 10) were also carried out to reveal the role of pH on the sonophotocatalytic activity of GCN. All pH values were adjusted using 0.1 M of NaOH and 0.1 M of HCl. The values of catalyst dosage and pH were selected following the references of other studies. At irradiation time intervals of every 0.5 h, the samples were collected from the mixture and filtered through a 0.22 µm nylon filter before UPLC analysis. After the catalyst dosage and pH were optimized, comparisons with other oxidation processes (US, Vis-L, US/Vis-L & US/Vis-L/P25) were also conducted. After the entire batch test carried out (Figure 3.2), the LC/MS test was conducted for sonophotocatalysis process (US/Vis-L/GCN) under optimum condition to identify intermediate formation.

Table 3.2: Operational condition for a series of batch tests of BPA oxidation by GCN

Series no.	**AOPs**	**Operational parameter (US frequency and power, temperature and mixing speed)**	**pH**	**Catalyst (gL^{-1})**	**Visible light (Vis-L, W)**
1	Sonocatalysis	35 kHz, 50 W, 20°C and 300 rpm	2,4,6,7,8, 10	0.05(GCN)	-
2	Sonocatalysis	35 kHz, 50 W, 20°C and 300 rpm	7	0.01, 0.05, 0.1, 0.2 and 0.3 (GCN)	-
3	Photocatalysis	20°C and 300 rpm	7	0.05 (GCN)	500
4	Sonolysis	35 kHz, 50 W, 20°C and 300 rpm	7	-	-
5	Photolysis	20°C and 300 rpm	7	-	500
6	Sono photocatalysis	35 kHz, 50 W, 20°C and 300 rpm	7	0.05 (GCN)	500
7	Sono photocatalysis	35 kHz, 50 W, 20°C and 300 rpm	7	0.05 (P25)	500

3.6 Reusability Test of GCN

After the tests completed, the synthesized sonophotocatalyst, GCN was recollected to identify the capability of the catalyst reuse. Following the sonophotocatalysis process for BPA removal, GCN was recollected by centrifuging the suspension after the test. Then, the separated GCN was washed at least three times with distilled water and subsequently dried overnight at room temperature. The dried GCN was weighted and reused for the subsequent sonophotocatalytic BPA removal under the same conditions (35 kHz, 50 W, 20°C, 300 rpm and pH 7): 1000 mL of BPA solution (10 mg L^{-1}) and reclaimed GCN (0.05 g L^{-1}). With five cycles of GCN reusability, the sonophotocatalytic oxidation efficiencies of BPA were investigated.

3.7 Analyses

Quantitative analysis of BPA was conducted by ultra performance liquid chromatography (UPLC, ACQUITYUPLC H Class, Waters) equipped with C18 column (50 mm × 2.1 mm × 1.7 µm). The mobile phase, acetonitrile (ACN) and water in a ratio of 60:40, was run in an isocratic mode with a flow rate of 0.30 mL min^{-1}, while column and sample temperatures were fixed at 40 and $10^{o}C$, respectively.

A high performance liquid chromatography- mass sprectrometry (HPLC-MS, Agilent Technologies) equipped with C18 column (2.1 mm × 100 mm × 1.8 µm) were applied to analyse the intermediates for the sonophotocatalytic oxidation of BPA. The mobile phase composition at a flow rate of 0.20 ml min^{-1} was first started with ACN/water 30/70 (v/v), increased linearly to 90/10 (v/v) in 8 min, kept for 2 min, and finally decreased to 30/70 (v/v) in 1 min and kept for another 2 min. To identify the intermediates, HPLC-MS in negative ion mode were applied with a scan range m/z 100-400.

Hydrogen peroxide (H_2O_2) concentration was determined using the KI method (Kormann, Bahnemann, & Hoffmann, 1988). The 2.0 mL of sample was mixed in a quartz cuvette containing 0.75 mL potassium biphthalate (0.10 M) and 0.75 mL of solution containing potassium iodide (0.4 M), sodium hydroxide (0.06 M), and ammonium molybdate (10^{-4} M). The mixed solutions were allowed to stand for 2 min before the absorbance was measured. All absorbance were measured using UV/vis spectrophotometer (Pharo 300, Merck).

CHAPTER 4

RESULTS AND DISCUSSION

4.1 Characterization of GCN

The X-ray diffraction (XRD) analysis was conducted to determine the phase composition of GCN (Figure 4.1). The XRD pattern signifies the interlayer stacking phase of GCN since it has binary peaks at 13.1^o and 27.4^o (Zhong et al., 2014), which can be indexed as (100) and (002) [JCPDS #87-1526], respectively. The strong XRD peak at 27.4^o was corresponding to aromatic interlayer stacking peak with a distance of 0.326 nm, which is consistent with the reported GCN (Chang et al., 2013). The weak peak (13.1^o) is due to an intralayer structural packing motif, which corresponds to a distance d = 0.675 nm (Liu et al., 2011).

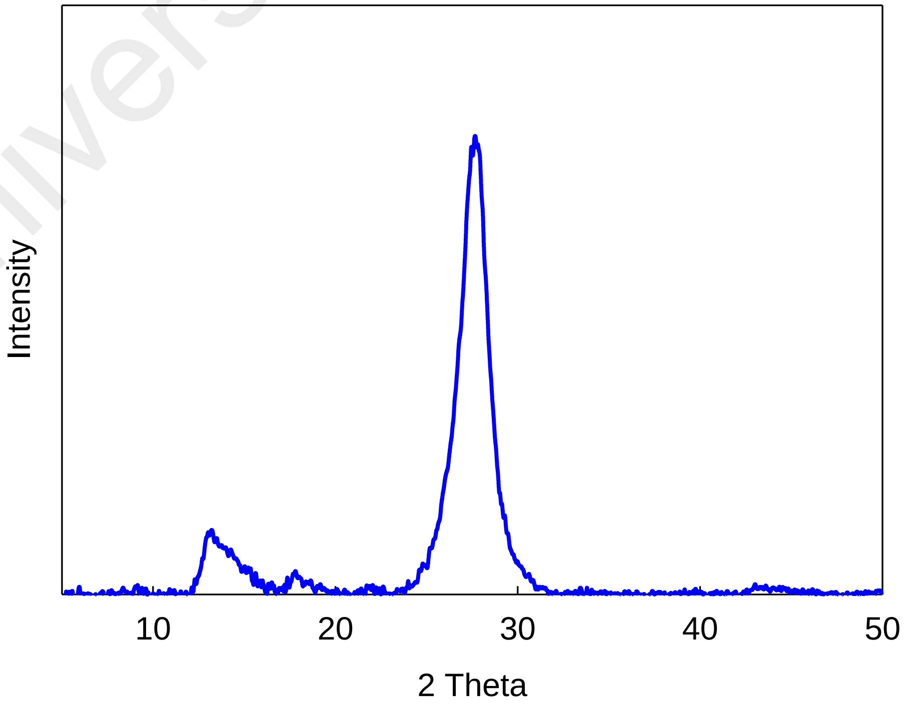

Figure 4.1: XRD pattern of graphitic carbon nitride (GCN)

The functional group analysis for GCN was conducted by Fourier Transform Infrared Spectroscopy (FTIR) (Figure 4.2). The intense bands at 1641, 1570, and 1410 cm^{-1} were assigned to the aromatic C-N stretching vibration, proving the successful synthesis of GCN. The sharp band at 807 cm^{-1} is attributed to the out-of-plane bending vibration characteristics of triazine molecules. The bands at 1320 and 1240 cm^{-1} corresponded the stretching vibration of C-N (-C)-C or C-NH-C. The broad band at 3100 – 3300 cm^{-1} can be assigned to the stretching modes of secondary and primary amines and their intermolecular hydrogen-bonding interactions. The stretching vibration of O-H is also contributed to the broad absorption in this region (Ji, Chang, Hu, Qin, & Shen, 2013). An additional broad band at 3350 cm^{-1} characterizes the O-H group of water molecule.

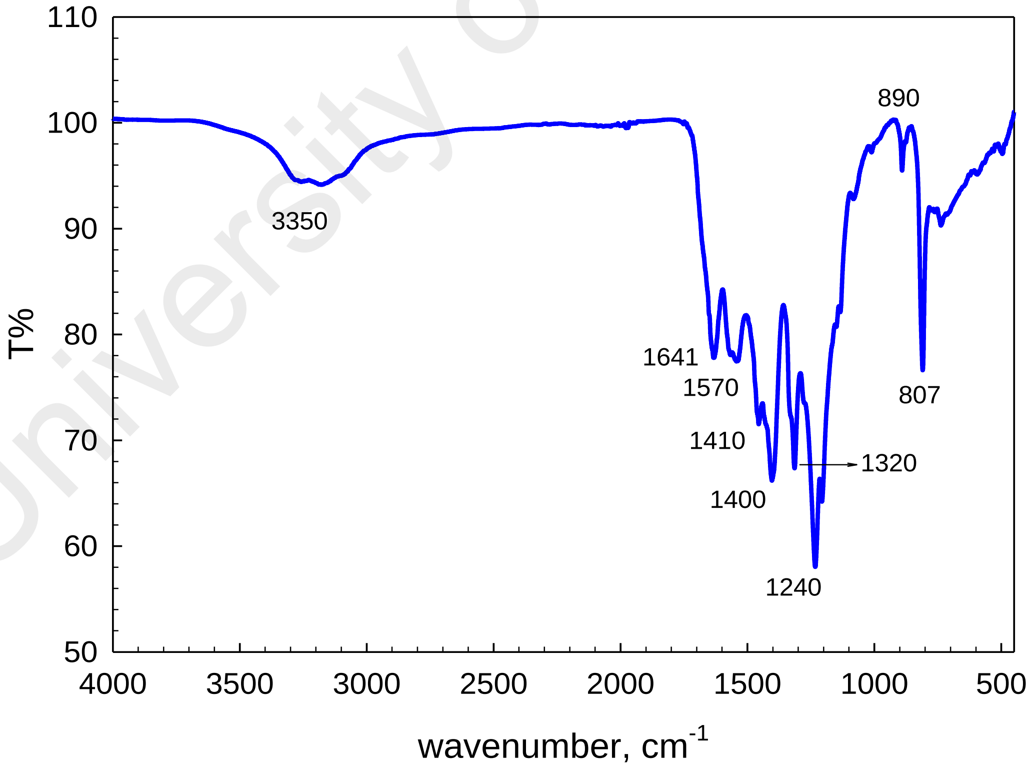

Figure 4.2: FTIR spectra of graphitic carbon nitride (GCN)

Figure 4.3 shows the optical absorbance spectra of GCN and TiO_2 (commercial name P25) obtained by UV-vis. The GCN demonstrated a Vis-L spectrum of absorbance band in the range of 350 to 400 nm while P25 had an ultraviolet (UV) absorbance band in 200~350 nm. Band gap energies of GCN and P25 were calculated via reflectance data using Tauc plot. Then plotting $(F(R)hv)^{1/2}$ against h_v, where Kubelka-Munk function F(R) is derived from equation as below:

$$F = \frac{(1-R^2)}{2R} \tag{4.1}$$

where R is absolute reflectance of the layer, and h_v is the photon energy. The band gap energies were determined by extrapolating the maximum slope of the curve to the photon energy axis. The obtained plot along with the calculated band gap energy is shown in the inset of Figure 4.3. The estimated approximate band gap energies of GCN and P25 were 2.7 eV and 3.2 eV, respectively.

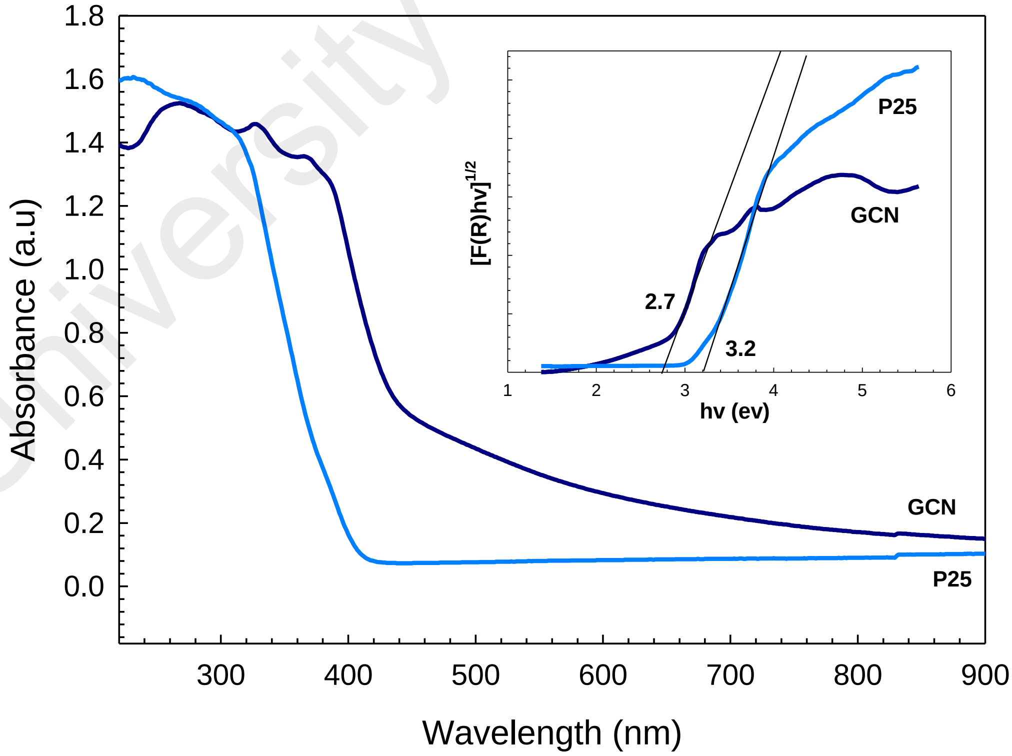

Figure 4.3: Absorbance and band gap energies of graphitic carbon nitride (GCN) and TiO_2 (P25)

4.2 BPA oxidation process by P25 (UV light)

Prior to oxidation, the adsorption behaviours of BPA by P25 were investigated in the dark for 1 h. As a result, about 15% of BPA (10 mg L^{-1} initial concentration) was removed by 0.05 g/L of P25. The adsorption equilibrated time and capacity of BPA by P25 were 30 min and 30.5 mg g^{-1}, respectively. The adsorption capacity was identified using the following equation:

$$q = \frac{\left[\left(C_0 - C_{eq} \right) \times V \right]}{m} \tag{4.2}$$

Where, q is the amount of adsorbate adsorbed (adsorption capacity) in mg, C_0 is initial concentration, C_{eq} is concentration after equilibrium, V is volume in L and m is mass of the sorbent in g. After the adsorption was equilibrated, the sonocatalysis was performed to degrade BPA with various operational conditions, which discussed further in this study.

4.2.1 Effect of frequency

In this study, the sonocatalytic oxidation of BPA was conducted with various frequencies ranging from 35 to 170 kHz under the fixed condition, in which US power, temperature and mechanical stirring speed were 50 W, 20 ± 1^{o}C and 300 rpm, respectively (Figure 4.4 A). The removal rates during the sonocatalysis were obtained using pseudo first-order kinetic model (Figure 4.4 B). Kinetic modelling not only allows estimation of degradation rates but also leads to suitable rate expressions characteristic of possible reaction mechanisms (Kuo, Wu, & Lin, 2010; Robati, 2013). The pseudo first-order kinetic equation is given as below (Azizian, 2004):

$$\frac{dC}{dt} = -kC \tag{4.3}$$

Where, C is the concentration of BPA, t is time, and k is the kinetic constant. The BPA removal percentages were 65%, 42% and 40% at the frequency 35, 100 and 170 kHz, respectively, for 2 h. The percentage of BPA removal was identified using the following equation:

$$\frac{C_0 - C_{eq}}{C_0} \times 100 \tag{4.4}$$

Where C_0 is the initial concentration of BPA and C_{eq} is the concentration of BPA after equilibrium. Thus, the highest rate constant of frequency was obtained at 35 kHz (7.6×10^{-3} min $^{-1}$). Determination coefficients, R^2 for first order kinetic model of US frequency were stated in table 4.1.

The US frequency is a critical parameter in sonocatalytic action. It can affect cavitation through modifying bubble number, bubble size, cavitation threshold, and temperatures during the collapse (Didenko, Nastich, Pugach, Polovinka, & Kvochka, 1994). It has two counteracting effects on the generation of hydroxyl radicals (·OH). As the frequency decreases, the size of the cavitation bubbles increases, however, the transfer of ·OH produced during the burst of cavitation into external organic matter reduces due to the decreases of temperature and pressure (Goel et al., 2004). As the frequency increases, the pulsation and collapse of the bubble occur more rapidly causing more radicals to escape from bubble. The mass transfer of ·OH also can be the highest when the frequency increases to the critical condition that maximizes the temperature and pressure of bubbles because of the optimum size cavitation (Capocelli et al., 2012). Cavitation at low frequency is highly effective to decompose organic molecules inside the bubble (Pétrier & Francony, 1997). However, the temperature and pressure can decrease at above the critical point of frequency as bubbles become smaller. Therefore, ultrasonic oxidation of organic matters can be significantly enhanced at the optimum frequency condition (J.-W. Kang, Hung, Lin, & Hoffmann, 1999).

Table 4.1: Determination coefficients, R^2 for first order kinetic model of US frequency

Experiment	**Test**	**Pseudo First Order**	
		K_1	**R^2**
US frequency (kHz)	30	0.007	0.981
	100	0.003	0.917
	170	0.002	0.790

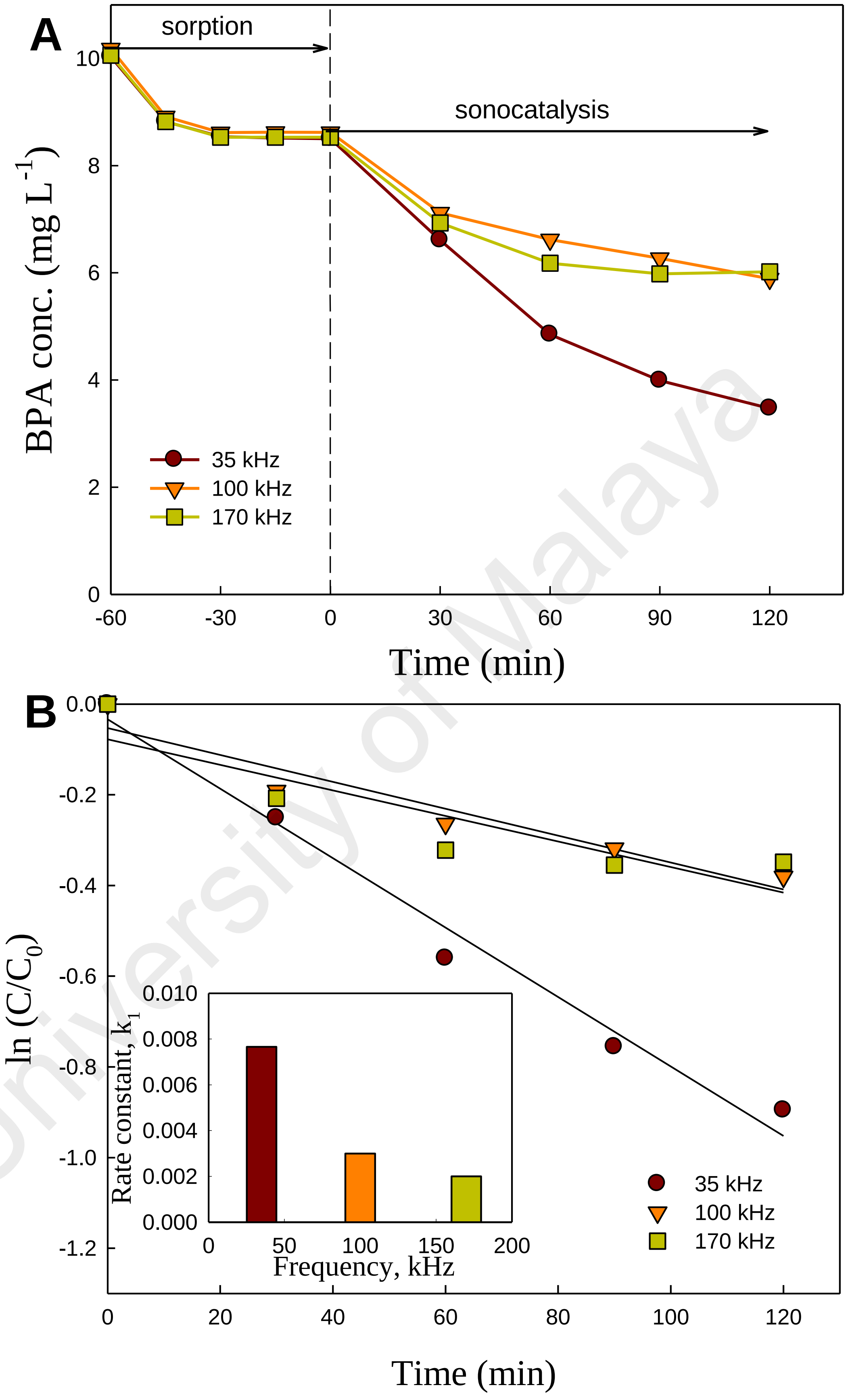

Figure 4.4: (A) Effect of ultrasound frequency on BPA degradation; US power = 50 W; stirring = 300 rpm; temperature = 20 ^{o}C, (B) pseudo-first-order kinetic model of ultrasound frequency effect on BPA degradation

4.2.2 Effect of power

By keeping the US frequency (35 kHz), temperature (20 ^{o}C), and stirring speed (300 rpm) constant, sonocatalytic removal of BPA were carried out at power intensities of 20W, 50W, and 100W. Figure 4.5 A shows the decrease of BPA concentration under three different power intensities. The rate constants of BPA removal were 2.8×10^{-3}, 7.6×10^{-3} and 3.2×10^{-3} min^{-1} at 20, 50, and 100 W of US power, respectively (Table 4.2). Figure 4.5 B shows the linear relation between ln (C_t/C_o) and time at different US powers obtained by pseudo first-order kinetics. The highest rate constant was obtained at 50 W US power. Guo et al. specified that the rate constant for 2,4-dinitrophenol degradation increased exponentially with the increase of US power intensity (Z. Guo, Zheng, Zheng, Hu, & Feng, 2005).

According to Gutierrez et.al (Gutierrez & Henglein, 1990), an increase in the acoustic power can be expected to increase the number of active cavitation bubbles and also the size of the individual bubbles. When higher acoustic power applied, the bubbles are exposed to greater negative pressures during the rarefaction cycle of ultrasound wave and also greater positive pressures in the subsequent compression cycle.

A cavitation bubble possesses its maximum potential energy at its maximum size. During bubbles collapse, this potential energy is partly converted into chemical reactions (formation of radicals and ions) and partly into heat, light and sound emission (Kanthale, Ashokkumar, & Grieser, 2008). The beneficial effect of US power could be attributed to the increased cavitation effect. However, too high US power can make cavitation bubbles grow largely in negative pressure-phase of ultrasonic wave, which results in inadequate collapse of cavitation bubbles. As a result, this led to a slower rate for BPA degradation (Z. Guo & Feng, 2009). Accordingly, in this study, the rate constant of BPA removal was decrease when 100W power applied.

Table 4.2: Determination coefficients, R^2 for first order kinetic model of US power

Experiment	**Test**	**Pseudo First Order**	
		K_1	**R^2**
US power (W)	20	0.002	0.951
	50	0.007	0.981
	100	0.003	0.970

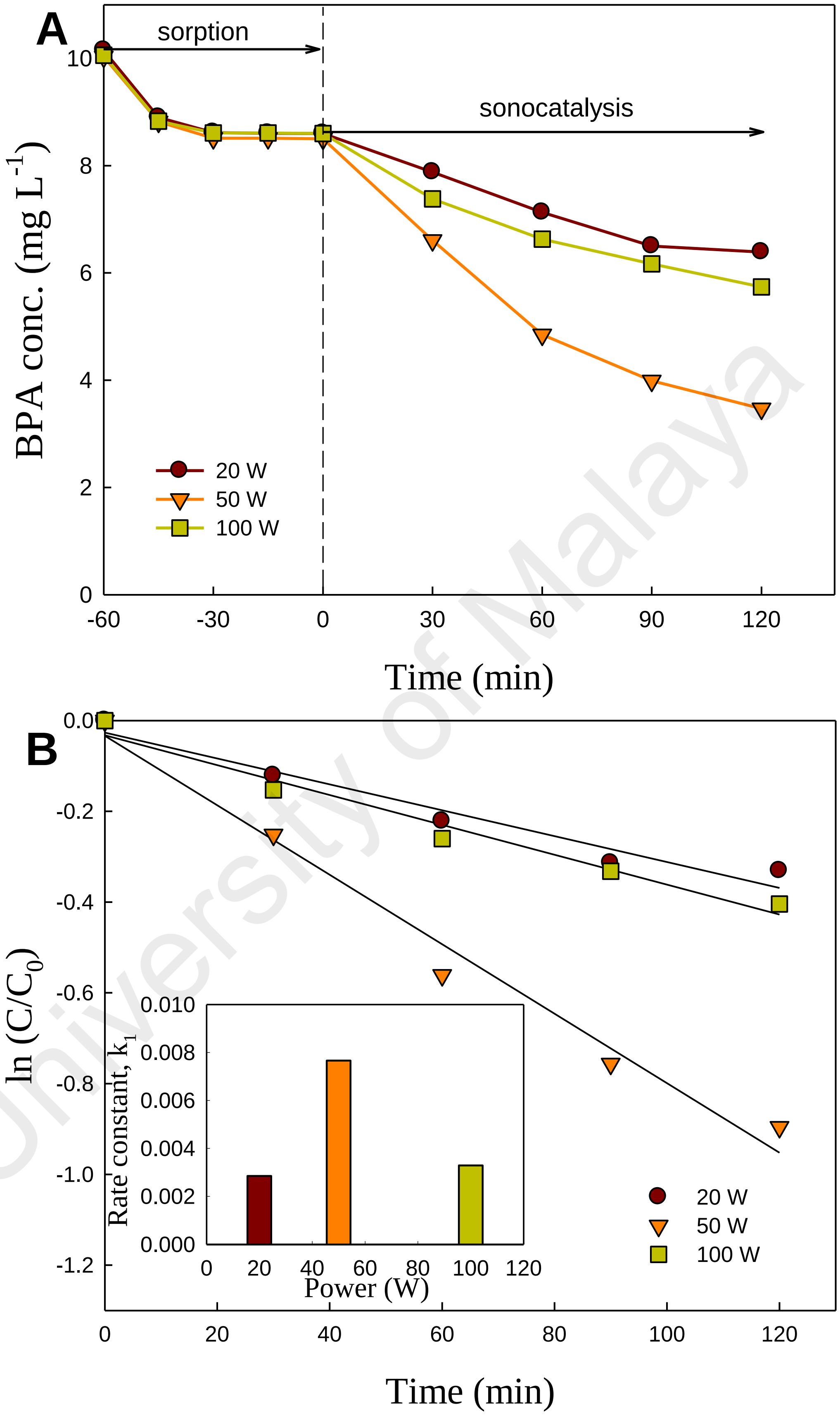

Figure 4.5: (A) Effect of ultrasound power on BPA degradation; US frequency = 35 kHz; stirring = 300 rpm; temperature = 20 ^{o}C, (B) pseudo-first-order kinetic model of ultrasound power effect on BPA degradation

4.2.3 Effect of mechanical stirring speed

To determine the effect of mechanical stirring speed (0, 100, 200, and 300 rpm), batch tests of BPA sonocatalytic removal were carried out at fixed US frequency, US power and temperature (35 kHz, 50W, and 20^{o}C), respectively (Figure 4.6). The highest rate constant (7.6×10^{-3} min^{-1}) was obtained at 300 rpm of stirring speed. The rate constants of BPA removal at 0, 100, and 200 rpm were 3.1×10^{-3}, 2.4×10^{-3}, and 2.1×10^{-3}min^{-1}, respectively (Table 4.3). Thus, oxidative rates were not linearly increased with an increase of the mechanical stirring speed. As it was observed, the BPA solution with the TiO_2 catalyst shows heterogeneous dispersion under the 100 and 200 rpm stirring speed. The rate constant without stirring was higher than those under 100 or 200 rpm stirring speed due to the homogeneous condition.

At the same time, the frequency effect is also related to the mechanical mixing in the degradation of BPA. When the mechanical stirring was applied in the experiment, the US frequency effect was opposite to the kinetic constants of BPA removal, even could be more complicated when a sonocatalyst is applied because the extent of homogeneous dispersion of the catalyst could be varied by microjets, microstrimming, and shock waves (K. Kang et al., 2015). According to Kang et. al, for the sonocatalysis of ibuprofen (IBP) removal without mixing showed the higher rate constant at higher frequency (500 kHz), but when the mechanical mixing applied, the lower frequency (35 kHz) obtained the higher rate constant of IBP removal.

The US frequency and mechanical stirring speed can have noteworthy effects on the speed of sonocatalytic removal of BPA. Apparently, these operational parameters are closely related to the diameter of the cavitation bubbles. The diameter of cavitation bubbles deceases as the frequency increases (Brotchie, Grieser, & Ashokkumar, 2009). In theory, larger bubbles created at low frequency can split into smaller bubbles when mechanical stirring applied. Accordingly, the number of bubbles and ·OH production increases. Meanwhile, the fine bubbles produced at higher frequency can potentially combine into larger bubbles with a mechanical stirring, rather than splitting to smaller bubbles and decreases the number of bubbles and ·OH, consequentially decelerating the reaction rate (Hanselmann & Windhab, 1998). This mechanism causes the highest rate constant of BPA removal at lower frequency (35 kHz) with mechanical stirring. The mechanical stirring is also important for the catalyst to be homogeneously dispersed in the BPA solution under the lower frequency (35 kHz).

Table 4.3: Determination coefficients, R^2 for first order kinetic model of stirring speed

Experiment	**Test**	**Pseudo First Order**	
		K_1	**R^2**
Stirring speed (rpm)	0	0.003	0.960
	100	0.002	0.975
	200	0.002	0.861
	300	0.007	0.981

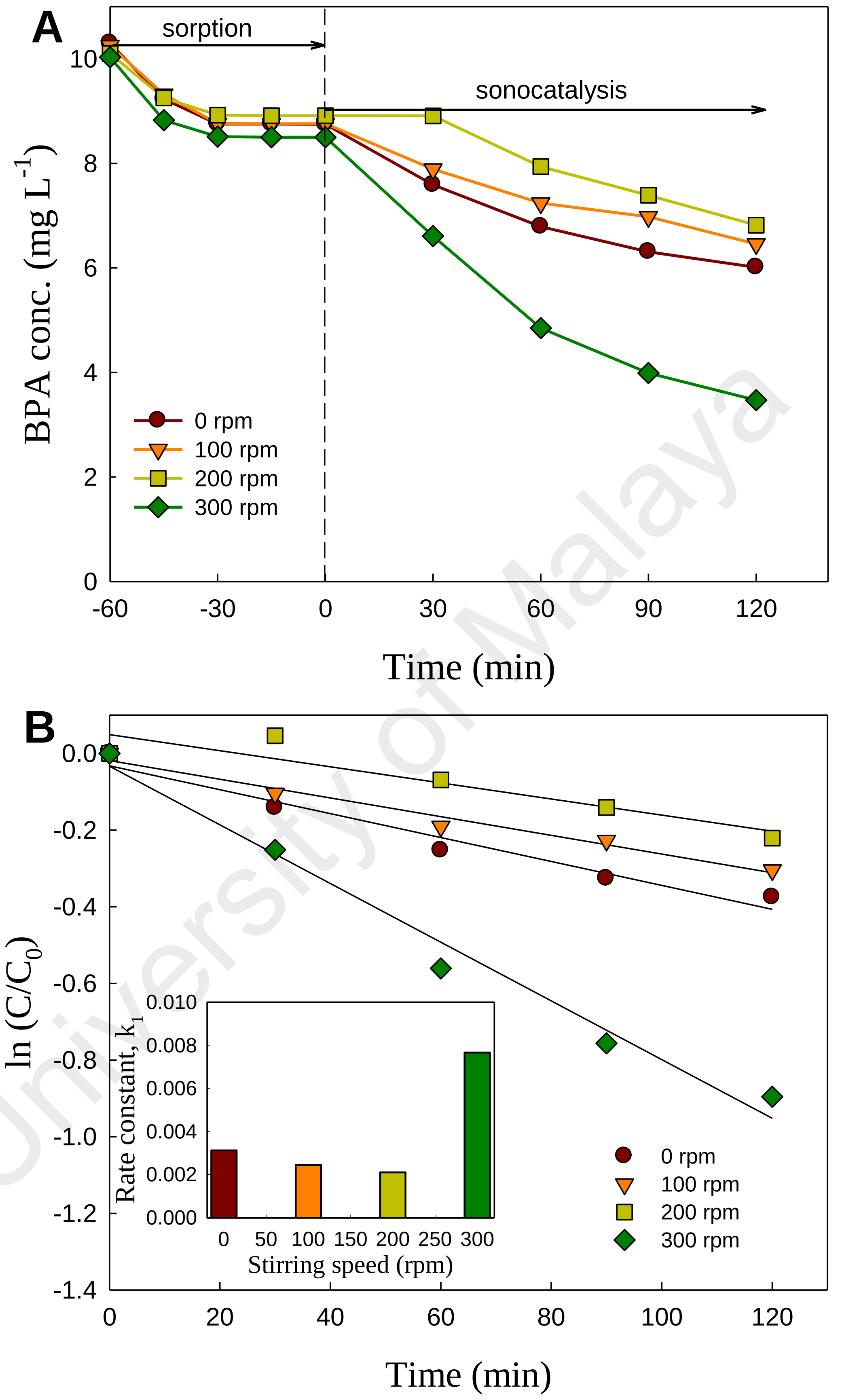

Figure 4.6: (A) Effect of mechanical stirring on BPA degradation; US frequency = 35 kHz; US power = 50 W; temperature = 20 °C, (B) pseudo-first-order kinetic model of mechanical stirring effect on BPA degradation

4.2.4 Effect of temperature

Along with US power, temperature is an important parameter in sonocatalysis because it could affect not only the activation energy but also the pollutant behaviour (K. Kang et al., 2015). In an ultrasonic reactor, the temperature increases rapidly with sonication if it is not controlled. In this study, kinetic tests of sonocatalytic BPA removal were conducted at various temperatures (10, 20, and 30 ±1 ^{o}C) with the fixed US frequency (35 kHz), US power (50 W) and mechanical stirring speed (300 rpm) (Figure 4.7). As a result, the rate constant of BPA removal at temperature 10, 20, and 30 ±1 ^{o}C were 2.5×10^{-3}, 7.6×10^{-3}, and 4.0×10^{-3} min^{-1}, respectively (Table 4.4), representing the highest rate constant was obtained at 20 ^{o}C.

An increase in temperature can increase the quantity of cavitation bubbles and results in the increase of degradation rate. At the same time, an increase in the temperature increases the water vapour in the bubbles and decreases the dissolved gases in the medium. Consequently, the collapse of the vaporous bubble is less effective due to the high temperature (Entezari & Kruus, 1996). However, this water vapour reduces the temperature and pressure generated when cavitation bubbles collapse and hence reduces the degradation efficiency on organic compounds (Tang et al., 2012). As the results, the rate constant of BPA oxidation at 20 ^{o}C is higher than at 30^{o}C. Wang et al. (J. Wang et al., 2009) reported that ultrasonic cavitation is weakened because of rapid gas volatilization from aqueous solution at high temperature.

Table 4.4: Determination coefficients, R^2 for first order kinetic model of temperature

Experiment	**Test**	**Pseudo First Order**	
		K_1	**R^2**
Temperature (°C)	10	0.002	0.859
	20	0.007	0.981
	30	0.004	0.979

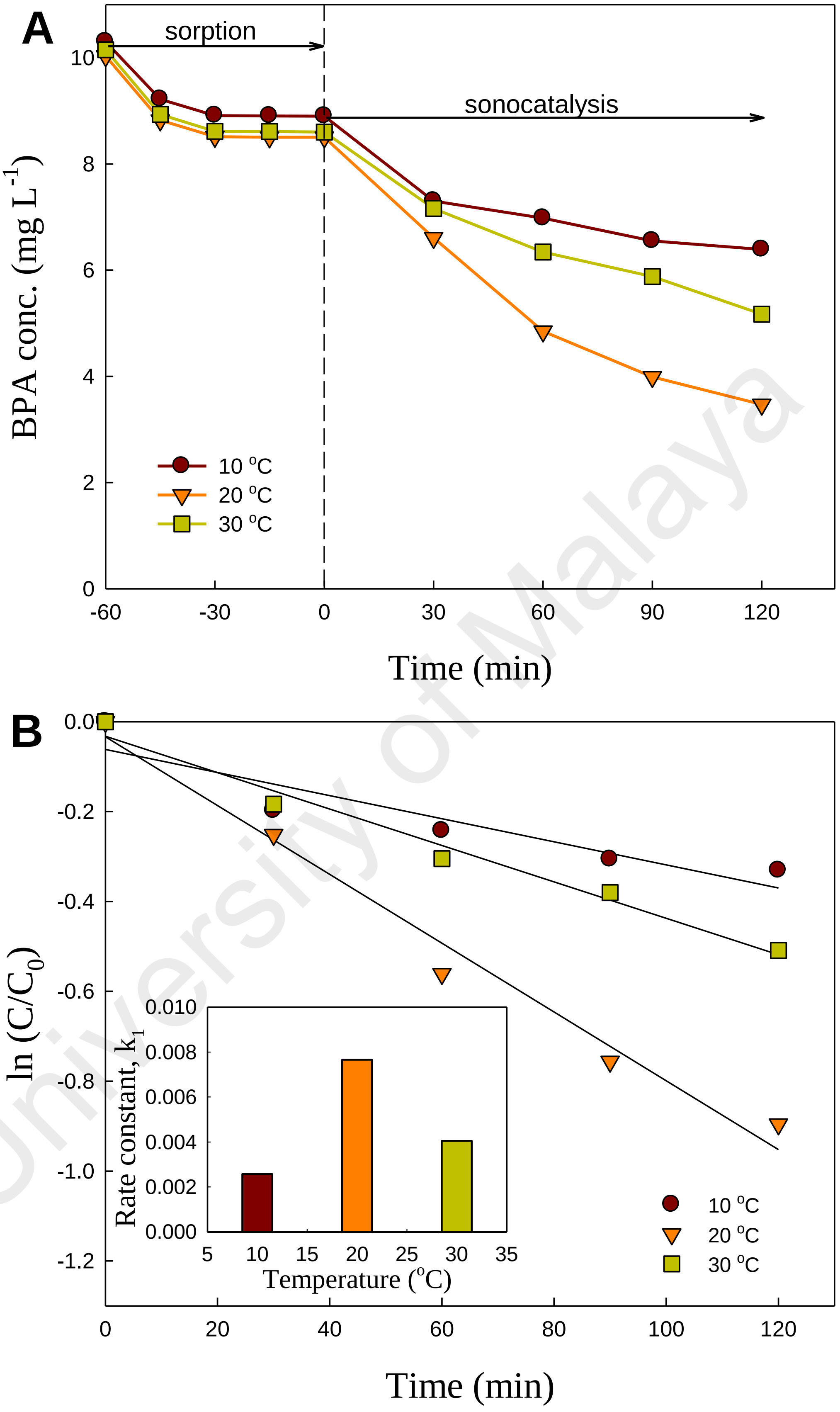

Figure 4.7: (A) Effect of temperature on BPA degradation; US frequency = 35 kHz; US power = 50 W; stirring = 300 rpm, (B) pseudo-first-order kinetic model of temperature effect on BPA degradation

4.3 BPA oxidation process by GCN (visible light)

This study focused on sonophotocatalytic degradation of BPA based on visible light irradiation by synthesized GCN. The kinetics of BPA removal by use of different types of AOPs (US and visible light) was applied. Furthermore, the main intermediates of BPA degradation were identified using a high performance liquid chromatography-mass spectrometry (HPLC/MS).

4.3.1 Effect of pH

Figure 4.8 displayed the pH effect on the degradation efficiency of BPA in the range 2-10. In this test, the adsorption behaviour of BPA by GCN was investigated for 1 h in dark condition. About 3.5 % of BPA was removed by 0.05 g L^{-1} of GCN with an adsorption capacity of 7.4 mg g^{-1}. After the dark reaction, the sonocatalytic degradation of BPA was carried out for 120 min. As shown in Figure 4.8 A, BPA was degraded rapidly at pH 2. For 2 h of degradation, more than 60% of BPA was degraded in most pH conditions, except pH 10. The degradation result at pH between 4 and 8 did not give significant change for BPA removal. The data was fitted by use of first order kinetic model Table 4.5 to obtain the kinetic constants (Figure 4.8 B) and the inset of Figure 4.8 B shows the k_1 vs pH. The result shows that k_1 was the highest at pH 2 (10.0×10^{-3} min^{-1}) while at pH 4 ~ 8 had almost similar kinetic constants (~9×10^{-3} min^{-1}). However, it was drastically reduced at pH 10 ($k_1 = 6.0 \times 10^{-3}$ min^{-1}).

Since BPA has two OH group (2 pK_a), the initial deprotonation occurs at pH 8 and second happens at pH 9.6 (Bautista-Toledo, Ferro-Garcia, Rivera-Utrilla, Moreno-Castilla, & Vegas Fernández, 2005). Thus, when pH above the pK_a value, hydrophobic interaction between GCN and BPA decreased and leads to electrostatic repulsion. The ionic form of BPA, Bis-phenolate anions, has higher tendency to stay in bulk aqueous phase instead of being near by the negatively charged cavitation microbubbles. As implosion occurred within the interface of microbubble and liquid produces the highest amount of ·OH, the electrostatic repulsion causes an increase of distance between BPA and ·OH, which would allow higher probability for ·OH to recombine as H_2O_2 instead of being used for BPA removal (Gültekin & Ince, 2008). More deprotonation of BPA at above pH 9.6 would further increase the effect of electrostatic repulsion. Hence, at pH 2, 4, 6 and 8, the compound exists mainly in molecular form, whereas at pH 10 it is completely ionic thus is less likely to approach the negatively charged cavity bubbles. As a consequence, the faster degradation of BPA at pH 2 than that at pH 4-8 and 10 is due to the more likely diffusion of the molecule at lower pH to the bubble-liquid interface, where the concentration of hydroxyl radicals is a maximum. Consequently, pH 7 was selected for the optimal experimental condition, because of the unnecessary of chemical treatment.

Table 4.5: Determination coefficients, R^2 for first order kinetic model of pH

Experiment	**Test**	**Pseudo First Order**	
		K_1	**R^2**
pH	2	0.010	0.970
	4	0.009	0.994
	6	0.009	0.993
	7	0.009	0.989
	8	0.009	0.954
	10	0.006	0.943

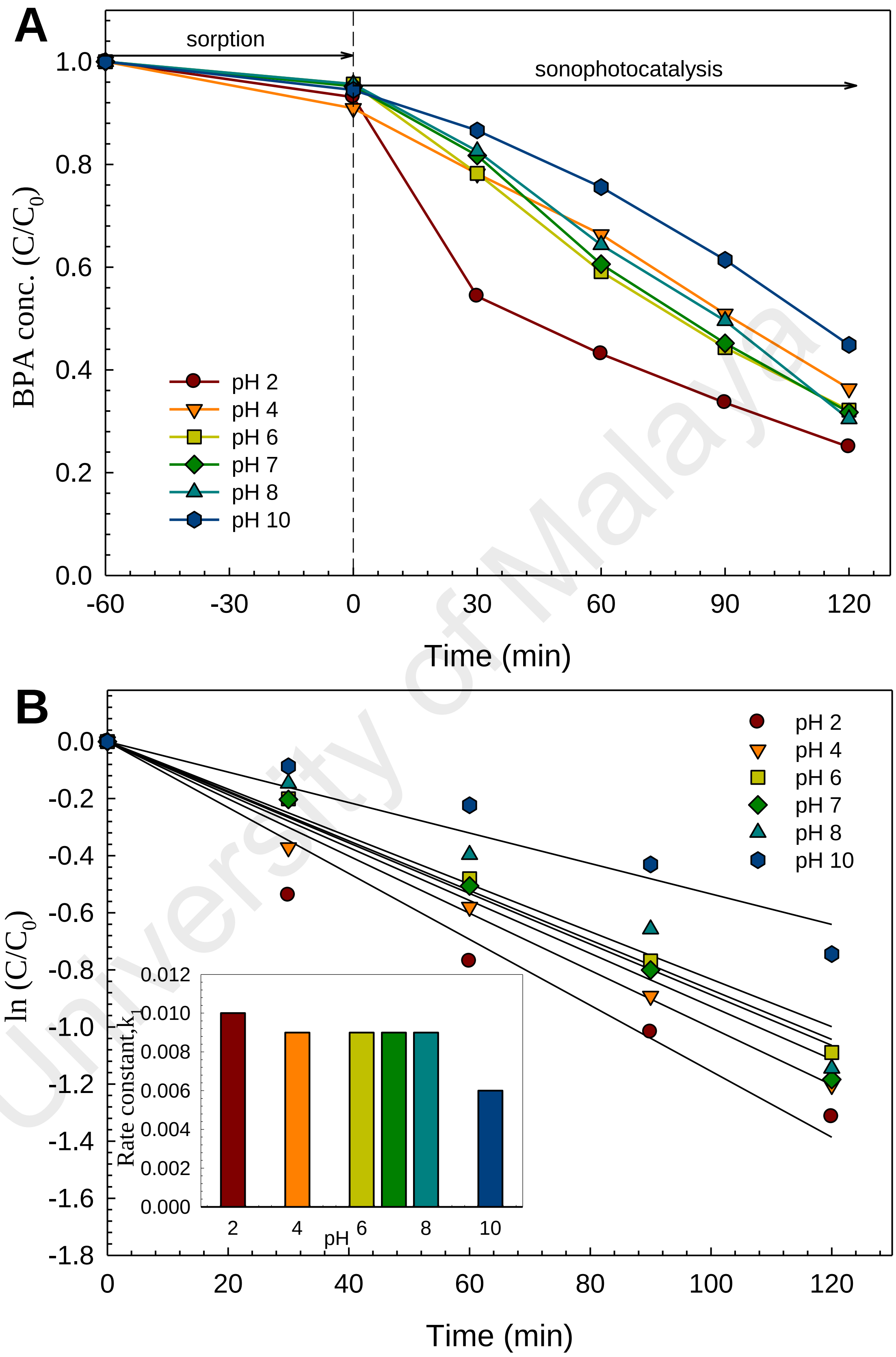

Figure 4.8: (A) pH effect of BPA solution on sonophotocatalyst under optimum condition (US frequency = 35 kHz; US power = 50 W; stirring = 300 rpm; temperature = 20 °C), (B) pseudo-first-order kinetic model of pH effect on BPA degradation

4.3.2 Effect of GCN loading

Figure 4.9 A shows the effect of GCN dosage (0.01, 0.05, 0.1, 0.2 and 0.3 g) on the sonocatalytic degradation of BPA. The rate constant of the BPA degradation increased drastically with an increase of GCN amounts from 0.01g (2.0 × 10^{-3} min^{-1}) to 0.1 g (14.0 × 10^{-3} min^{-1}). Therefore, it can infer that the BPA degradation efficiency could be improved by the presence of additional active sites or total surface area of GCN. However, when the dosage of GCN was more than 0.1 g, the rate constant steadily increased to 20.0 × 10^{-3} min^{-1} 0.3 g GCN. The data was fitted by use of first order kinetic model Table 4.6 to obtain the kinetic constants (Figure 4.9 B).

The overdose effect has been reported by other photocatalysis studies (Kaneco et al., 2004; Wong & Chu, 2003), where an abundant of photocatalyst would decrease the light penetration onto the bottom of the reactor while increase the light scattering effect. Therefore, in the photocatalysis, there is an optimal dosage so that degradation efficiency could be inhibited with a dosage higher than optimal. It is noteworthy that in our study the BPA degradation rate did not decrease even with overdose of catalyst as reported by Wong & Chu.

This could be related to the synergetic sonication process where ultrasound irradiation continuously exfoliate the bulk GCN particles and reduce agglomeration (particle-particle interactions). Yet, judging from the economical point of view, the optimal dosage of GCN was determined to be 0.05 g since further mass increment was not significant. Therefore, 0.05 g was used in further tests.

Table 4.6: Determination coefficients, R^2 for first order kinetic model of catalyst dosage

Experiment	**Test**	**Pseudo First Order**	
		K_1	**R^2**
Catalyst dosage (g)	0.01	0.002	0.974
	0.05	0.009	0.989
	0.1	0.014	0.978
	0.2	0.018	0.956
	0.3	0.020	0.956

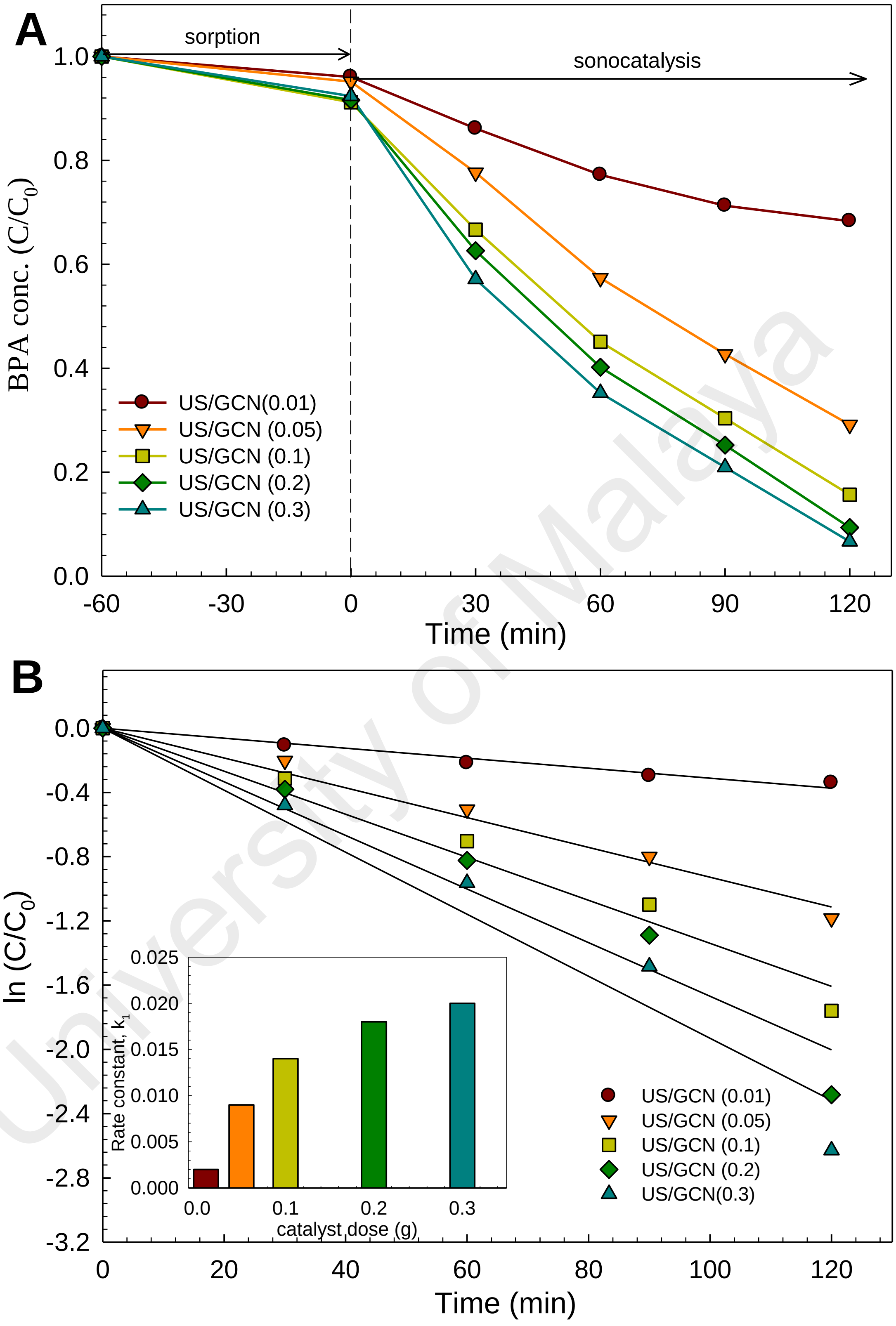

Figure 4.9: (A) Effect of catalyst dosage on BPA degradation under optimum condition. (US frequency = 35 kHz; US power = 50 W; stirring = 300 rpm; temperature = 20 °C), (B) pseudo-first-order- kinetic model of catalyst dosage effect on BPA degradation

4.4 Sonophotocatalytic effect on BPA

After the optimum condition were identified for all four parameters (US frequency, US power, mechanical stirring speed and temperature), the effect of advance oxidation process (AOP) were applied on BPA degradation with the presence of P25 as sonophotocatalyst. The AOP effect on BPA degradation by P25 was investigated under UV light. This research further investigated based on the effect of AOP on BPA degradation with the presence of sonophotocatalyst GCN under visible light. The detailed study was discussed below.

4.4.1 AOP effect on BPA degradation by P25

Under the optimized condition (35 kHz frequency, 50W power, 300 rpm stirring speed and 20^{o}C temperature), the effect of sole US, UV, combined US/UV, US/P25, UV/P25 and US/UV/P25 were investigated (Figure 4.10 A). The rate constants of BPA removal by sonolysis and photolysis were 4.7×10^{-3} and 2.0×10^{-3} min^{-1}, respectively. The rate constant (11.4×10^{-3}min^{-1}) by sonophotolysis was higher than rate constant (7.0×10^{-3}min^{-1}) of sonocatalysis and rate constant of (6.0×10^{-3}min^{-1}) photocatalysis. Sonophotocatalysis had the highest rate constant (28.0×10^{-3} min^{-1}) compared to the other catalytic processes (Figure 4.10 B). The combination of US/UV/P25 had almost 96 % of BPA removal in 120 min under the optimum conditions. Sonophotocatalytic degradation generally occurs faster than that during the respective individual processes at similar operating conditions (Taghizadeh & Abdollahi, 2011). Determination of coefficients, R^2 for first order kinetic model of different AOP were listed in table 4.7

Interestingly, a synergistic effect has been obtained under the experimental condition, as can be easily verified from the degradation rate constants obtained under the combined effect of sonophotocatalysis which was greater than the sum of the reaction rate constant of sonocatalysis and photocatalysis employed separately (Selli, 2002). The synergy can be quantified as the normalized difference between the sum of those obtained under separate photocatalysis and sonocatalysis. According to the following equation the synergistic effect was found to be 53%.

$$Synergy = \frac{k_{sonophotocatalysis} - (k_{sonocatalysis} + k_{photocatalysis})}{k_{sonophotocatalysis}} \qquad (4.5)$$

In general, sonolysis alone, without the presences of any catalyst was found to produce active ·OH, which are capable of attacking the organic compound in solution (Davydov et al., 2001). Although ·OH can be produced by the sonolysis of water, they are most likely not produced in sufficient quantities to achieve a higher rate of BPA degradation. Direct photolysis using an artificial UV light seems to be not efficient in BPA degradation because oxidative intermediate species (mainly ·OH) are not generated (Monteagudo, Durán, San Martín, & García, 2014). This method instead generates intermediated from the pollutant molecules which could be more hazardous than the parent pollutant molecule (Joseph, Puma, Bono, & Krishnaiah, 2009). When photocatalysis process applied, TiO_2 will play a role to produce ·OH which will enhance the degradation rate of BPA. After absorbing light, the excited BPA molecules inject an electron into the conduction band of TiO_2 where it is captured by surface adsorbed O_2 to form $·O_2^-$. The interfacial electron transfer can inhibit the fast electron-hole recombination on TiO_2, and the holes have sufficient time to react with H_2O to generate

·OH. Only UV has no any interfacial electron transfer takes place, therefore the photolysis has the lowest rate constant in BPA degradation (Tangestaninejad, Moghadam, Mirkhani, Mohammadpoor-Baltork, & Salavati, 2008; K. Zhang, Zhang, Chen, & Oh, 2011).

The oxidation process of BPA is ·OH dependent, therefore the presence of TiO_2 in an ultrasonic system should results in the formation of ·OH in the irradiated solutions. Increasing in the formation of ·OH can be explained by the well-known mechanism of hot spots and sonoluminescence (Shimizu, Ogino, Dadjour, & Murata, 2007; Tangestaninejad et al., 2008). The cavitation can be increased by the heterogeneous nucleation of bubbles, resulting in the induction of hot spot in the solution. Temperatures can reach to 30 000 K in these hot spots, causing the pyrolysis of H_2O molecules to form ·OH. The produced H_2O_2 by recombination of ·OH may also interact with the surface of TiO_2 and produce a number of oxidizing agents, which can facilitate the degradation of BPA. Sonoluminescence involves an intense UV-light, which excite the TiO_2 particles to act as a photocatalyst during sonication (Tangestaninejad et al., 2008).

On the other hand, the combination of oxidation processes (US/UV), results higher rate constant on degradation of BPA compared to the sole US or UV at similar operating conditions. In general, combination of AOPs will be more efficient compared to the sole AOP degradation rate because the combination of AOP will produce more oxidative intermediate species (·OH). Basically, US application produces H_2O_2, which is reduced by exposure to UV light. This is because UV tends to split H_2O_2 to form OH. This enhances the higher degradation rate of BPA under US/UV combination process compared to solo US and UV.

As a result, the highest degradation rate was obtained by sonophotocatalysis under the optimum condition. As explained above, sonocatalyst and photocatalyst are producing ·OH. In addition, an electric interaction between the bubbles and TiO_2 particles has an important role on the synergetic effect between US and UV light (Bejarano-Pérez & Suárez-Herrera, 2007; Tangestaninejad et al., 2008). According to the electric field theory, the fragmentation of microbubbles induced by ultrasound is accompanied by the formation of places of high density of negative charge that can produce intense electric fields when those bubbles come near to the locally charged TiO_2 particles (K. Suslick, Doktycz, & Flint, 1990). The strong electric fields produced in this way can induce local discharges that can generate reactive species (·OH) that can increase the reaction rate of BPA degradation on the surface of TiO_2 particles.

The beneficial effect of sonophotocatalysis may be attributed to several reasons, namely: (i) increased production of ·OH in the reaction mixture through reactions (1) and (2) (Kavitha & Palanisamy, 2011), (ii) enhanced mass transfer between the liquid phase and the TiO_2 surface (Wu, Zivanovic, Hayes, & Weiss, 2008), and (iii) increased catalytic activity due to ultrasound de-aggregating catalyst particles, thus increasing surface area (Silva et al., 2007). The action of photocatalysis towards ultrasound increases organic degradation due to the TiO_2 particles, providing extra nuclei for bubble formation (Tuziuti, Yasui, Iida, Taoda, & Koda, 2004). Nevertheless, a detrimental effect on sonolytic efficiency may take place because of sound attenuation (Berberidou, Poulios, Xekoukoulotakis, & Mantzavinos, 2007).

Table 4.7: Determination coefficients, R^2 for first order kinetic model of different AOP

Experiment	**Test**	**Pseudo First Order**	
		K_1	**R^2**
AOP	US	0.004	0.989
	UV	0.002	0.970
	UV/P25	0.006	0.994
	US/P25	0.007	0.981
	US/UV	0.011	0.990
	US/UV/P25	0.028	0.983

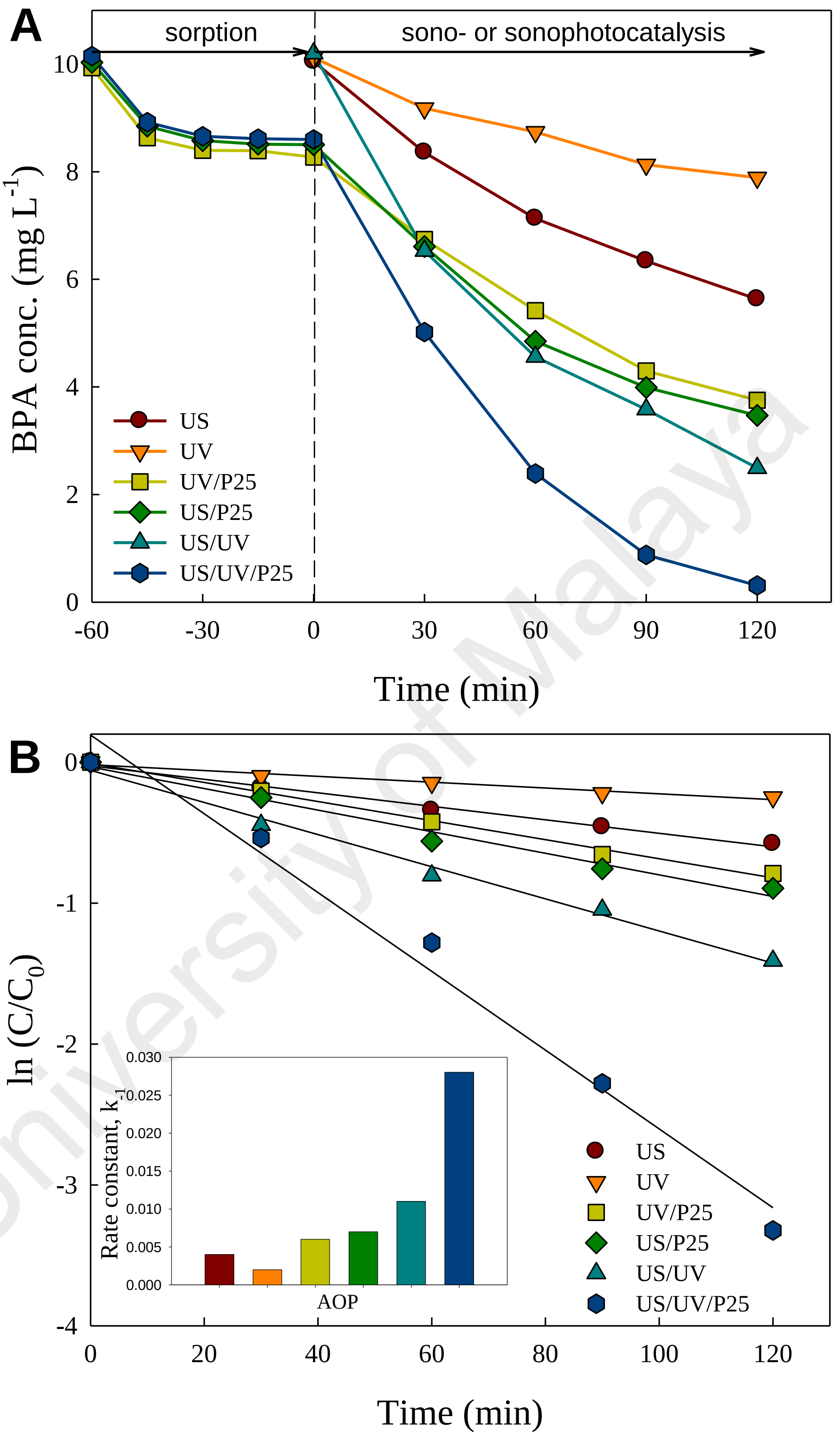

Figure 4.10: (A) Sonocatalytic effect with different AOP application on BPA degradation under optimum condition, (US frequency = 35 kHz, US power = 50 W; stirring = 300 rpm; temperature = 20 ^{o}C); (B) pseudo-first-order kinetic model of BPA degradation at different AOP condition

4.4.2 AOP effect on BPA degradation by GCN

Various AOPs using GCN were conducted to remove BPA and their performances were compared with TiO_2 based Vis-L/US. The solution pH and GCN dosage applied were 7 and 0.05 g, respectively. The kinetics of BPA removal by various AOPs based on GCN or TiO_2 was depicted at Figure 4.11A.

The rate constants of BPA removal by photolysis (Vis-L only) and sonolysis (US only) were 1.0×10^{-3} min^{-1} and 4.0×10^{-3} min^{-1}, respectively. Thus, the US based oxidation is 4 times faster than Vis-L based oxidation. In addition, the rate constant of sonocatalysis (US/GCN, 9.0×10^{-3} min^{-1}) was much higher than those of photocatalysis (Vis-L/GCN, 5.0×10^{-3} min^{-1}) and sonophotolysis (US/Vis-L, 7.0×10^{-3} min^{-1}). This infers that the catalyst plays an important role in BPA degradation with the assist of AOP. Interestingly, the Vis-L and GCN based sonophotocatalysis had the highest rate constant (Vis-L/US/GCN, $14.0 \times 10^{-3} min^{-1}$) and the order of BPA oxidation rate constants was as follows: Vis-L/US/GCN > US/GCN >Vis-L/US ≈Vis-L/US/P25 >Vis-L/GCN > US >Vis-L. Due to the synergetic effect of individual compartment, the sonophotocatalysis had the highest speed of BPA removal (Madhavan et al., 2010; Mrowetz, Pirola, & Selli, 2003; Taghizadeh & Abdollahi, 2011).

In detail, sonophotocatalysis could overcome the problem existed in the discrete process by (i) increasing in the active surface area of catalyst via acoustic wave that can prevent the aggregation of particles, (ii) continuously cleaning the surface of catalyst via ultrasound and eventually increasing the photocatalytic performance by the Vis-L, and finally (iii) promoting the mass transport of BPA to the catalyst surface (Kaur & Singh, 2007). Because of these advantages, the Vis-L/US/GCN had almost 80.6% of BPA removal in 120 min and the fastest rate compared to other AOPs (Taghizadeh & Abdollahi, 2011).

As comparison, the Vis-L/US/P25 was also investigated. In the dark test, P25 removed 14% of BPA so that its sorption capacity was 28.2 mg g^{-1}. Although GCN had a lower sorption capacity than P25, it had two times higher degradation rate than P25 ($7.0 \times 10^{-3} min^{-1}$) in the sonophotocatalysis, demonstrating that GCN is effective in the catalytic activity in the basis of US and Vis-L system. The wider band gap (3.2 eV) of P25 restricts its excitation to UV spectrum. On the other hand, GCN has good physicochemical stability, harvesting visible light with a band gap of 2.7 eV and suitable redox potential to efficiently catalyze reactions. These make GCN to be promising candidate for visible light enhancement. The data was fitted by use of first order kinetic model Table 4.8 to obtain the kinetic constants (Figure 4.11 B).

Table 4.8: Determination coefficients, R^2 for first order kinetic model of AOP effect

Experiment	**Test**	**Pseudo First Order**	
		K_1	**R^2**
AOP	Vis-L	0.001	0.942
	US	0.004	0.989
	Vis-L/GCN	0.005	0.995
	US/GCN	0.009	0.989
	Vis-L/US	0.007	0.998
	Vis/US/GCN	0.014	0.976
	Vis-L/US/P25	0.007	0.975

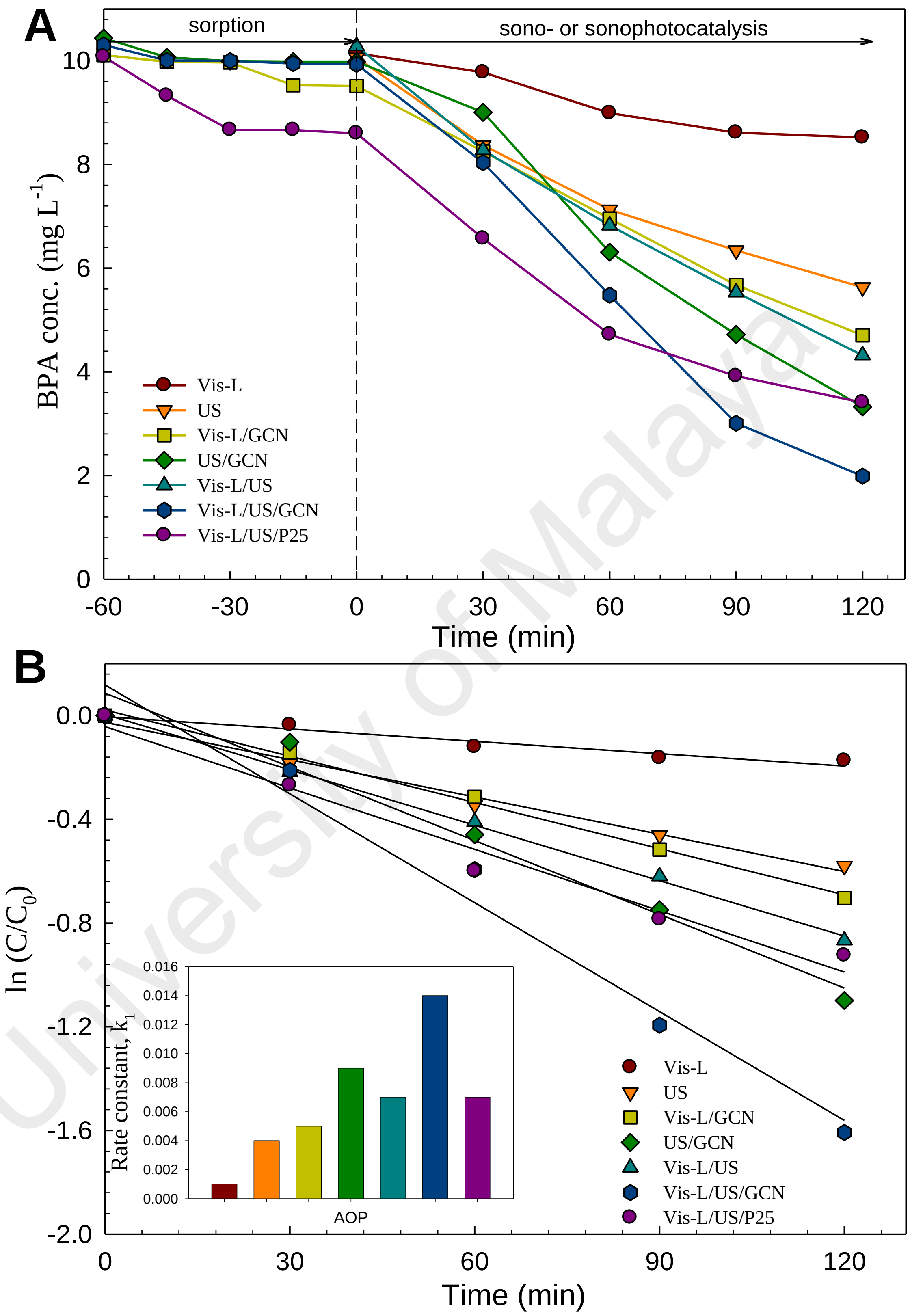

Figure 4.11: (A) Sonocatalytic effect with different AOP application on BPA degradation under optimum condition (US frequency = 35 kHz; US power = 50 W; stirring = 300 rpm; temperature = 20 °C); (B) pseudo-first-order kinetic model of BPA degradation at different AOP condition.

4.5 Hydrogen peroxide (H_2O_2) formation during BPA oxidation

The formations of hydrogen peroxide (H_2O_2) during the BPA degradation process by P25 and GCN under UV light and visible light respectively were investigated. As a comparison, the formation of H_2O_2 without BPA in the solution was also identified to understand more on the mechanism of the sonophotocatalysis process. The study was discussed more in the section below.

4.5.1 BPA oxidation by US/UV/P25

The formation of H_2O_2 by various AOPs was investigated. Exponential BPA degradation over time indicates the data fits the first-order kinetics. According to reaction (2.3), the presence of H_2O_2 is due to the recombinant of ·OH produced when water molecules being fragmented by US irradiation (R. A. Torres, Pétrier, et al., 2008). Therefore, the concentration of H_2O_2 in solution is an indirect measure of the concentration of ·OH. Figure 4.12 shows the formation of H_2O_2 by US, US/UV, and US/UV/P25 during degradation of BPA (10 mg L^{-1}) over 120 min. After 60 min, the rate of accumulation was stabilized, suggesting that rate of production and consumption (recombination and scavenging reactions) of ·OH was almost equivalent (Berberidou et al., 2007). To confirm the above mechanism, the production of H_2O_2 by US, US/UV and US/UV/P25 was measured to evaluate H_2O_2 formation without BPA. In the absence of BPA, H_2O_2 formation increased linearly, but was lower in the presence of BPA, indicating that a fraction of the ·OH formed reacts with BPA, and that ·OH-mediated oxidation is a BPA decomposition pathway (Gültekin & Ince, 2008). The concentration of H_2O_2 with/without BPA followed the order of US/UV/P25 > US > US/UV. The degradation rate of BPA followed the order US/UV/P25 > US/UV > US. Generally, US application produces H_2O_2, which is reduced by exposure to UV light. This is because UV tends to split H_2O_2 to form ·OH, which can enhance the degradation rate of BPA. Using US/UV/P25, the formation of H_2O_2 increased further in the absence of BPA because the catalyst reacts with UV light to form ·OH. The ·OH attacks BPA mainly at the interface of cavitation bubbles because of the hydrophobic and slightly volatile characteristics of BPA (R. A. Torres, Nieto, et al., 2008).

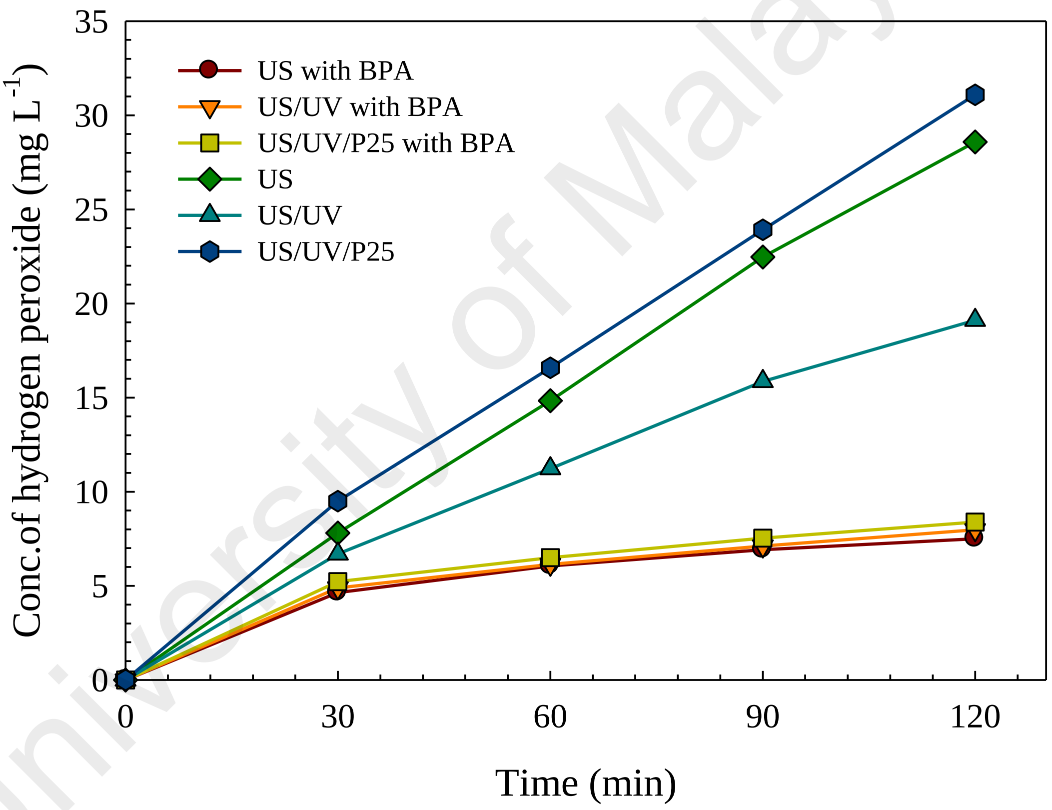

Figure 4.12: Hydrogen peroxide formation of BPA degradation at different AOPs applications under optimum condition: US frequency = 35 kHz, US power = 50W; stirring = 300 rpm; temperature = 20°C

4.5.2 BPA oxidation by US/Vis-L/GCN

In order to obtain the correlation between the oxidation rate of BPA and the oxidizing power of AOPs, the amount of H_2O_2 was measured under the same conditions with the kinetics. Hydrogen peroxide (H_2O_2) increased linearly up to 28~34 mg L^{-1} at 120 min in the absence of BPA (Figure 4.13 A) whiles it increased non-linearly when BPA was added under the same conditions (Figure 4.13 B). Therefore, it can determine that a fraction of ·OH formed reacts with BPA and ·OH-mediated oxidation is one of the decomposition pathways of BPA (Gültekin & Ince, 2008). The ·OH attack on BPA is mainly carried out at the interface of the cavitation because of the hydrophobic and slightly volatile characteristics of BPA (R. A. Torres, Nieto, et al., 2008).

The US irradiation creates cavitation in aqueous phase to produce hydrogen (·H) and hydroxyl radicals (·OH) through generating extreme temperature (>3000^{o}C) and pressure (>300 atm) (K. S. Suslick & Flannigan, 2008). Consequently, ·OH oxidizes BPA and intermediate species are produced. The unused ·OH can be recombined to H_2O_2 (R. A. Torres, Pétrier, et al., 2008).

$$H_2O \overset{)))}{\rightarrow} \bullet OH + \bullet H \tag{4.6}$$

$$\bullet OH + BPA \rightarrow \text{ Intermediate products} \tag{4.7}$$

$$\bullet OH + \bullet OH \rightarrow H_2O_2 \tag{4.8}$$

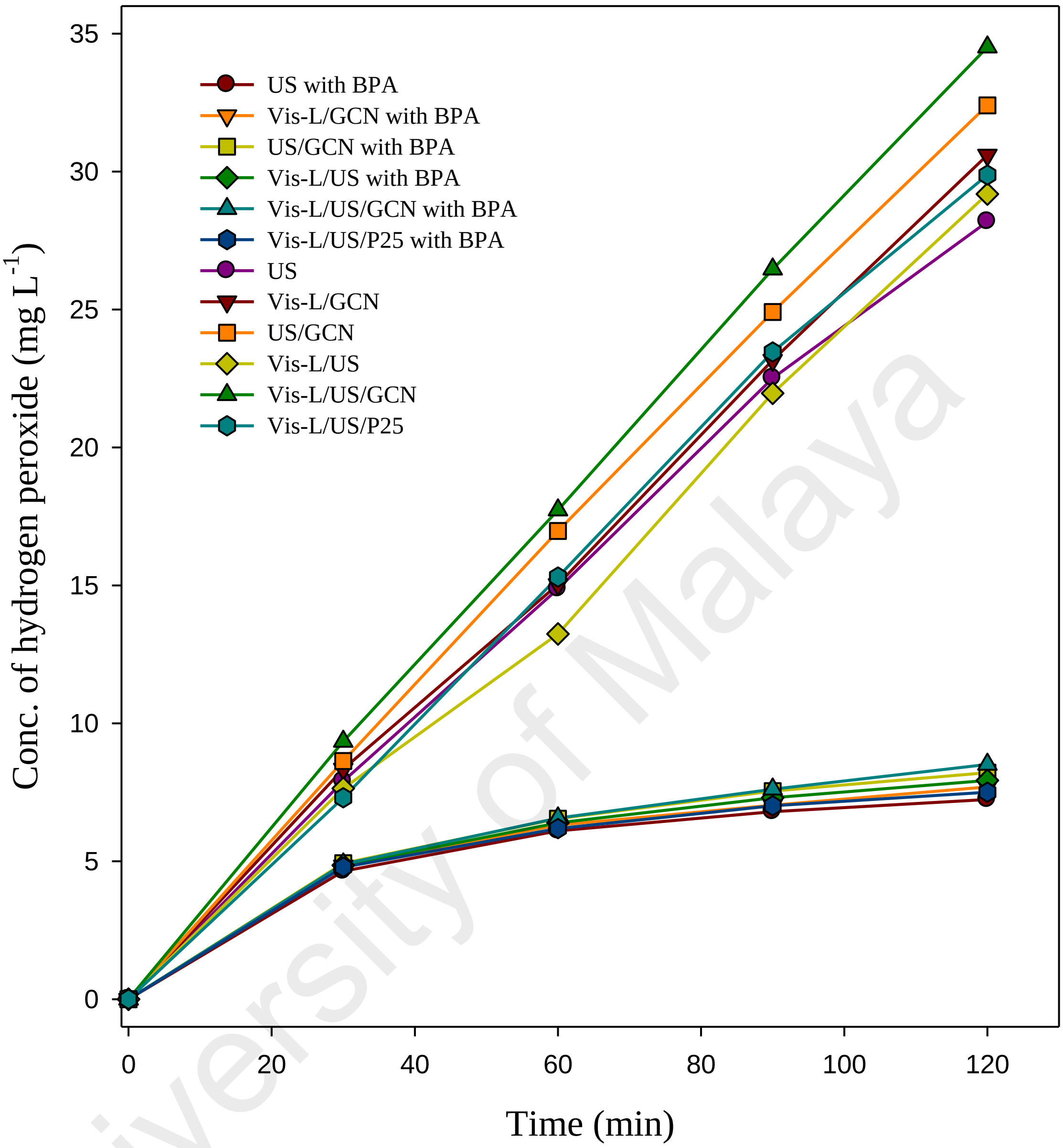

Figure 4.13: Hydrogen peroxide formation of BPA degradation at different AOPs applications under optimum condition: US frequency = 35 kHz, US power = 50W; stirring = 300 rpm; temperature = 20^{o}C

When Vis-L irradiates a photocatalyst such as GCN or TiO_2, electrons (e_{CB}^-) move from the valence band (VB) to the conduction band (CB), producing positively charged holes (h_{VB}^+). Then, h^+_{VB} reacts not only with H_2O or hydroxyl group attached on the surface of catalyst, but also directly with BPA.

$$\text{GCN or TiO}_2 \xrightarrow{\text{VL}} e^-_{CB} + h^+_{VB} \tag{4.9}$$

$$h^+_{VB} + OH^- \rightarrow \bullet OH \text{ and/or } h^+_{VB} + H_2O \rightarrow \bullet OH + \bullet H \tag{4.10}$$

$$h^+_{VB} + BPA \rightarrow \text{ Intermediate products} \tag{4.11}$$

$$\bullet OH + \bullet OH \rightarrow H_2O_2 \tag{4.12}$$

As shown above, BPA is mainly eliminated by ·OH and h^+_{VB}. However, since the BPA removed by h^+_{VB} cannot be measured, the following rationale was established by assuming that the amounts of consumed H_2O_2 is equal to the amounts of depleted ·OH for BPA removal. The H_2O_2 consumed for the removal of BPA can be calculated by subtracting H_2O_2 produced with BPA from H_2O_2 produced without BPA. Then, the usage rate of consumed H_2O_2 is the divided value of consumed H_2O_2 by the removed BPA.

$$[H_2O_2]_{\text{consumed for BPA removal}} = [H_2O_2]_{\text{production without BPA}} - [H_2O_2]_{\text{production with BPA}} \tag{4.13}$$

$$\text{Usage rate (R) of } [H_2O_2]_{\text{consumed}} = \frac{[BPA]_{\text{removed}}}{[H_2O_2]_{\text{consumed}}} \tag{4.14}$$

Where R is the usage rate of consumed H_2O_2 and has the following relationship since it depends on the concentration of BPA:

$$\frac{d[R]}{d[BPA]} = k \quad (4.15)$$

$$[R]_{BPA} = k[BPA] \quad (4.16)$$

Where k is the slope of linear relationship between the usage rate (R) and BPA concentration.

Based on the explanation, the linear relationships between the usage rate of consumed H_2O_2 and concentration of BPA were made for US, Vis-L/US, Vis-L/US/P25 and Vis-L/US/GCN (Table 4.9 and Figure 4.14). All cases had a determination coefficient (R^2) higher than 0.86. The slopes for US, Vis-L/US and Vis-L/US/P25 were 0.116, 0.115 and 0.186, respectively, whiles Vis-L/US/GCN had a relatively lower slope (0.018). Thus, for the case of US, the proposed relationship is plausible since BPA is mainly removed by ·OH generated by the splitting of water molecules. The cases of Vis-L/US and Vis-L/US/P25 had similar (or even higher) slopes of usage rate to US since decomposition of H_2O_2 could be promoted by Vis-L and TiO_2. However, in the case of Vis-L/US/GCN, the slope (0.018) was much lower than US, Vis-L/US or Vis-L/US/P25. Accordingly, it can infer that the electron transport at the GCN surface is activated by Vis-L, and the usage rate of consumed H_2O_2 can be lowered by BPA removed by h^+_{VB} as shown in Eq. (4.9) to (4.11). However, based on the data analysis, it is plausible that Vis-L does not create h^+_{VB} on the surface of P25.

Table 4.9: Usage rate of H_2O_2 consumed for BPA removal based on the kinetics of BPA removal

Time	**US**	**Vis-L/GCN**	**US/GCN**	**Vis-L/US**	**Vis-L/US/GCN**	**Vis-L/US/P25**
30	0.518	0.359	0.264	0.720	0.426	0.806
60	0.334	0.293	0.352	0.505	0.399	0.425
90	0.237	0.238	0.303	0.324	0.367	0.284
120	0.211	0.210	0.275	0.281	0.305	0.232

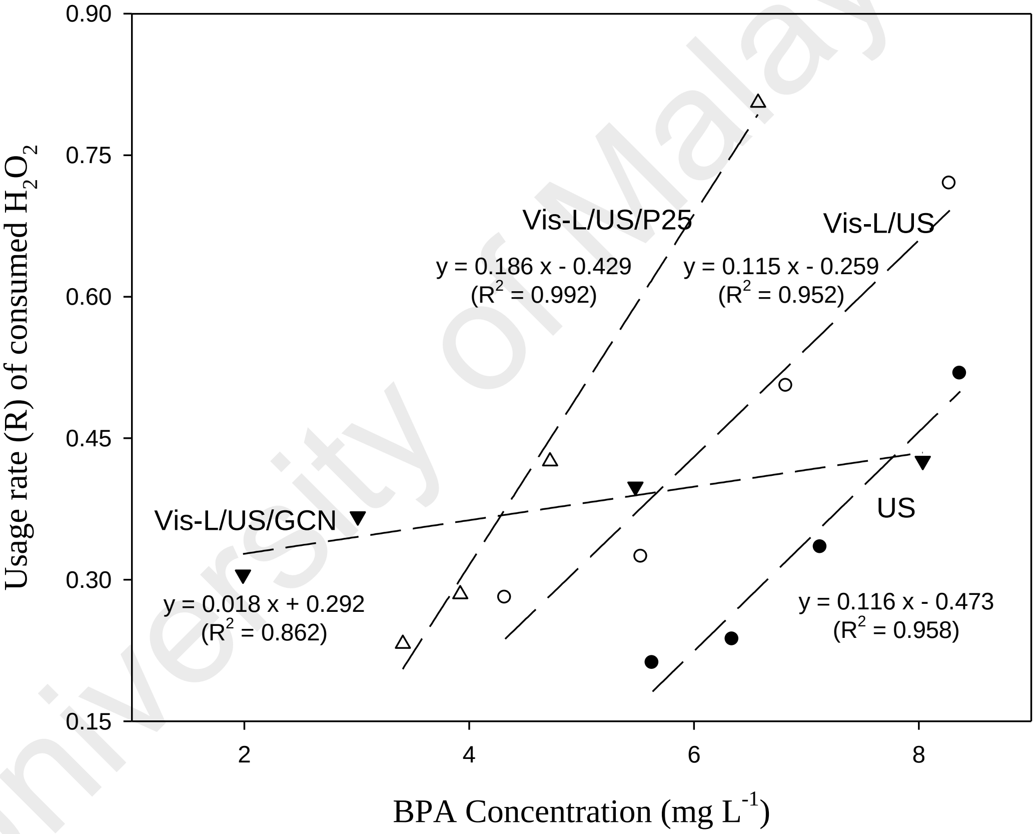

Figure 4.14: Relationship of usage rate of consumed H_2O_2 and BPA concentration

4.6 Intermediate formation during BPA oxidation

The formations of intermediate during the BPA degradation by P25 and GCN under UV light and visible light respectively were investigated. The highest rate constant was obtained under sonophotocatalytic process, US/UV/P25 and US/Vis-L/GCN and was carried out in 300 minutes for each test. The study was discussed more in the section below.

4.6.1 BPA oxidation by US/UV/P25

The highest rate constant was obtained under sonophotocatalytic (US/UV/P25) degradation of BPA (10 mgL^{-1}) for 120 min with the rate constant 28.0×10^{-3} min^{-1}. Further investigation for intermediate production by sonophotocatalytic degradation was carried out under the optimum condition for 300 min until BPA in water fully mineralized. The intermediate products formed were examined by HPLC-MS analysis in negative electroscopy modes. Five by-products by sonophotocatalytic degradation of BPA were identified by the molecular ions and mass fragment peaks and also by comparison with HPLC-MS library data (Table 4.10). But the other intermediates were not identified because of their low concentration in the reaction mixture.

Figure 4.15 shows the peak areas of extracted ion chromatography (EIC) of these product ions changed with the irradiation time. In this study, the five main intermediates identified under the US/UV/P25 system were monohydroxylated bisphenol A, (A); 4-isopropenylphenol, (B); monohydroxylated 4-isopropenylphenol, (C); dihydroxylated bisphenol A, (D); and 4-hydroxyacetophenone, (E).

In the photocatalytic degradation of bisphenol A with TiO_2, various intermediate products such as phenol, p-hydroquinone, p-isopropenylphenol, and 4-hydroxyphenyl-2-propanol have been identified by several researchers (Fukahori, Ichiura, Kitaoka, & Tanaka, 2003; Horikoshi, Tokunaga, Hidaka, & Serpone, 2004; Ohko et al., 2001; Watanabe et al., 2003). The intermediates of BPA sonolysis are relatively complicated. Kitajima et al. (Kitajima, Hatanaka, & Hayashi, 2006) identified only one intermediate (2,3-dihydro-2-methylbenzofuran) during BPA sonolysis in O_2 saturated water.

The BPA by-products confirm that during the sonochemical treatment BPA is mainly degraded through ·OH radical reactions. At the same time, the combined ultrasound/photocatalysis system, however, benefits from the individual strengths of each process, eliminating BPA completely as well as all hydrophilic and hydrophobic intermediates.

Table 4.10: Main BPA intermediated formed by sonophotocatalysis (US/UV/P25) by HPLC/MS

	Structure	**Molecular formula**	**Retention time (min)**	**ES negative M – H**	**Molecular weight (*M*)**
BPA	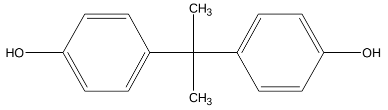 Bisphenol A	$C_{15}H_{16}O_2$	4.6	227	228
A	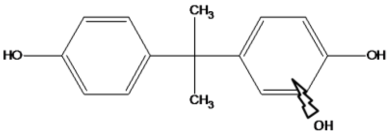 Monohydroxylated bisphenol A	$C_{15}H_{16}O_3$	3.7	243	244
B	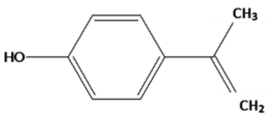 4-isopropenylphenol	$C_9H_{10}O$	1.9	133	134
C	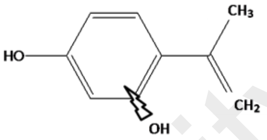 Monohydroxylated 4-isopropenylphenol	$C_9H_{10}O_2$	1.6	149	150
D	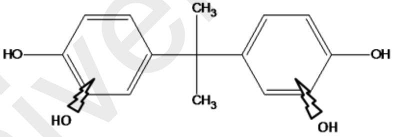 Dihydroxylated bisphenol A	$C_{15}H_{16}O_4$	2.8	259	260
E	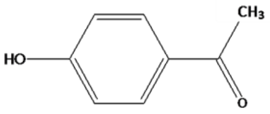 4-hydroxyacetophenone	$C_8H_8O_2$	2.2	135	136

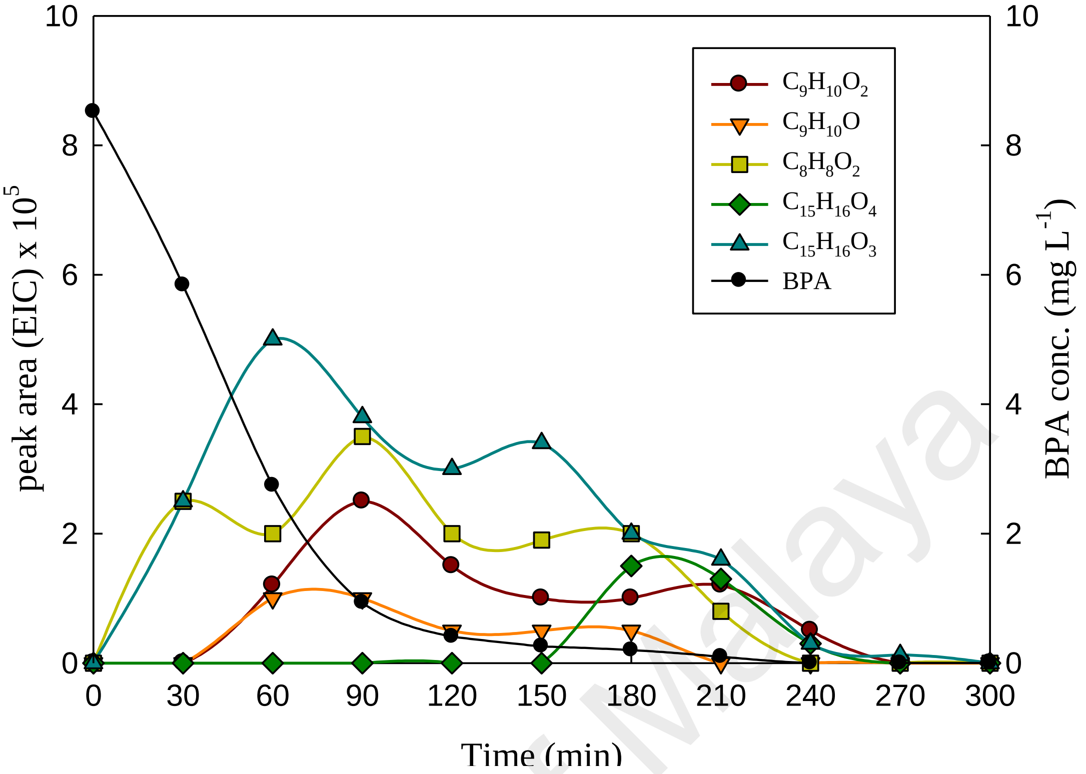

Figure 4.15: Intermediates formation of BPA degradation at UV/US/P25 applications under optimum condition, (US frequency = 35 kHz, US power = 50 W; stirring = 300 rpm; temperature = 20 °C) at 300 min

Figure 4.16 illustrates the sonophotodegradation pathway of BPA in the US/UV/P25 application. The BPA degradation mechanism involves initial reactions by hydroxyl radicals. The first ·OH reactions, yielded monohydroxylated BPA, (A) and 4-hydroxyacetophenone, (E). Subsequent hydroxylation of monohydroxylated BPA led to the 4-isopropenyl phenol (B) and dihydroxylated BPA (D). Further oxidation of 4-isopropenyl phenol led to monohydroxylated 4-isopropenyl phenol (C).

Many reports on the photocatalytic degradation of organic compounds in aqueous solutions have suggested the important role of ·OH (C. Guo et al., 2009; Kaneco et al., 2004). In this work, BPA might be concentrated at the interface of catalyst during the ultrasonic treatment, where it can be easily degraded by ·OH. In the TiO_2 sonophotocatalysis of aromatic compounds, initial hydroxylation of aromatic rings by hydroxyl radicals is believed to play a role in a sequential ring cleavage; a number of researchers have reported the detection of partially hydroxylated aromatic compounds and ring-ruptured products (Ohko et al., 2001; Y. Wang & Hong, 2000). Therefore, C, D and E intermediates are presumably further oxidized through ring-rupturing reactions into aliphatic compounds containing carboxylic acid (Fukahori et al., 2003; Kaneco et al., 2004; Konstantinou, Sakkas, & Albanis, 2002). Then, carboxylic acid produced in small amounts, followed by H_2O and evolution of CO_2 gas. Therefore, with sonophotocatalytic degradation of BPA via hydroxylation, compounds A and E could be formed by direct attack of ·OH. Compounds B and C could be formed in the reaction route of BPA→ A→ B→C. Compound D could be produced as the pathways of BPA→ A→ D.

Unlike the target compound, the more hydrophilic by-products prefer the solution bulk and thus have low probabilities of reaction with ·OH because of the short life of ·OH. Most of the ·OH recombine to produce H_2O_2 rather than reacting with by-products. By combination of photocatalytic treatment, the hydrophilic byproducts that are generated, easily adsorbed and become decarboxylated on the TiO_2 surface. This allows a faster degradation in the US/UV/P25 treatment.

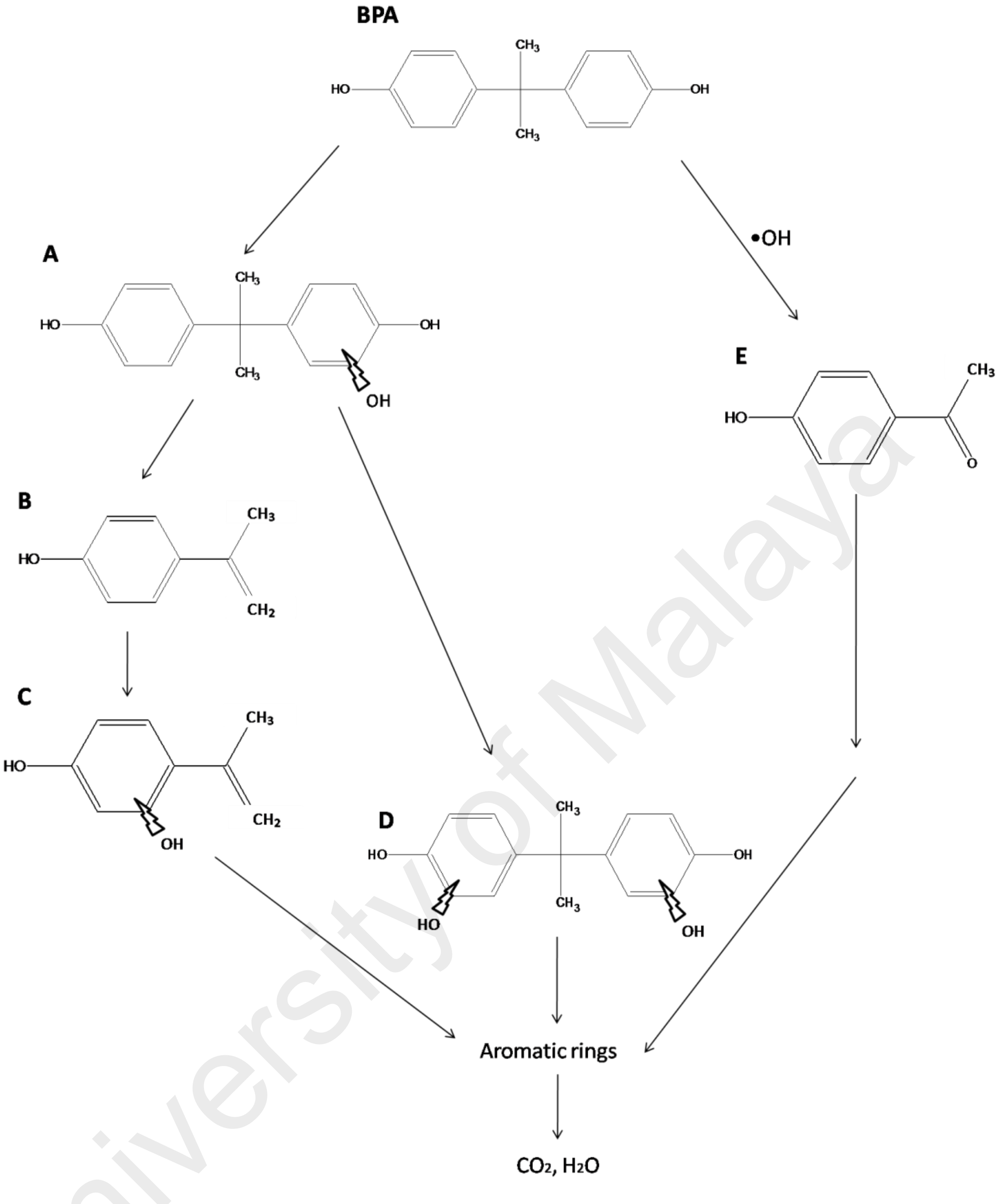

Figure 4.16: Proposed reaction pathways of bisphenol A (BPA) degradation

4.6.2 BPA oxidation by US/Vis-L/GCN

Further investigation for sonophotocatalytic degradation pathway using GCN was carried out for 300 min. The intermediate species were examined by HPLC-MS analysis in negative electroscopy modes. Five by-products were identified by the molecular ions and mass fragment peaks and also by comparison with HPLC-MS library data (Table 4.11). The BPA concentrations and peak areas of extracted ion chromatography (EIC) of by-products changed with the irradiation time are illustrated in Figure 4.17. In the sonophotocatalytic degradation of BPA with the presence of GCN, various intermediate by-products such as monohydroxylated BPA (A), dihydroxylated BPA (B), 4-hydroxyacetophenone (C), 4-isopropenylphenol (D) and 4-hydroxybenzaldehyde (E) were also confirmed by other studies (Fukahori et al., 2003; Horikoshi et al., 2004; Ohko et al., 2001; Watanabe et al., 2003).

Table 4.11: Main BPA intermediates formed by sonophotocatalysis (Vis-L/US/GCN) and identified by HPLC/MS

Species	Structure	Molecular formula	Retention time (min)	ES negative M – H	Molecular weight (*M*)
BPA	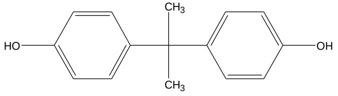 Bisphenol A	$C_{15}H_{16}O_2$	4.6	227	228
A	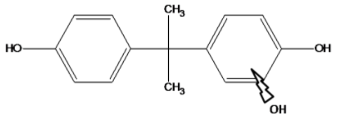 Monohydroxylated BPA	$C_{15}H_{16}O_3$	3.7	243	244
B	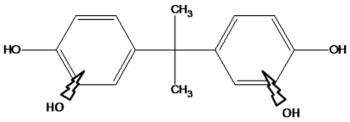 Dihydroxylated BPA	$C_{15}H_{16}O_4$	2.8	259	260
C	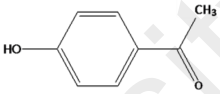 4-hydroxyacetophenone	$C_8H_8O_2$	2.3	135	136
D	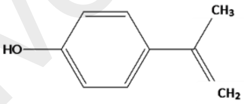 4-isopropenylphenol	$C_9H_{10}O$	1.9	133	134
E	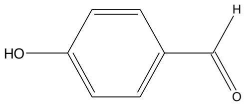 4-hydroxybenzaldehyde	$C_7H_6O_2$	2.1	121	122

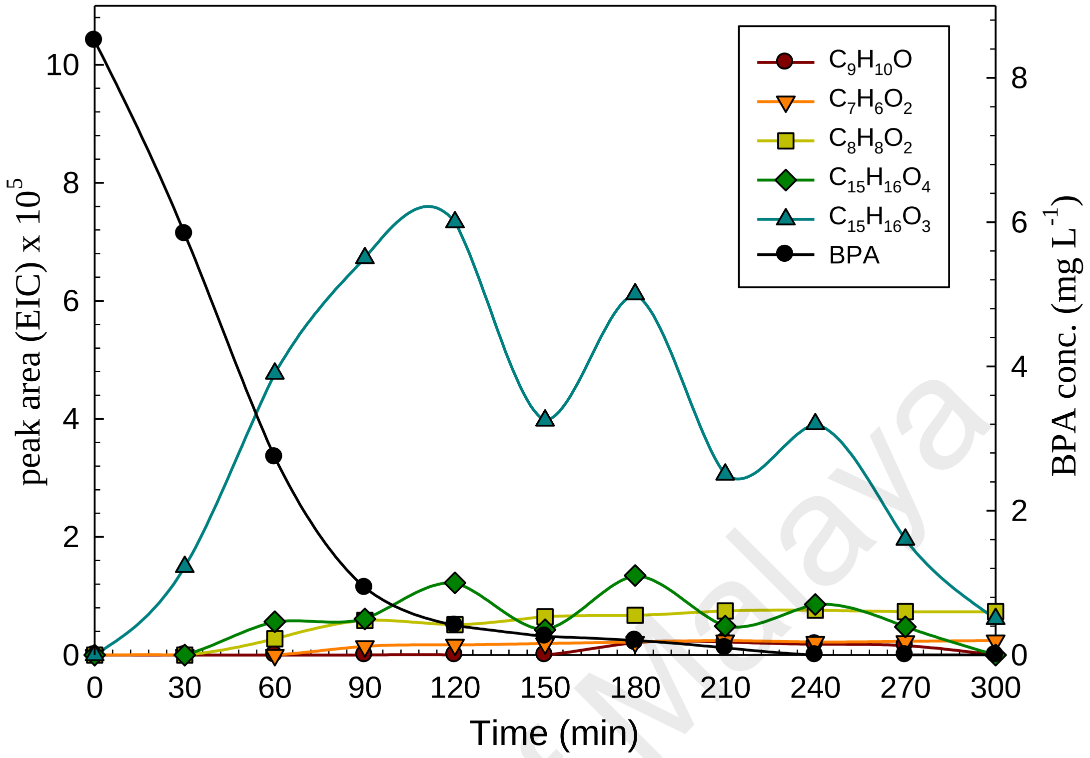

Figure 4.17: Intermediates formation of BPA degradation at Vis-L/US/GCN applications under optimum condition, (US frequency = 35 kHz, US power = 50 W; stirring = 300 rpm; temperature = 20 °C) at 300 min

Figure 4.18 shows the proposed mechanism of degradation pathway based on the kinetic results of Figure 4.17. As a result, monohydroxylated BPA increased up to 7.5×10^5 of EIC until 120 min and decreased to 0.4×10^5 at 300 min with oscillation. Similar to monohydroxylated BPA, dihydroxylated BPA had an oscillated EIC and finally disappeared at 300 min. Meanwhile, 4-hydroxyacetophenone and 4-hydroxybenzaldehyde were detected after 30 and 60 minutes, respectively, but were equilibrated without oscillation. In the case of 4-isopropenylphenol, a trace amount was detected after 150 min and completely removed at 240 min.

Based on these phenomena, it can conclude that monohydroxylated BPA and dihydroxylated BPA sequentially increased due to the attack of ·OH on BPA, and these intermediates were further decomposed to 4-hydroxyacetophenone and 4-hydroxybenzaldehyde.However, 4-hydroxyacetophenone and 4-hydroxybenzaldehyde became final by-products instead of being decomposed to other by-products. As a by-product of dihydroxylated BPA, 4-isopropenylphenol might be decomposed into CO_2 and water.

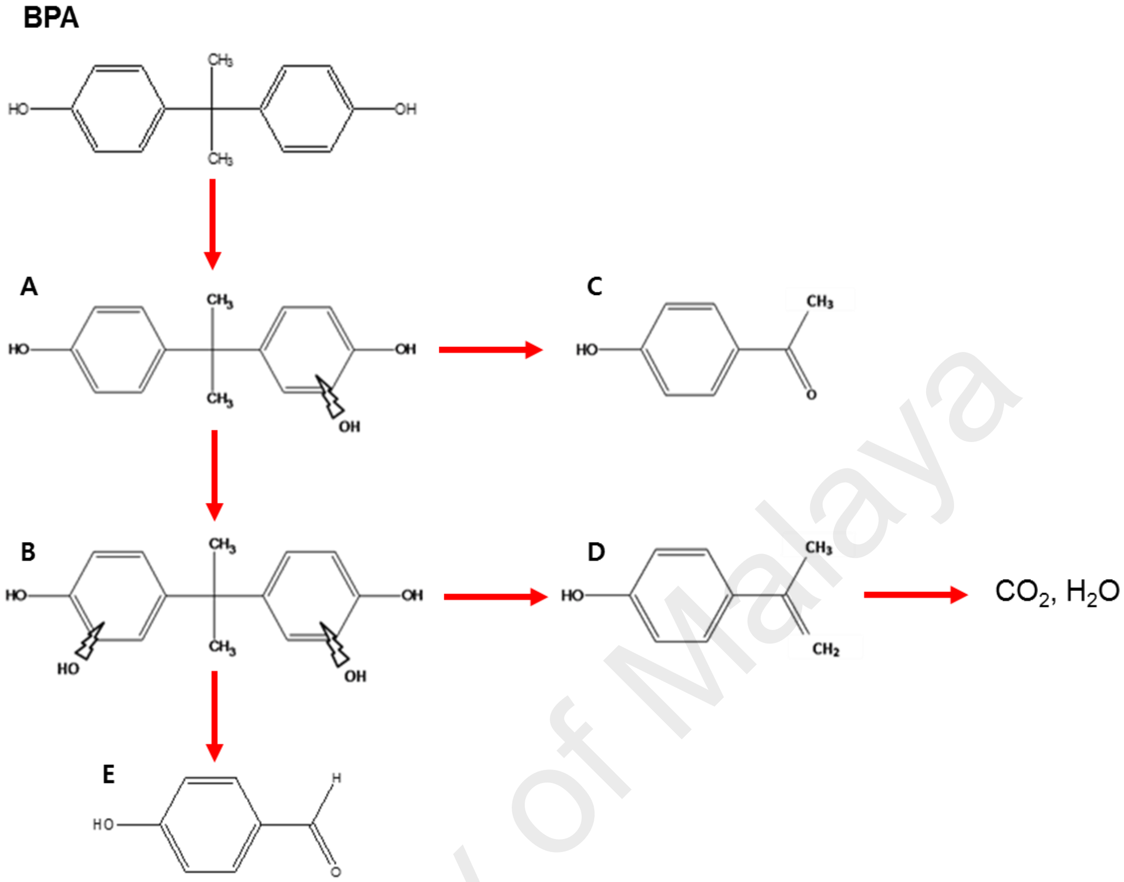

Figure 4.18: Proposed reaction pathways of bisphenol A (BPA) degradation

4.7 Recycle and Reusability

Five cycles of the sonophotocatalytic oxidation of BPA were conducted under the same condition with previous batch tests. This test was carried out to identify the capability of the catalyst (GCN) reuse. Figure 4.19A shows the sonophotocatalytic rate constant of BPA degradation under optimum condition according to the recycle number of GCN reused. The rate constant of the first cycle was 13.0×10^{-3} min^{-1}whiles the second and third cycles were almost similar (12.0×10^{-3} min^{-1}) (Figure 4.19B). There is a light decrease in rate constant occurred at fourth (10.0×10^{-3} min^{-1}) and fifth cycles (8.0×10^{-3} min^{-1}), respectively.

The rate constant of the first recycle test was lower compared to the rate constant (14.0×10^{-3} min^{-1}) of original BPA degradation test on sonophotocatalysis. Therefore, it can suggest that GCN could have a minor loss of activity at every cycle. This is because all the samples of BPA were filtered through a 0.22 µm nylon filter before the UPLC analysis. Filtering method is important to avoid the tiny particles which dispersed in aqueous medium to lead problem in UPLC analysis. Since the five cycle were carried out under the same condition, but the catalyst dosage was decrease at every cycle due to the filtering method which leads to the decrease of rate constant of BPA as increasing the recycling cycle.

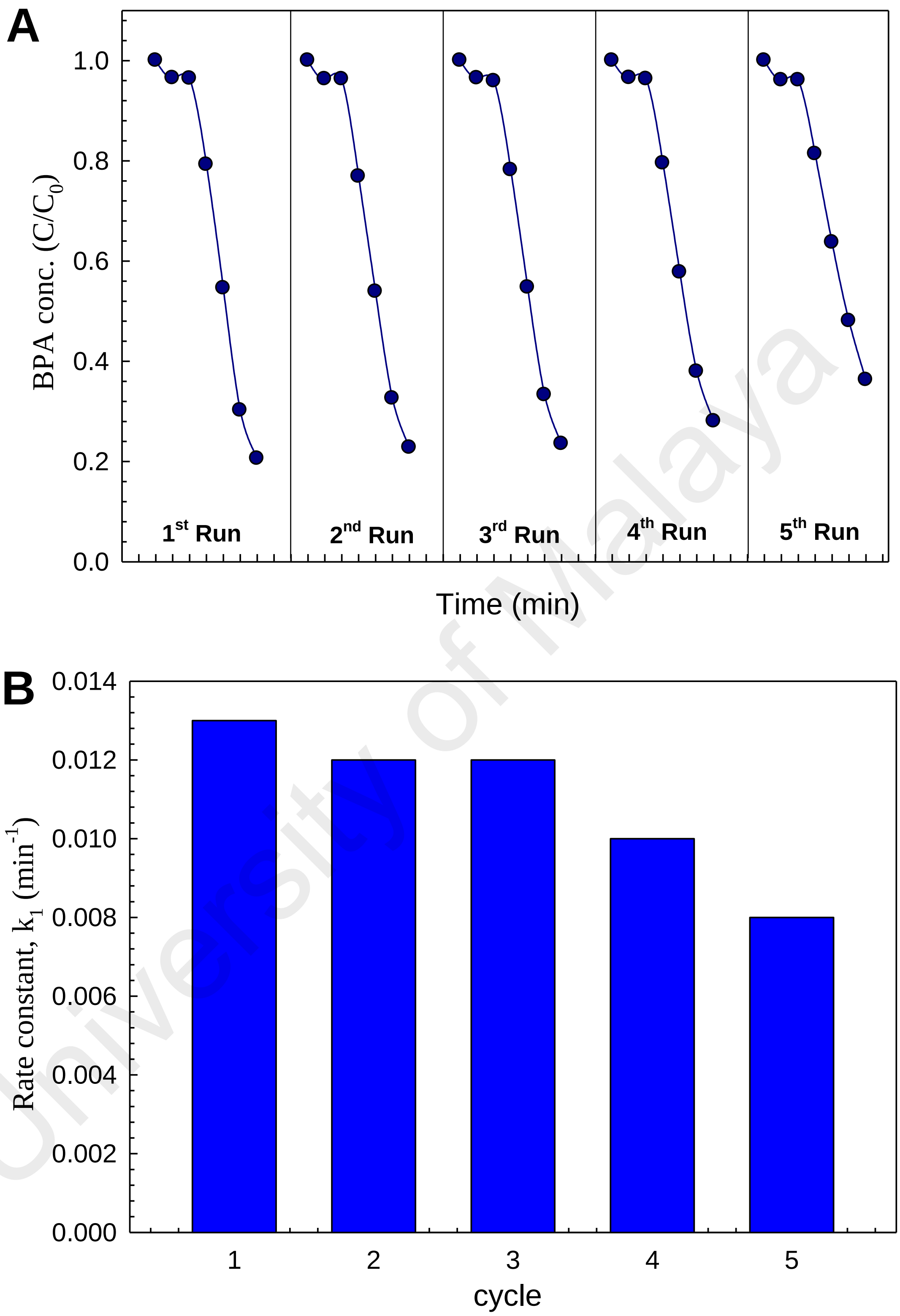

Figure 4.19: (A) Recycles of GCN in sonophotocatalysis for the removal of BPA under optimum condition (US frequency = 35 kHz, US power = 50 W; stirring = 300 rpm; temperature = 20 ^{o}C); (B) Rate constant of GCN in sonophotocatalysis for five cycles

CHAPTER 5

CONCLUSIONS AND RECOMMENDATIONS

5.1 Conclusions

The foremost aim of this thesis was to operate and investigate the Bisphenol A (BPA) degradation by the constructed reactor which combined with ultrasound (US) and Ultraviolet (UV) / Visible Light (Vis-L) generators. The foresaid goal was successfully achieved by finding out the effectiveness of energy based AOPs on BPA removal. The preliminary phase of this study identified the optimum conditions (US frequency, 35 kHz; US power, 50 W; mechanical stirring speed, 300 rpm; and temperature, 20°C) for BPA removal by sonocatalysis (US/P25). These conditions resulted in about 65% removal of BPA after 120 min. The percentage of BPA removal was calculated using equation 4.2.

After the optimum conditions of the selected parameters were successfully identified, the BPA degradation was carried out for sonophotocalalysis (US/UV/P25) process. Although US-mediated degradation of BPA occurs mainly through reactions with ·OH, a portion of BPA was removed by sonolysis and photolysis under the optimum conditions. Use of sonophotocatalysis application resulted in degradation of 96% of BPA in 120 min. This result indicates the effectiveness of energy based Advance Oxidation Processes (AOP) on the BPA degradation. The findings of this study suggest that TiO_2-based sonophotocatalysis has a synergistic effect as can be easily verified from the degradation rate constants obtained under the combined effect of sonophotocatalysis (US/UV/P25) which was greater than the sum of the reaction rate constants of sonocatalysis (US/P25) and photocatalysis (UV/P25) employed separately. According to equation 4.5, the synergic effect was found about to be 53%.

Intermediates of BPA degradation were identified and BPA degradation pathways were proposed based on the HPLC-MS analytical data. Five main intermediates were formed during the sonophotocatalytic degradation. They were monohydroxylated bisphenol A, 4-isopropenylphenol, monohydroxylated 4-isopropenylphenol, dihydroxylated bisphenol A, and 4-hydroxyacetophenone. The findings of this study suggest that TiO_2-based sonophotocatalysis facilitates complete removal of non-polar pollutants and their intermediates that are not susceptible to photocatalyst-mediated degradation.

In order to operate energy-saving sonophotocatalysis process, the final phase of sonophotocatalysis process to remove BPA was applied by developing nano-structured graphitic carbon nitride (GCN) by the use of nontoxic precursor chemicals. GCN was developed as environmental-friendly sonophotocatalyst and it displayed good visible-light-driven photocatalytic performance. The effect on initial pH of BPA solution and sonophotocatalyst (GCN) dosage were investigated under the optimum condition. pH 7 and 0.05 g of GCN was determined in all test.

A series of batch tests were conducted for effect of sonocatalysis (US/GCN), photocatalysis (Vis-L/GCN) and combination of sonophotocatalysis (Vis-L/US/GCN). As comparison to sonophotocatalysis (Vis-L/US/GCN) process, Vis-L/US/P25 test was conducted. Batch test results indicated that Vis-L/US/GCN (14.0×10^{-3} min^{-1}) had two times higher degradation rate than Vis-L/US/P25 (7.0×10^{-3} min^{-1}), inferring that GCN is effective in the catalytic activity in Vis-L/US. In the sonophotocatalytic degradation of BPA with the presence of GCN, various intermediate by-products such as monohydroxylated BPA, dihydroxylated BPA, 4-hydroxyacetophenone, 4-isopropenylphenol and 4-hydroxybenzaldehyde were identified.

Based on the H_2O_2 production analyses and data interpretation, the surface of GCN can be activated by Vis-L so that electrons are transported from VB and holes (h^+_{VB}) are being utilized in the removal of BPA. In addition, bulk layered GCN can be effectively exfoliated by US irradiation. Since the synthesis of GCN is facile, simple and economical, we could expect that a large-scale production of GCN could be applicable and further makes the energy-based AOP become more practical.

5.2 Recommendations

The following recommendations are taken into considerations for future research works.

- For the primary work, the polluted wastewater used was synthetically prepared in laboratory. However, this solution might be different with the real wastewater because the real wastewater consists of mixture of few types of pollutants

- The amount of hydroxyl radicals (·OH) and superoxide radical anion ($\cdot O_2^-$) could be quantitatively analysed for additional information on the surface reactions.

References

Andreozzi, R., Caprio, V., Insola, A., & Marotta, R. (1999). Advanced oxidation processes (AOP) for water purification and recovery. *Catalysis Today, 53*(1), 51-59.

Azizian, S. (2004). Kinetic models of sorption: a theoretical analysis. *Journal of colloid and Interface Science, 276*(1), 47-52.

Bahena, C. L., Martínez, S. S., Guzmán, D. M., & Hernández, M. d. R. T. (2008). Sonophotocatalytic degradation of alazine and gesaprim commercial herbicides in TiO 2 slurry. *Chemosphere, 71*(5), 982-989.

Bahnemann, D. (2004). Photocatalytic water treatment: solar energy applications. *Solar energy, 77*(5), 445-459.

Bautista-Toledo, I., Ferro-Garcia, M., Rivera-Utrilla, J., Moreno-Castilla, C., & Vegas Fernández, F. (2005). Bisphenol A removal from water by activated carbon. Effects of carbon characteristics and solution chemistry. *Environ. Sci. Technol., 39*(16), 6246-6250.

Bejarano-Pérez, N. J., & Suárez-Herrera, M. F. (2007). Sonophotocatalytic degradation of congo red and methyl orange in the presence of TiO 2 as a catalyst. *Ultrasonics Sonochemistry, 14*(5), 589-595.

Berberidou, C., Poulios, I., Xekoukoulotakis, N., & Mantzavinos, D. (2007). Sonolytic, photocatalytic and sonophotocatalytic degradation of malachite green in aqueous solutions. *Applied Catalysis B: Environmental, 74*(1), 63-72.

Bickley, R. I., Gonzalez-Carreno, T., Lees, J. S., Palmisano, L., & Tilley, R. J. (1991). A structural investigation of titanium dioxide photocatalysts. *Journal of Solid State Chemistry, 92*(1), 178-190.

Brotchie, A., Grieser, F., & Ashokkumar, M. (2009). Effect of power and frequency on bubble-size distributions in acoustic cavitation. *Physical review letters, 102*(8), 084302.

Capocelli, M., Joyce, E., Lancia, A., Mason, T. J., Musmarra, D., & Prisciandaro, M. (2012). Sonochemical degradation of estradiols: Incidence of ultrasonic frequency. *Chemical Engineering Journal, 210*, 9-17.

Chang, C., Fu, Y., Hu, M., Wang, C., Shan, G., & Zhu, L. (2013). Photodegradation of bisphenol A by highly stable palladium-doped mesoporous graphite carbon nitride (Pd/mpg-C 3 N 4) under simulated solar light irradiation. *Applied Catalysis B: Environmental, 142*, 553-560.

Chen, X., & Mao, S. S. (2007). Titanium dioxide nanomaterials: synthesis, properties, modifications, and applications. *Chem. Rev, 107*(7), 2891-2959.

Chen, Y., & Dionysiou, D. D. (2006). Effect of calcination temperature on the photocatalytic activity and adhesion of TiO 2 films prepared by the P-25 powder-modified sol–gel method. *Journal of Molecular Catalysis A: Chemical, 244*(1), 73-82.

Chiang, K., Lim, T. M., Tsen, L., & Lee, C. C. (2004). Photocatalytic degradation and mineralization of bisphenol A by TiO 2 and platinized TiO 2. *Applied Catalysis A: General, 261*(2), 225-237.

Chiha, M., Hamdaoui, O., Baup, S., & Gondrexon, N. (2011). Sonolytic degradation of endocrine disrupting chemical 4-cumylphenol in water. *Ultrasonics sonochemistry, 18*(5), 943-950.

Chong, M. N., Jin, B., Chow, C. W., & Saint, C. (2010). Recent developments in photocatalytic water treatment technology: a review. *Water Research, 44*(10), 2997-3027.

Cleuvers, M. (2004). Mixture toxicity of the anti-inflammatory drugs diclofenac, ibuprofen, naproxen, and acetylsalicylic acid. *Ecotoxicology and Environmental Safety, 59*(3), 309-315.

Comninellis, C., Kapalka, A., Malato, S., Parsons, S. A., Poulios, I., & Mantzavinos, D. (2008). Advanced oxidation processes for water treatment: advances and trends for R&D. *Journal of Chemical Technology and Biotechnology, 83*(6), 769-776.

Daghrir, R., Drogui, P., & Robert, D. (2013). Modified TiO2 for environmental photocatalytic applications: a review. *Industrial & engineering chemistry research, 52*(10), 3581-3599.

Daughton, C. G., & Ternes, T. A. (1999). Pharmaceuticals and personal care products in the environment: agents of subtle change? *Environmental health perspectives, 107*(Suppl 6), 907.

Davydov, L., Reddy, E. P., France, P., & Smirniotis, P. G. (2001). Sonophotocatalytic destruction of organic contaminants in aqueous systems on TiO 2 powders. *Applied Catalysis B: Environmental, 32*(1), 95-105.

Deborde, M., Rabouan, S., Mazellier, P., Duguet, J.-P., & Legube, B. (2008). Oxidation of bisphenol A by ozone in aqueous solution. *Water Research, 42*(16), 4299-4308.

Didenko, Y. T., Nastich, D., Pugach, S., Polovinka, Y., & Kvochka, V. (1994). The effect of bulk solution temperature on the intensity and spectra of water sonoluminescence. *Ultrasonics, 32*(1), 71-76.

Entezari, M. H., & Kruus, P. (1996). Effect of frequency on sonochemical reactions II. Temperature and intensity effects. *Ultrasonics sonochemistry, 3*(1), 19-24.

Falconer, I. R., Chapman, H. F., Moore, M. R., & Ranmuthugala, G. (2006). Endocrine-disrupting compounds: A review of their challenge to sustainable and safe water supply and water reuse. *Environmental toxicology, 21*(2), 181-191.

Fent, K., Weston, A. A., & Caminada, D. (2006). Ecotoxicology of human pharmaceuticals. *Aquatic toxicology, 76*(2), 122-159.

Fuerhacker, M. (2003). Bisphenol A emission factors from industrial sources and elimination rates in a sewage treatment plant. *Water science and technology, 47*(10), 117-122.

Fujishima, A., Rao, T. N., & Tryk, D. A. (2000). Titanium dioxide photocatalysis. *Journal of Photochemistry and Photobiology C: Photochemistry Reviews, 1*(1), 1-21.

Fukahori, S., Ichiura, H., Kitaoka, T., & Tanaka, H. (2003). Capturing of bisphenol A photodecomposition intermediates by composite TiO 2–zeolite sheets. *Applied Catalysis B: Environmental, 46*(3), 453-462.

Fulazzaky, M. A., Seong, T. W., & Masirin, M. I. M. (2010). Assessment of water quality status for the Selangor River in Malaysia. *Water, Air, and Soil Pollution, 205*(1-4), 63.

Garoma, T., & Matsumoto, S. (2009). Ozonation of aqueous solution containing bisphenol A: Effect of operational parameters. *Journal of hazardous materials, 167*(1), 1185-1191.

Goel, M., Hongqiang, H., Mujumdar, A. S., & Ray, M. B. (2004). Sonochemical decomposition of volatile and non-volatile organic compounds—a comparative study. *Water Research, 38*(19), 4247-4261.

Gonze, E., Fourel, L., Gonthier, Y., Boldo, P., & Bernis, A. (1999). Wastewater pretreatment with ultrasonic irradiation to reduce toxicity. *Chemical Engineering Journal, 73*(2), 93-100.

Gültekin, I., & Ince, N. H. (2008). Ultrasonic destruction of bisphenol-A: the operating parameters. *Ultrasonics sonochemistry, 15*(4), 524-529.

Guo, C., Ge, M., Liu, L., Gao, G., Feng, Y., & Wang, Y. (2009). Directed synthesis of mesoporous TiO2 microspheres: catalysts and their photocatalysis for bisphenol A degradation. *Environmental science & technology, 44*(1), 419-425.

Guo, Z., & Feng, R. (2009). Ultrasonic irradiation-induced degradation of low-concentration bisphenol A in aqueous solution. *Journal of hazardous materials, 163*(2), 855-860.

Guo, Z., Zheng, Z., Zheng, S., Hu, W., & Feng, R. (2005). Effect of various sono-oxidation parameters on the removal of aqueous 2, 4-dinitrophenol. *Ultrasonics sonochemistry, 12*(6), 461-465.

Gutierrez, M., & Henglein, A. (1990). Chemical action of pulsed ultrasound: observation of an unprecedented intensity effect. *Journal of Physical Chemistry, 94*(9), 3625-3628.

Hanselmann, W., & Windhab, E. (1998). Flow characteristics and modelling of foam generation in a continuous rotor/stator mixer. *Journal of Food Engineering, 38*(4), 393-405.

Herrmann, J.-M., Mozzanega, M.-N., & Pichat, P. (1983). Oxidation of oxalic acid in aqueous suspensions of semiconductors illuminated with UV or visible light. *Journal of Photochemistry, 22*(4), 333-343.

Höhne, C., & Püttmann, W. (2008). Occurrence and temporal variations of the xenoestrogens bisphenol A, 4-tert-octylphenol, and tech. 4-nonylphenol in two German wastewater treatment plants. *Environmental Science and Pollution Research, 15*(5), 405-416.

Hong, C.-S., Wang, Y., & Bush, B. (1998). Kinetics and products of the TiO 2, photocatalytic degradation of 2-chlorobiphenyl in water. *Chemosphere, 36*(7), 1653-1667.

Horikoshi, S., Tokunaga, A., Hidaka, H., & Serpone, N. (2004). Environmental remediation by an integrated microwave/UV illumination method: VII. Thermal/non-thermal effects in the microwave-assisted photocatalyzed mineralization of bisphenol-A. *Journal of photochemistry and photobiology A: Chemistry, 162*(1), 33-40.

Jermann, D., Pronk, W., Boller, M., & Schäfer, A. I. (2009). The role of NOM fouling for the retention of estradiol and ibuprofen during ultrafiltration. *Journal of Membrane Science, 329*(1), 75-84.

Ji, H., Chang, F., Hu, X., Qin, W., & Shen, J. (2013). Photocatalytic degradation of 2, 4, 6-trichlorophenol over g-C3N4 under visible light irradiation. *Chemical Engineering Journal, 218,* 183-190.

Jones, O. A., Green, P. G., Voulvoulis, N., & Lester, J. N. (2007). Questioning the excessive use of advanced treatment to remove organic micropollutants from wastewater. *Environmental science & technology, 41*(14), 5085-5089.

Joseph, C. G., Puma, G. L., Bono, A., & Krishnaiah, D. (2009). Sonophotocatalysis in advanced oxidation process: A short review. *Ultrasonics Sonochemistry, 16*(5), 583-589.

Jyothi, K., Yesodharan, S., & Yesodharan, E. (2014). Ultrasound (US), Ultraviolet light (UV) and combination (US+ UV) assisted semiconductor catalysed degradation of organic pollutants in water: Oscillation in the concentration of hydrogen peroxide formed in situ. *Ultrasonics sonochemistry, 21*(5), 1787-1796.

Kaneco, S., Rahman, M. A., Suzuki, T., Katsumata, H., & Ohta, K. (2004). Optimization of solar photocatalytic degradation conditions of bisphenol A in water using titanium dioxide. *Journal of photochemistry and photobiology A: Chemistry, 163*(3), 419-424.

Kang, J.-H., Kondo, F., & Katayama, Y. (2006). Human exposure to bisphenol A. *Toxicology, 226*(2-3), 79-89.

Kang, J.-W., Hung, H.-M., Lin, A., & Hoffmann, M. R. (1999). Sonolytic destruction of methyl tert-butyl ether by ultrasonic irradiation: the role of O3, H2O2, frequency, and power density. *Environmental science & technology, 33*(18), 3199-3205.

Kang, K., Jang, M., Cui, M., Qiu, P., Na, S., Son, Y., & Khim, J. (2015). Enhanced sonocatalytic treatment of ibuprofen by mechanical mixing and reusable magnetic core titanium dioxide. *Chemical Engineering Journal, 264*, 522-530.

Kanthale, P., Ashokkumar, M., & Grieser, F. (2008). Sonoluminescence, sonochemistry (H 2 O 2 yield) and bubble dynamics: frequency and power effects. *Ultrasonics sonochemistry, 15*(2), 143-150.

Katsumata, H., Kawabe, S., Kaneco, S., Suzuki, T., & Ohta, K. (2004). Degradation of bisphenol A in water by the photo-Fenton reaction. *Journal of photochemistry and photobiology A: Chemistry, 162*(2), 297-305.

Kaur, S., & Singh, V. (2007). Visible light induced sonophotocatalytic degradation of Reactive Red dye 198 using dye sensitized TiO_2. *Ultrason. Sonochem., 14*(5), 531-537.

Kavitha, S., & Palanisamy, P. (2011). Photocatalytic and sonophotocatalytic degradation of reactive red 120 using dye sensitized TiO2 under visible light. *International Journal of Civil and Environmental Engineering, 3*(1), 1-6.

Keller, V., Bernhardt, P., & Garin, F. (2003). Photocatalytic oxidation of butyl acetate in vapor phase on TiO 2, Pt/TiO 2 and WO 3/TiO 2 catalysts. *Journal of Catalysis, 215*(1), 129-138.

Kim, S. D., Cho, J., Kim, I. S., Vanderford, B. J., & Snyder, S. A. (2007). Occurrence and removal of pharmaceuticals and endocrine disruptors in South Korean surface, drinking, and waste waters. *Water Research, 41*(5), 1013-1021.

Kitajima, M., Hatanaka, S.-i., & Hayashi, S. (2006). Mechanism of O 2-accelerated sonolysis of bisphenol A. *Ultrasonics, 44*, e371-e373.

Kočí, K., Matějů, K., Obalová, L., Krejčíková, S., Lacný, Z., Plachá, D., . . . Šolcová, O. (2010). Effect of silver doping on the TiO 2 for photocatalytic reduction of CO 2. *Applied Catalysis B: Environmental, 96*(3), 239-244.

Kolpin, D. W., Furlong, E. T., Meyer, M. T., Thurman, E. M., Zaugg, S. D., Barber, L. B., & Buxton, H. T. (2002). Pharmaceuticals, hormones, and other organic wastewater contaminants in US streams, 1999− 2000: A national reconnaissance. *Environmental science & technology, 36*(6), 1202-1211.

Konstantinou, I. K., Sakkas, V. A., & Albanis, T. A. (2002). Photocatalytic degradation of propachlor in aqueous TiO 2 suspensions. Determination of the reaction pathway and identification of intermediate products by various analytical methods. *Water Research, 36*(11), 2733-2742.

Kormann, C., Bahnemann, D. W., & Hoffmann, M. R. (1988). Photocatalytic production of hydrogen peroxides and organic peroxides in aqueous suspensions of titanium dioxide, zinc oxide, and desert sand. *Environmental science & technology, 22*(7), 798-806.

Krejčíková, S., Matějová, L., Kočí, K., Obalová, L., Matěj, Z., Čapek, L., & Šolcová, O. (2012). Preparation and characterization of Ag-doped crystalline titania for photocatalysis applications. *Applied Catalysis B: Environmental, 111*, 119-125.

Kuo, C.-Y., Wu, C.-H., & Lin, H.-Y. (2010). Photocatalytic degradation of bisphenol A in a visible light/TiO 2 system. *Desalination, 256*(1), 37-42.

Lee, H.-B., Peart, T. E., Gris, G., & Chan, J. (2002). Endocrine-disrupting chemicals in industrial wastewater samples in Toronto, Ontario. *Water quality research journal of Canada, 37*(2), 459-472.

Lifka, J., Ondruschka, B., & Hofmann, J. (2003). The use of ultrasound for the degradation of pollutants in water: aquasonolysis–a review. *Engineering in life sciences, 3*(6), 253-262.

Liu, J., Zhang, T., Wang, Z., Dawson, G., & Chen, W. (2011). Simple pyrolysis of urea into graphitic carbon nitride with recyclable adsorption and photocatalytic activity. *Journal of Materials Chemistry, 21*(38), 14398-14401.

Lotsch, B. V., & Schnick, W. (2005). Thermal Conversion of Guanylurea Dicyanamide into Graphitic Carbon Nitride via Prototype CN X Precursors. *Chemistry of materials, 17*(15), 3976-3982.

Madhavan, J., Grieser, F., & Ashokkumar, M. (2010). Combined advanced oxidation processes for the synergistic degradation of ibuprofen in aqueous environments. *Journal of hazardous materials, 178*(1), 202-208.

Meneses, M., Pasqualino, J. C., & Castells, F. (2010). Environmental assessment of urban wastewater reuse: treatment alternatives and applications. *Chemosphere, 81*(2), 266-272.

Mills, A., & Le Hunte, S. (1997). An overview of semiconductor photocatalysis. *Journal of photochemistry and photobiology A: Chemistry, 108*(1), 1-35.

Monteagudo, J., Durán, A., San Martín, I., & García, S. (2014). Ultrasound-assisted homogeneous photocatalytic degradation of Reactive Blue 4 in aqueous solution. *Applied Catalysis B: Environmental, 152*, 59-67.

Mrowetz, M., Pirola, C., & Selli, E. (2003). Degradation of organic water pollutants through sonophotocatalysis in the presence of TiO 2. *Ultrasonics sonochemistry, 10*(4), 247-254.

Ohko, Y., Ando, I., Niwa, C., Tatsuma, T., Yamamura, T., Nakashima, T., . . . Fujishima, A. (2001). Degradation of bisphenol A in water by TiO2 photocatalyst. *Environmental science & technology, 35*(11), 2365-2368.

Ohno, T., Sarukawa, K., Tokieda, K., & Matsumura, M. (2001). Morphology of a TiO 2 photocatalyst (Degussa, P-25) consisting of anatase and rutile crystalline phases. *Journal of Catalysis, 203*(1), 82-86.

Park, C., Choi, E., Jeon, H., Lee, J., Sung, B., Cho, Y., & Ko, K. (2014). Effect of nitrate on the degradation of bisphenol A by UV/H2O2 and ozone/H2O2 oxidation in aqueous solution. *Desalination and Water Treatment, 52*(4-6), 797-804.

Petrier, C., & Casadonte, D. (2001). The sonochemical degradation of aromatic and chloroaromatic contaminants. *Adv. Sonochem, 6*, 91-109.

Pétrier, C., & Francony, A. (1997). Ultrasonic waste-water treatment: incidence of ultrasonic frequency on the rate of phenol and carbon tetrachloride degradation. *Ultrasonics sonochemistry, 4*(4), 295-300.

Petrier, C., Jeunet, A., Luche, J. L., & Reverdy, G. (1992). Unexpected frequency effects on the rate of oxidative processes induced by ultrasound. *Journal of the American Chemical Society, 114*(8), 3148-3150.

Petrier, C., Lamy, M.-F., Francony, A., Benahcene, A., David, B., Renaudin, V., & Gondrexon, N. (1994). Sonochemical degradation of phenol in dilute aqueous solutions: comparison of the reaction rates at 20 and 487 kHz. *The Journal of Physical Chemistry, 98*(41), 10514-10520.

Rizzo, L. (2011). Bioassays as a tool for evaluating advanced oxidation processes in water and wastewater treatment. *Water Research, 45*(15), 4311-4340.

Robati, D. (2013). Pseudo-second-order kinetic equations for modeling adsorption systems for removal of lead ions using multi-walled carbon nanotube. *Journal of Nanostructure in Chemistry, 3*(1), 1-6.

Rodgers-Gray, T. P., Jobling, S., Morris, S., Kelly, C., Kirby, S., Janbakhsh, A., . . . Tyler, C. R. (2000). Long-term temporal changes in the estrogenic composition of treated sewage effluent and its biological effects on fish. *Environmental science & technology, 34*(8), 1521-1528.

Rykowska, I., & Wasiak, W. (2006). Properties, threats, and methods of analysis of bisphenol A and its derivatives. *Acta chromatographica, 16*, 7.

Sánchez-Avila, J., Bonet, J., Velasco, G., & Lacorte, S. (2009). Determination and occurrence of phthalates, alkylphenols, bisphenol A, PBDEs, PCBs and PAHs in an industrial sewage grid discharging to a Municipal Wastewater Treatment Plant. *Science of the Total Environment, 407*(13), 4157-4167.

Santhi, V., Sakai, N., Ahmad, E., & Mustafa, A. (2012). Occurrence of bisphenol A in surface water, drinking water and plasma from Malaysia with exposure assessment from consumption of drinking water. *Science of the Total Environment, 427*, 332-338.

Seger, B., & Kamat, P. V. (2009). Fuel cell geared in reverse: photocatalytic hydrogen production using a TiO2/Nafion/Pt membrane assembly with no applied bias. *The Journal of Physical Chemistry C, 113*(43), 18946-18952.

Selli, E. (2002). Synergistic effects of sonolysis combined with photocatalysis in the degradation of an azo dye. *Physical Chemistry Chemical Physics, 4*(24), 6123-6128.

Shimizu, N., Ogino, C., Dadjour, M. F., & Murata, T. (2007). Sonocatalytic degradation of methylene blue with TiO 2 pellets in water. *Ultrasonics sonochemistry, 14*(2), 184-190.

Silva, A. M., Nouli, E., Carmo-Apolinário, Â. C., Xekoukoulotakis, N. P., & Mantzavinos, D. (2007). Sonophotocatalytic/H 2 O 2 degradation of phenolic compounds in agro-industrial effluents. *Catalysis Today, 124*(3), 232-239.

Snyder, S. A., Westerhoff, P., Yoon, Y., & Sedlak, D. L. (2003). Pharmaceuticals, personal care products, and endocrine disruptors in water: implications for the water industry. *Environmental Engineering Science, 20*(5), 449-469.

Song, L., Zhang, S., Wu, X., & Wei, Q. (2012). A metal-free and graphitic carbon nitride sonocatalyst with high sonocatalytic activity for degradation methylene blue. *Chemical Engineering Journal, 184*, 256-260.

Staehelin, J., & Hoigne, J. (1985). Decomposition of ozone in water in the presence of organic solutes acting as promoters and inhibitors of radical chain reactions. *Environmental science & technology, 19*(12), 1206-1213.

Sumpter, J. P. (2005). Endocrine disrupters in the aquatic environment: an overview. *Acta hydrochimica et hydrobiologica*, *33*(1), 9-16.

Suslick, K., Doktycz, S., & Flint, E. (1990). On the origin of sonoluminescence and sonochemistry. *Ultrasonics, 28*(5), 280-290.

Suslick, K. S., & Flannigan, D. J. (2008). Inside a collapsing bubble: sonoluminescence and the conditions during cavitation. *Annu. Rev. Phys. Chem., 59*, 659-683.

Suzuki, T., Nakagawa, Y., Takano, I., Yaguchi, K., & Yasuda, K. (2004). Environmental fate of bisphenol A and its biological metabolites in river water and their xeno-estrogenic activity. *Environmental science & technology, 38*(8), 2389-2396.

Suzuki, Y., Arakawa, H., Maezawa, A., & Uchida, S. (1999). Ultrasonic enhancement of photo-catalytic oxidation of surfactant. *International Journal of Photoenergy, 1*(1), 60-64.

Taghizadeh, M. T., & Abdollahi, R. (2011). Sonolytic, sonocatalytic and sonophotocatalytic degradation of chitosan in the presence of TiO 2 nanoparticles. *Ultrasonics sonochemistry, 18*(1), 149-157.

Tang, S. K., Teng, T. T., Alkarkhi, A. F., & Li, Z. (2012). Sonocatalytic degradation of rhodamine B in aqueous solution in the presence of TiO2 coated activated carbon. *APCBEE Procedia, 1*, 110-115.

Tangestaninejad, S., Moghadam, M., Mirkhani, V., Mohammadpoor-Baltork, I., & Salavati, H. (2008). Sonochemical and visible light induced photochemical and sonophotochemical degradation of dyes catalyzed by recoverable vanadium-containing polyphosphomolybdate immobilized on TiO 2 nanoparticles. *Ultrasonics Sonochemistry, 15*(5), 815-822.

Tay, K. S., Rahman, N. A., & Abas, M. R. B. (2012). Degradation of bisphenol A by ozonation: rate constants, influence of inorganic anions, and by-products. *Maejo International Journal of Science and Technology, 6*(1).

Ternes, T. A., Meisenheimer, M., McDowell, D., Sacher, F., Brauch, H.-J., Haist-Gulde, B., . . . Zulei-Seibert, N. (2002). Removal of pharmaceuticals during drinking water treatment. *Environmental science & technology, 36*(17), 3855-3863.

Torres, R., Abdelmalek, F., Combet, E., Pétrier, C., & Pulgarin, C. (2007). A comparative study of ultrasonic cavitation and Fenton's reagent for bisphenol A degradation in deionised and natural waters. *Journal of hazardous materials, 146*(3), 546-551.

Torres, R. A., Nieto, J. I., Combet, E., Pétrier, C., & Pulgarin, C. (2008). Influence of TiO 2 concentration on the synergistic effect between photocatalysis and high-frequency ultrasound for organic pollutant mineralization in water. *Applied Catalysis B: Environmental, 80*(1), 168-175.

Torres, R. A., Pétrier, C., Combet, E., Carrier, M., & Pulgarin, C. (2008). Ultrasonic cavitation applied to the treatment of bisphenol A. Effect of sonochemical parameters and analysis of BPA by-products. *Ultrasonics sonochemistry, 15*(4), 605-611.

Torres, R. A., Pétrier, C., Combet, E., Moulet, F., & Pulgarin, C. (2007). Bisphenol A mineralization by integrated ultrasound-UV-iron (II) treatment. *Environmental science & technology, 41*(1), 297-302.

Tuziuti, T., Yasui, K., Iida, Y., Taoda, H., & Koda, S. (2004). Effect of particle addition on sonochemical reaction. *Ultrasonics, 42*(1), 597-601.

Wang, J., Guo, Y., Liu, B., Jin, X., Liu, L., Xu, R., . . . Wang, B. (2011). Detection and analysis of reactive oxygen species (ROS) generated by nano-sized TiO 2 powder under ultrasonic irradiation and application in sonocatalytic degradation of organic dyes. *Ultrasonics sonochemistry, 18*(1), 177-183.

Wang, J., Jiang, Z., Zhang, L., Kang, P., Xie, Y., Lv, Y., . . . Zhang, X. (2009). Sonocatalytic degradation of some dyestuffs and comparison of catalytic activities of nano-sized TiO 2, nano-sized ZnO and composite TiO 2/ZnO powders under ultrasonic irradiation. *Ultrasonics sonochemistry, 16*(2), 225-231.

Wang, Y., & Hong, C.-S. (2000). TiO 2-mediated photomineralization of 2-chlorobiphenyl: the role of O 2. *Water Research, 34*(10), 2791-2797.

Watanabe, N., Horikoshi, S., Kawabe, H., Sugie, Y., Zhao, J., & Hidaka, H. (2003). Photodegradation mechanism for bisphenol A at the TiO 2/H 2 O interfaces. *Chemosphere, 52*(5), 851-859.

Wong, C., & Chu, W. (2003). The direct photolysis and photocatalytic degradation of alachlor at different TiO 2 and UV sources. *Chemosphere, 50*(8), 981-987.

Wu, T., Zivanovic, S., Hayes, D. G., & Weiss, J. (2008). Efficient reduction of chitosan molecular weight by high-intensity ultrasound: Underlying mechanism and effect of process parameters. *Journal of agricultural and food chemistry, 56*(13), 5112-5119.

Xu, J., Li, Y., Peng, S., Lu, G., & Li, S. (2013). Eosin Y-sensitized graphitic carbon nitride fabricated by heating urea for visible light photocatalytic hydrogen evolution: the effect of the pyrolysis temperature of urea. *Physical Chemistry Chemical Physics, 15*(20), 7657-7665.

Xu, P., Janex, M.-L., Savoye, P., Cockx, A., & Lazarova, V. (2002). Wastewater disinfection by ozone: main parameters for process design. *Water Research, 36*(4), 1043-1055.

Yan, S., Li, Z., & Zou, Z. (2009). Photodegradation performance of g-C3N4 fabricated by directly heating melamine. *Langmuir, 25*(17), 10397-10401.

Zhang, J., Chen, X., Takanabe, K., Maeda, K., Domen, K., Epping, J. D., . . . Wang, X. (2010). Synthesis of a Carbon Nitride Structure for Visible-Light Catalysis by Copolymerization. *Angewandte Chemie International Edition, 49*(2), 441-444.

Zhang, K., Zhang, F. J., Chen, M. L., & Oh, W. C. (2011). Comparison of catalytic activities for photocatalytic and sonocatalytic degradation of methylene blue in present of anatase TiO 2–CNT catalysts. *Ultrasonics Sonochemistry, 18*(3), 765-772.

Zhong, X., Jin, M., Dong, H., Liu, L., Wang, L., Yu, H., . . . Wang, J.-g. (2014). TiO_2 nanobelts with a uniform coating of g-C_3N_4 as a highly effective heterostructure for enhanced photocatalytic activities. *J. Solid State Chem., 220*, 54-59.

Zhu, L., Meng, Z.-D., Park, C.-Y., Ghosh, T., & Oh, W.-C. (2013). Characterization and relative sonocatalytic efficiencies of a new MWCNT and CdS modified TiO 2 catalysts and their application in the sonocatalytic degradation of rhodamine B. *Ultrasonics sonochemistry, 20*(1), 478-484.

LIST OF PUBLICATIONS AND PAPERS PRESENTED

Paper published

1. Sharmini Sunasee, Wong, K. T., Lee, G., Pichiah, S., Ibrahim, S., Park, C., Kim, N. C., Yoon, Y., Jang, M. (2017). Titanium dioxide-based sonophotocatalytic mineralization of Bisphenol A and its intermediates. *Environmental Science and Pollution Research*, 1-12
2. Sharmini Sunasee, Leong, K. H., Wong, K. T., Lee, G., Pichiah, S., Nah, I. W., Jeon, B., Yoon, Y., Jang, M. (2017). Sonophotocatalytic degradation of Bisphenol A and its intermediates with graphitic carbon nitride. *Environmental Science and Pollution Research*, 1-12.

Conference Presentations

1. Sharmini Sunasee, Min Jang. "Synthesis of magnetic graphene based sonophotocatalyst and sonophotocatalytic process to remove bisphenol A (BPA) in water". 18th Malaysian International Chemical Congress (18 MICC). 3-5 November (2014) Kuala Lumpur, Malaysia.
2. Sharmini Sunasee, Saravanan, P., Cui, M., Shaliza, I., Jang, M. "Bisphenol A degradation by sonophotocatalysis with presence of nano-structured graphitic carbon nitride". 2nd Asia-Oceania Sonochemical Society Conference (AOSS-2). 25-28 July (2015) Kuala Lumpur, Malaysia.